ISSN: 2408-2384 (Online)
ISSN: 1686-5456 (Print)

Environment and Natural Resources Journal

Volume 21, Number 1, January-February 2023

Environment and Natural Resources Journal (EnNRJ)
Volume 21, Number 1, January - February 2023 ISSN: 1686-5456 (Print)
ISSN: 2408-2384 (Online)

AIMS AND SCOPE

The Environment and Natural Resources Journal is a peer-reviewed journal, which provides insight scientific knowledge into the diverse dimensions of integrated environmental and natural resource management. The journal aims to provide a platform for exchange and distribution of the knowledge and cutting-edge research in the fields of environmental science and natural resource management to academicians, scientists and researchers. The journal accepts a varied array of manuscripts on all aspects of environmental science and natural resource management. The journal scope covers the integration of multidisciplinary sciences for prevention, control, treatment, environmental clean-up and restoration. The study of the existing or emerging problems of environment and natural resources in the region of Southeast Asia and the creation of novel knowledge and/or recommendations of mitigation measures for sustainable development policies are emphasized.

The subject areas are diverse, but specific topics of interest include:

- Biodiversity
- Climate change
- Detection and monitoring of polluted sources e.g., industry, mining
- Disaster e.g., forest fire, flooding, earthquake, tsunami, or tidal wave
- Ecological/Environmental modelling
- Emerging contaminants/hazardous wastes investigation and remediation
- Environmental dynamics e.g., coastal erosion, sea level rise
- Environmental assessment tools, policy and management e.g., GIS, remote sensing, Environmental Management System (EMS)
- Environmental pollution and other novel solutions to pollution
- Remediation technology of contaminated environments
- Transboundary pollution
- Waste and wastewater treatments and disposal technology

Schedule
Environment and Natural Resources Journal (EnNRJ) is published 6 issues per year in January-February, March-April, May-June, July-August, September-October, and November-December.

Publication Fees
There is no cost of the article-processing and publication.

Ethics in publishing
EnNRJ follows closely a set of guidelines and recommendations published by Committee on Publication Ethics (COPE).

Environment and Natural Resources Journal (EnNRJ)
Volume 21, Number 1, January - February 2023
ISSN: 1686-5456 (Print)
ISSN: 2408-2384 (Online)

Editorial Office Address
Research Management and Administration Section,
Faculty of Environment and Resource Studies, Mahidol University
999, Phutthamonthon Sai 4 Road, Salaya, Phutthamonthon, Nakhon Pathom, Thailand, 73170
Phone +662 441 5000 ext. 2108 Fax. +662 441 9509-10
Website: https://ph02.tci-thaijo.org/index.php/ennrj/index
E-mail: ennrjournal@gmail.com

Environment and Natural Resources Journal (EnNRJ)

Volume 21, Number 1, January - February 2023 ISSN: 1686-5456 (Print)
ISSN: 2408-2384 (Online)

CONTENT

Pilot-Scale Modelling of Aerated Lagoon Technology for the Treatment of Landfill Leachate: Case Study Hrybovychi Plant

Myroslav Malovanyy[1], Volodymyr Zhuk[2], Ivan Tymchuk[1*], Ruslan Grechanik[1], Vira Sliusar[1], Nataliya Vronska[1], Anastasiya Marakhovska[1], and Andriy Sereda[1]

[1]*Viacheslav Chornovil Institute of Sustainable Development, Lviv Polytechnic National University, S. Bandera Str. 12, Lviv 79013, Ukraine*

[2]*Institute of Civil Engineering and Building Systems, Lviv Polytechnic National University, S. Bandera Str. 12, Lviv 79013, Ukraine*

ARTICLE INFO

Received: 26 Apr 2022
Received in revised: 11 Aug 2022
Accepted: 22 Aug 2022
Published online: 12 Oct 2022
DOI: 10.32526/ennrj/21/202200103

Keywords:
Aerobic biological treatment/ Leachate/ Pilot-scale treatment unit/ Solid waste landfill

*** Corresponding author:**
E-mail: i.s.tymchuk@gmail.com

ABSTRACT

Results of experimental pilot-scale study of aerobic pre-treatment of the leachate of the Hrybovychi municipal solid waste (MSW) landfill (Ukraine) in batch reactor mode and in semi-continuous mode are presented. The dependencies of key pollution indicators, namely biological oxygen demand, chemical oxygen demand, pH, suspended solids, and total Kjeldahl nitrogen (TKN), during a 30-day periodical aeration process were obtained. The first 15 days treatment was in the batch reactor mode treating an initial volume of raw leachate. The second 15 days treatment was in a semi-continuous reactor mode: 400 L of aerobically pre-treated leachate were pumped to the next treatment stage and consequently the same volume of raw leachate was added in the bioreactor tank. Aerobic biological treatment of Hrybovychi landfill leachate using the developed method achieved significant treatment effects, namely 55.3% of the total Kjeldahl nitrogen, 27% of COD, 70.2% of BOD_5 and 66.5% of BOD_{tot}. Time dependences of TKN, COD, BOD_5, and BOD_{tot} are well fitted by simple exponential trends, which correspond to first-order reactions. Landfill leachate, aerobically pre-treated in the pilot-scale treatment unit, can be discharged for final treatment to the bio-plateau or to the wastewater treatment plant.

1. INTRODUCTION

Municipal solid waste (MSW) landfills are big sources of chemical and biological environmental pollution (Degtyar and Galkina, 2019; Grynchyshyn, 2019). MSW landfills are particularly dangerous in terms of their impact on the surface water bodies and groundwater in the area of influence of these environmentally hazardous objects (Samoylik and Molchanova, 2017; Vaverková et al., 2020). According to expert estimations, more than 99% of Ukrainian MSW landfills do not meet European requirements, and the volume of household waste tends to increase (National Strategy for Waste Management in Ukraine Until 2030, 2017).

Leachate is the most harmful impact of landfills and dumps on the environment. Leachate is actively formed in the landfill body when moisture content of deposited solid waste is more than 55%, and due to precipitation that exceeds the evaporation from the landfill surface (Municipal Solid Waste Landfills, 2005). Landfill leachates are highly concentrated water solutions of various toxic organic and inorganic substances (Melnyk et al., 2014; Popovych et al., 2020; Teng et al., 2021). In the absence of strict control of hydrosphere pollution (Iurchenko et al., 2016; Tulaydan et al., 2017), and due to problems with monitoring of this pollution (Odnorih et al., 2020), development of effective methods to prevent contamination of surface waters and aquifers by leachates is especially important.

The most common technologies for leachate treatment are biological anaerobic and aerobic methods and membrane processes, continuing with a final stage of secondary treatment at municipal wastewater treatment plants (WWTP) (Dereli et al., 2020; Malovanyy et al., 2018) or artificial wetlands (Popovych et al., 2020; Malovanyy et al., 2021). Membrane treatments, including the most widespread

Citation: Malovanyy M, Zhuk V, Tymchuk I, Grechanik R, Sliusar V, Vronska N, Marakhovska A, Sereda A. Pilot-scale modelling of aerated lagoon technology for the treatment of landfill leachate: Case study Hrybovychi Plant. Environ. Nat. Resour. J. 2023;21(1):1-8. (https://doi.org/10.32526/ennrj/21/202200103)

reverse osmosis, are energy-expensive, and implementation of these processes requires significant capital and operating costs (Dushkyn et al., 2011). It is also advisable to use different energy-saving systems (Shchur et al., 2021). Anaerobic biological treatment of leachate (Mojiri et al., 2021; Zamri et al., 2017) could be economical due to the obtaining of biogas, a renewable energy source (Voytovych et al., 2020). However, its implementation on an industrial scale requires strict adherence to the process parameters, and since the leachate composition can vary widely upon time, this technology is challenging to implement.

Aerobic methods of biological leachate treatment have a number of advantages compared to anaerobic methods: flexibility of use, convenience of an output to a steady mode of maintenance, and quick adaptation to variable leachate composition and flow rate (Miao et al., 2019; Wang et al., 2018). Aerobic reactors are much simpler in design and less expensive than anaerobic ones, they can be automated and operated much easier. It is interesting to note the study on leachate treatment from Pulau Burung Landfill Site (PBLS), located in Bayram Forest Reserve, Malaysia (Zamri et al., 2017). The researchers selected this site because it is semi-aerobic and recirculates the leachate. PBLS has been in operation for over 20 years and the resulting leachate is mature, with a high COD and concentration of ammonium nitrogen and a low BOD_5/COD ratio. However, the use of adsorbent material, in this case, ion exchange resin, as a second stage after aeration requires the development of methods for its processing or disposal, which involves additional costs.

An effective way to increase the effect of biological treatment of landfill leachate is the use of sequencing batch reactors SBR (Jagaba et al., 2021; Tałałaj et al., 2021), SBR with carriers (Koc-Jurczyk and Jurczyk, 2020), microaeration (Wei et al., 2021), etc. A combination of aerobic and anaerobic methods of leachate treatment is both promising and effective (El-Gohary and Kamel, 2016; Sun et al., 2015). However, treating solid waste landfill leachate in this coordinated manner is energy-intensive and more expensive than aerobic treatment. Treatment using the aeration method with higher plants is interesting (Chen et al., 2022). However, this method is more suitable for domestic wastewater treatment, as it has a more predictable chemical composition.

The main deficiency of aerobic and anaerobic biological methods of landfill leachate treatment is the need for additional stages for more deep treatment to meet the requirements for discharge into open water courses (Lebron et al., 2021; Malovanyy et al., 2018). The most common solution is the use of combined multi-stage treatment methods, where biological methods are combined with reverse osmosis (Tałałaj et al., 2021), treatment with strong oxidants, including ozonation (Yang et al., 2022), and Fenton process (El Mrabet et al., 2020), followed by precipitation enhanced by coagulation and flocculation (De et al., 2019; Malovanyy et al., 2018). Oxidation and sorption are especially necessary and effective for the treatment of mature leachate and for the removal of heavy metal ions (Taghavi et al., 2021).

Aerated lagoons is a simple, economic and effective method for aerobic biological treatment of landfill leachate from organic contaminants and ammonium nitrogen (Broughton and Shilton, 2012; Malovanyy et al., 2018). A typical example of the long-time treatment of mature leachate in aerated lagoons is the Bell House landfill (England), where leachate was treated in four aerated lagoons connected in series (Mehmood et al., 2009). The average COD of raw leachate was equal to 1,740 mg/L, whereas COD decreased to 620 mg/L after the first lagoon, 510 mg/L after the second, 492 mg/L after the third, and 426 mg/L after the fourth, corresponding to a total treatment effect of 75.5%. The average ammonium nitrogen concentration in the raw leachate was 965.2 mg/L, and total treatment effect in the four lagoons was 99.0%.

Technology of biological aerobic treatment of landfill leachate in laboratory conditions, simulating the process in an aerated lagoon, was studied by Malovanyy et al. (2018). The information on its successful application predicts the prospects for its application as a pre-treatment stage in the complex technology of leachate treatment at Hrybovychi MSW landfill (Lviv Region, Ukraine). The purpose of the paper was an experimental pilot-scale study of aerobic treatment of the leachate of the Hrybovychi MSW landfill in the batch reactor mode and in semi-continuous mode.

2. METHODOLOGY

2.1 Materials

Hrybovychi MSW landfill leachate was used in this study as tested leachate. Hrybovychi MSW landfill with a total area of about 38 ha is located in the west part of Ukraine, 2 km to the north from Lviv city (49.90N; 24.04E). It served as the main MSW landfill of Lviv city from 1958 until 2016, and now it is under technical remediation process. The main parameters of raw Hrybovychi MSW landfill leachate, sampled in November 2021, are presented in Table 1.

Thus, significantly excessive concentrations of contaminants were detected in the Hrybovychi MSW landfill leachate. The study of biological leachate treatment under aeration conditions was aimed to find the treatment effects using BOD_5, COD and TKN as key pollutant indicators.

Table 1. The average chemical composition of Hrybovychi MSW landfill leachate

#	Pollution indicators	Unit	Value	TLV*
1	Ammonium nitrogen	mg/L	548.1	2
2	Total Kjeldahl nitrogen (TKN)	mg/L	889.3	10
3	BOD_5	mg/L	192.0	15
4	COD	mg/L	5,082.0	80
5	Suspended solids (SS)	mg/L	3,011.0	-
6	Iron	mg/L	10.7	0.3
7	Cadmium	mg/L	0.005	0.001
8	Cobalt	mg/L	0.028	0.1
9	Manganese	mg/L	0.015	0.1
10	Nickel	mg/L	0.09	0.1
11	Lead	mg/L	0.12	0.03
12	Strontium	mg/L	0.022	7
13	Total dissolved solids (TDS)	mg/L	15,245.0	-
14	Chlorides	mg/L	3,900.0	350

*TLV - threshold limit value for the output in open water courses in Ukraine

2.2 Pilot-scale aeration treatment unit

Biological aerobic treatment of Hrybovychi MSW landfill leachate was studied at the pilot treatment unit with a capacity of 400 L/day. Aeration was carried out in a bioreactor with diameter D=1.6 m, total depth H=1.8 m and leachate depth h=1.4 m, equipped with a jet pump aerator (P=2.2 kW), as shown in Figure 1. Standard oxygen transfer rate was equal to 0.9±0.1 kg O_2/h.

The optimal aeration parameters (timing and intensity) were determined during the research. Previous laboratory studies have shown that the optimal duration of the non-stationary period for the start of the process of aerobic biological treatment is 7-15 days (Malovanyy et al., 2018). Pilot studies have confirmed these figures. Microbiocenosis was gradually self-inoculated in the bioreactor in the process of aeration (Dos Santos et al., 2022; Malovanyy et al., 2018), which resulted in a gradual biological treatment of leachate.

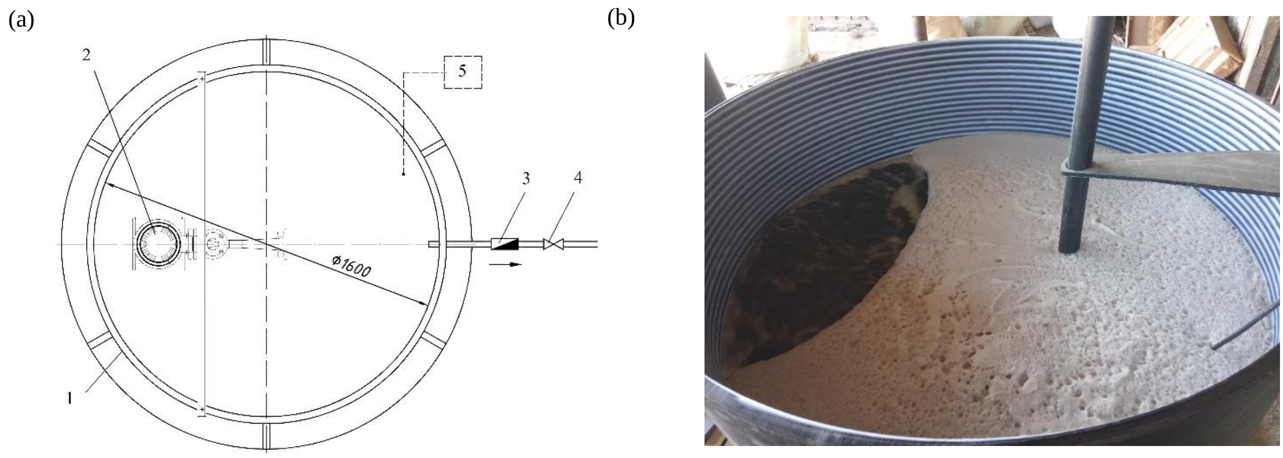

Figure 1. Pilot-scale bioreactor treatment unit: Principal scheme (a); leachate aeration process (b); 1-reservoir, 2-jet aerator, 3-water meter, 4-valve, 5-oximeter/pH meter/TDS meter

Periodical aeration process was used, with 12 h of aeration per day. Control samples of leachate were taken for laboratory analysis every 24 h. Previously published methods (Baird et al., 2017) were used for the analysis of key pollutant indicators, namely BOD_5, BOD_{tot}, COD, SS, TKN, and pH.

Dependencies of key pollution indicators during the 30-day periodical aeration process were obtained experimentally. The first 15 days treatment in the batch reactor mode treating the same initial volume of raw leachate. Another 15 days treatment in the continuous reactor mode and 400 L of aerobically pre-treated leachate were pumped to the next treatment stage, and consequently the same volume of raw leachate was added in the bioreactor tank, thus in continuous mode hydraulic retention time (HRT) was equal to seven days.

3. RESULTS AND DISCUSSION

Experimental dependence of the TKN on the duration of biochemical aerobic treatment of leachate is presented in Figure 2. During batch reactor mode of aerobic leachate treatment, the concentration of TKN decreased from 889.3 mg/L to 397.2 mg/L, corresponding to a treatment effect of 55.3%. The high rate of TKN decreasing can be explained by the intensive conversion of ammonium nitrogen from aqueous to gaseous phase at pH higher than pH 7 (Abood et al., 2014). The results obtained in this batch reactor mode can be approximated by a simple exponential dependence, corresponding to the first-order reaction:

$$C_{TKN} = 833.5 \exp\ (-0.551t) \qquad (1)$$

Where; C_{TKN} is the TKN concentration in mg/L; t is time in days; coefficient of determination of the dependence (1) R^2=0.959.

The most relevant factor in the treatment process is COD (Koc-Jurczyk and Jurczyk, 2020). Dependence of the COD of the leachate on the duration of its aerobic biochemical treatment at the pilot-scale treatment unit (Figure 3) shows that in first 15 days of the batch reactor mode the value of COD decreased by about 27%, which is quite typical for medium and mature leachates, containing high levels of hard oxidizing organic substances (Miao et al., 2019). For the batch reactor mode, the approximate equation is:

$$C_{COD} = 5{,}007 \exp\ (-0.0204t) \qquad (2)$$

Where; C_{COD} is the value of COD, mg/L, and coefficient R^2=0.983.

Average treatment effect by COD, obtained in the continuous mode at HRT=7 days, is found to be 26.5%, and this result correlates quite well with the treatment of mature leachate of Bell House landfill (UK) in aerated lagoons, where the average COD at the inlet was 1,740 mg/L and after 56 days of aeration was reduced to 620 mg/L, corresponding to the treatment effect of 64% (Mehmood et al., 2009). Extrapolating the exponential dependence (2) to the value of the (HRT) of 56 days, the estimated treatment effect of Hrybovychi leachate by COD could be about 69%.

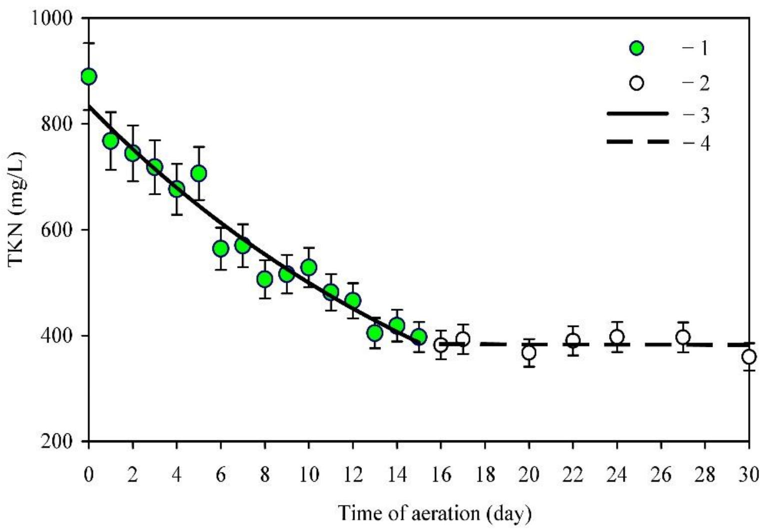

Figure 2. Content of total Kjeldahl nitrogen in Hrybovychi leachate during its aeration in the pilot-scale treatment unit: 1-batch reactor mode; 2-semi-continuous mode; 3-trend line (1); 4-average value of 385 mg/L

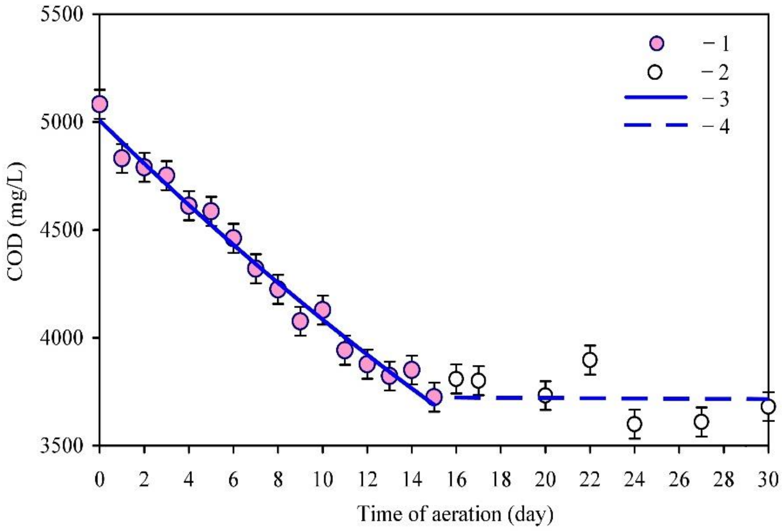

Figure 3. Change of COD in Hrybovychi leachate during the aeration process at the pilot-scale treatment unit: 1-batch reactor mode; 2-semi-continuous mode; 3-trend line (2); 4-average value of 3,732 mg/L

The average treatment effect by BOD_5 of Hrybovychi landfill leachate was found to be 70.2% (Figure 4), which is much higher than the treatment effect on COD, and an exponential approximation with R^2=0.849 is obtained:

$$C_{BOD_5} = 176.9 \exp\ (-0.075t) \tag{3}$$

At the same time, slightly less than 74.6% was obtained by (De et al., 2019) after three days of aeration treatment of Kolkata landfill leachate (India), which can be explained by a significantly higher degree of biodegradability of Kolkata leachate with a BOD_5/COD ratio of 0.36.

Similar results were obtained for BOD_{tot} (Figure 5):

$$C_{BOD_{tot}} = 586 \exp\ (-0.076t) \tag{4}$$

Where; C_{BODtot} is the value of BOD_{tot}, mg/L; R^2=0.9487.

The average effect of leachate treatment on BOD_{tot} is found to be 66.5%. It should be noted the high value of the ratio BOD_{tot}/BOD_5=3.57 when entering the regular semi-continuous operating mode of the aerobic biological treatment, which can be explained by the low rate of biochemical oxidation of biodegradable organics in Hrybovychi leachate, comparing, for instance, the Kolkata leachate (De et al., 2019).

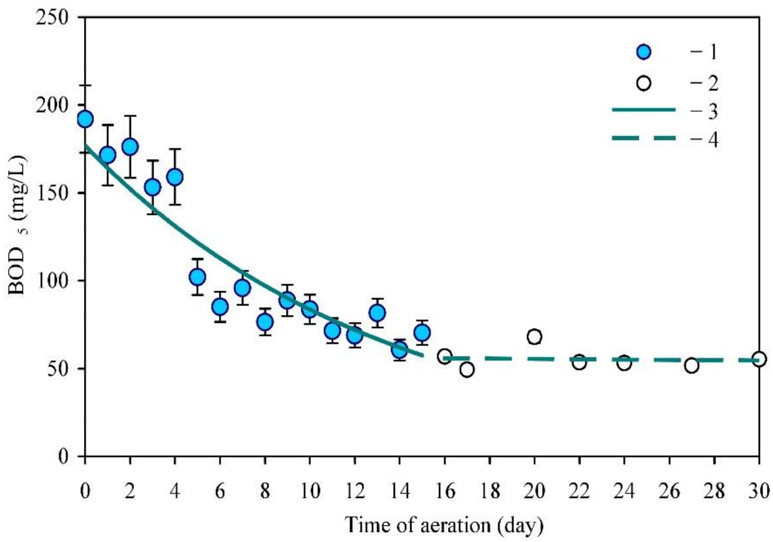

Figure 4. Change of BOD_5 in Hrybovychi leachate during the aeration process at the pilot-scale treatment unit: 1-batch reactor mode; 2-semi-continuous mode; 3-trend line (3); 4-average value of 57.3 mg/L

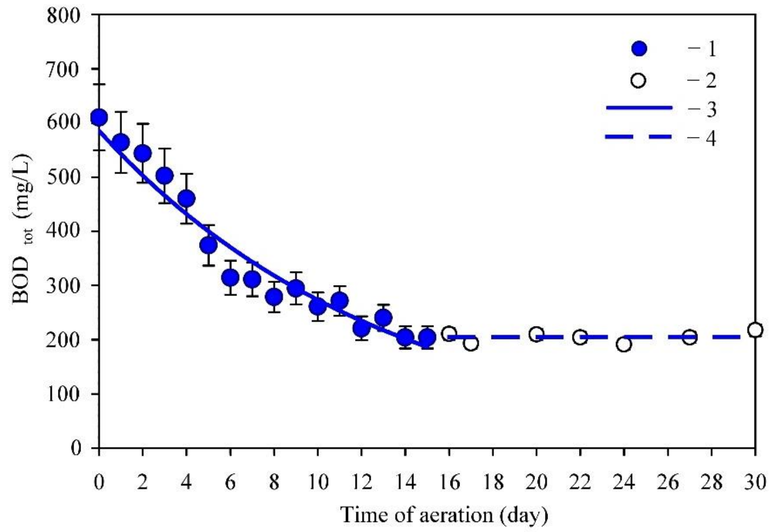

Figure 5. Change of BOD_{tot} in Hrybovychi leachate during the aeration process at the pilot-scale treatment unit: 1-batch reactor mode; 2-semi-continuous mode; 3-trend line (4); 4-average value of 204.4 mg/L

Clear trends of relatively rapid increasing of the pH value at the beginning of the aeration and slow asymptotic increasing to the 12-15 days of aeration are obtained (Figure 6). This tendency is analogical to reported by (Mehmood et al., 2009), where mean pH of raw leachate was 7.2, while the mean pH after 4-stage aerated lagoon with HRT=56 days was 8.5. This permanent growth of pH is probably caused by the nature of biochemical processes of the leachate oxidation by aerobic microbiocenosis, and for the first 12 days of aeration of Hrybovychi leachate the exponential association equation is obtained (R^2=0.971):

$$\mathrm{pH} = 0.623 \times [15.64 - \exp(-0.536t)] \quad (5)$$

In the semi-continuous mode of operation pH of leachate was stabilized at an average value of 9.74 with small (±0.05) variations in both directions (Figure 6), which is something above the upper optimal limit for biological treatment process estimated about pH=8.5.

During the phase of biochemical treatment of the leachate, a monotonic but insignificant increase in the content of suspended solids was observed (Figure 7). This can be explained by the gradual growth of the microbiocenosis biomass involved in the biochemical treatment process. Simple linear trend can be used to approximate the experimental results:

$$C_{SS} = 193 + 1.91t \quad (6)$$

Where; C_{SS} is suspended solids content, mg/L; R^2=0.8448.

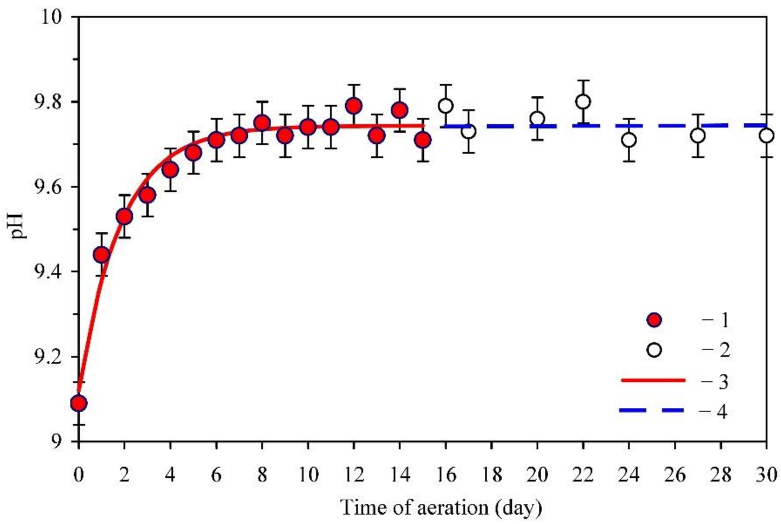

Figure 6. Change of pH in Hrybovychi leachate during the aeration process at the pilot-scale treatment unit: 1-batch reactor mode; 2-semi-continuous mode; 3-trend line (5); 4-average value 9.74

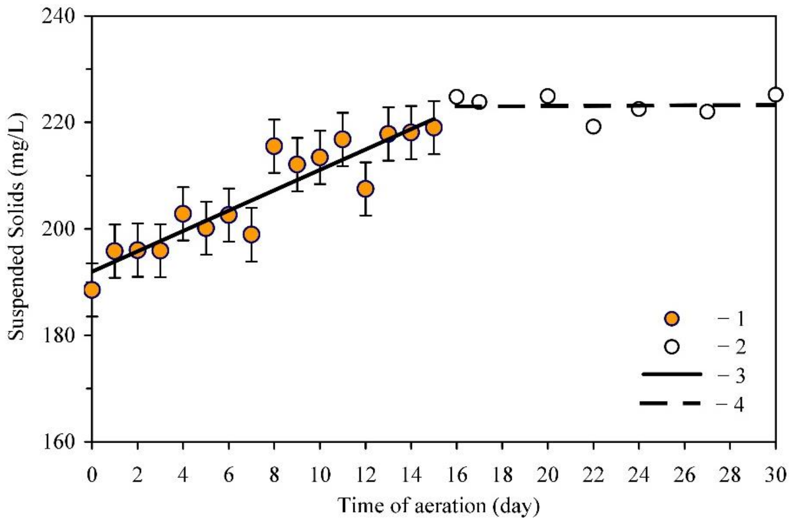

Figure 7. Change of C_{SS} in Hrybovychi leachate during the aeration process at the pilot-scale treatment unit: 1-batch reactor mode; 2-semi-continuous mode; 3-trend line (6); 4-average values 223 mg/L

The average content of suspended solids in the continuous operation mode of the pilot plant C_{SS}=223 mg/L is 31% of the average value of suspended solids of 700 mg/L obtained for full-scale aerated lagoons (Mehmood et al., 2009). Such a low level of suspended solids can be explained by the short duration of the pilot plant study, and over time this value should stabilize at a much higher equilibrium value, similar to (Mehmood et al., 2009).

4. CONCLUSION

Based on the analysis of the pilot-scale results optimal parameters for the aerobic biological treatment of leachates of typical Ukrainian MSW landfills are obtained. Initial batch reactor mode should continue about 15 days to reach sufficiently high treatment effects on baseline pollution indicators. Aerobic biological treatment of landfill leachate using the developed method allows achieving treatment effect of 55.3% on the total Kjeldahl nitrogen, 27% on COD and 63.3% on BOD. Time dependences of TKN, COD, BOD_5, and BOD_{tot} with sufficiently high accuracy can be described by simple exponential dependences, respectively (1)-(4), which correspond to first-order reactions. The peculiarities of the change of pH and suspended solids at the batch reactor mode of the treatment process are explained by the self-inoculation of the activated sludge microbiocenosis. Landfill leachate, aerobically pre-treated in the pilot-scale treatment unit, can be discharged for the final treatment to the bio-plateau or to the wastewater treatment plant.

ACKNOWLEDGEMENTS

This research was supported by the Ministry of Education and Science of Ukraine, grant DZ/107-2021 “Development of the Technology for Preliminary Treatment of Municipal Solid Waste Landfill Leachates”.

REFERENCES

Abood AR, Bao J, Du J, Zheng D, Luo Y. Non-biodegradable landfill leachate treatment by combined process of agitation, coagulation, SBR and filtration. Waste Management 2014; 34(2):439-47.

Baird RB, Eaton AD, Rice EW. Standard Methods for the Examination of Water and Wastewater. 23rd ed. Washington, DC, USA: American Public Health Association, American Water Works Association, Water Environment Federation; 2017.

Broughton A, Shilton A. Tracer studies on an aerated lagoon. Water Science Technology 2012;65(4):611-7.

Chen X, Zhong F, Chen Y, Wu J, Cheng S. The interaction effects of aeration and plant on the purification performance of horizontal subsurface flow constructed wetland. International Journal of Environmental Research and Public Health 2022;19(3):1583-93.

De S, Hazra T, Dutta A. Sustainable treatment of municipal landfill leachate by combined association of air stripping, fenton oxidation, and enhanced coagulation. Environmental Monitoring and Assessment 2019;191(2):1-14.

Degtyar M, Galkina H. Research of main factors affecting the efficiency leachate treatment. Scientific Notes of Taurida National V.I. Vernadsky University, Series: Technical Sciences 2019;69(5):62-8. (in Ukrainian).

Dereli RK, Giberti M, Liu Q, Flynn D, Casey E. Benchmarking leachate co-treatment strategies in municipal wastewater treatment plants under dynamic conditions and energy prices. Journal of Environmental Management 2020;260:Article No. 110129.

dos Santos VHJM, de Medeiros Engelmann P, Marconatto L, dos Anjos Borgea LG, de Lara Palhano P, Augustin AH, et al.

Exploratory analysis of the microbial community profile of the municipal solid waste leachate treatment system: A case study. Waste Management 2022;141:125-35.

Dushkyn S, Kovalenko A, Dehtyar M, Shevchenko T. Resource-Saving Wastewater Treatment Technologies. Kharkiv, Ukraine: KNAME; 2011. (in Russian).

El-Gohary FA, Kamel G. Characterization and biological treatment of pre-treated landfill leachate. Ecological Engineering 2016;94:268-74.

El Mrabet I, Benzina M, Valdés H, Zaitan H. Treatment of landfill leachates from Fez City (Morocco) using a sequence of aerobic and fenton processes. Scientific African 2020;8:e00434.

Grynchyshyn N. Properties of the filtrate formed after termination of the operation of the landfill. Bulletin of Lviv State University of Life Safety 2019;19:122-7. (in Ukrainian).

Iurchenko V, Lebedeva E, Brigada E. Environmental safety of the sewage disposal by the sewerage pipelines. Procedia Engineering 2016;134:181-6.

Jagaba AH, Kutty SRM, Lawal IM, Abubakar S, Hassan I, Zubairu I, et al. Sequencing batch reactor technology for landfill leachate treatment: A state-of-the-art review. Journal of Environmental Management 2021;282:Article No. 111946.

Koc-Jurczyk J, Jurczyk Ł. The characteristics of organic compounds in landfill leachate biologically treated under different technological conditions. Journal of Ecological Engineering 2020;21(3):104-11.

Lebron YA, Moreira VR, Brasil YL, Silva AF, de Souza Santos LV, Lange LC, et al. A survey on experiences in leachate treatment: common practices, differences worldwide and future perspectives. Journal of Environmental Management 2021;288:Article No. 112475.

Malovanyy M, Moroz O, Popovich V, Kopiy M, Tymchuk I, Sereda A, et al. The perspective of using the “open biological conveyor” method for purifying landfill filtrates. Environmental Nanotechnology, Monitoring and Management 2021;16:Article No. 100611.

Malovanyy M, Zhuk V, Sliusar V, Sereda A. Two stage treatment of solid waste leachates in aerated lagoons and at municipal wastewater treatment plants. Eastern-European Journal of Enterprise Technologies 2018;1(10):23-30.

Mehmood M, Adetutu E, Nedwell D, Ball AS. In situ microbial treatment of landfill leachate using aerated lagoons. Bioresource Technology 2009;100(10):2741-4.

Melnyk A, Kuklinska K, Wolska L, Namiesnik J. Chemical pollution and toxicity of water samples from stream receiving leachate from controlled municipal solid waste (MSW) landfill. Environmental Research 2014;135:253-61.

Miao L, Yang G, Tao T, Peng Y. Recent advances in nitrogen removal from landfill leachate using biological treatments: A review. Journal of Environmental Management 2019;235:178-85.

Mojiri A, Zhou J, Ratnaweera H, Ohashi A, Ozaki N, Kindaichi T, et al. Treatment of landfill leachate with different techniques: An overview. Water Reuse 2021;11(1):66-96.

Municipal Solid Waste Landfills. Basic Design Points: DBN V.2.4-2-2005. Kyiv, Ukraine: State Committee of Ukraine on Construction and Architecture; 2005. (in Ukrainian).

National Strategy for Waste Management in Ukraine Until 2030. Order of the Cabinet of Ministers of Ukraine dated November 8, 2017 No. 820-p. Kyiv, Ukraine: Cabinet of Ministers of Ukraine [Internet]. 2017 [cited 2022 Aug 15]. Available from: https://zakon.rada.gov.ua/laws/show/820-2017-p. (in Ukrainian).

Odnorih Z, Manko R, Malovanyy M, Soloviy K. Results of surface water quality monitoring of the western bug river Basin in Lviv Region. Journal of Ecological Engineering 2020;21(3):18-26.

Popovych V, Telak J, Telak O, Malovanyy M, Yakovchuk R, Popovych N. Migration of hazardous components of municipal landfill leachates into the environment. Journal of Ecological Engineering 2020;21(1):52-62.

Samoylik M, Molchanova A. Ecological aspects of influence of solid domestic wastes on the environment. Filtrate. Bulletin of Poltava State Agrarian Academy 2017;1-2:88-91. (in Ukrainian).

Shchur I, Lis M, Biletskyi Y. Passivity-based control of water pumping system using BLDC motor drive fed by solar PV array with battery storage system. Energies 2021;14(23):67-84.

Sun H, Peng Y, Shi X. Advanced treatment of landfill leachate using anaerobic-aerobic process: Organic removal by simultaneous denitritation and methanogenesis and nitrogen removal via nitrite. Bioresource Technology 2015;177:337-45.

Taghavi K, Naghipour D, Ashrafi SD, Salehi M. The removal of heavy metals from the leachate of aged landfill: The application of the Fenton process and nanosilica absorbent. Environment and Natural Resources Journal 2021;19(6):427-34.

Tałałaj IA, Bartkowska I, Biedka P. Treatment of young and stabilized landfill leachate by integrated sequencing batch reactor (SBR) and reverse osmosis (RO) process. Environmental Nanotechnology, Monitoring and Management 2021;16:Article No. 100502.

Teng C, Zhou K, Peng C, Chen W. Characterization and treatment of landfill leachate: A review. Water Research 2021;203: Article No. 117525.

Tulaydan Y, Malovanyy M, Kochubei V, Sakalova H. Treatment of high-strength wastewater from ammonium and phosphate ions with the obtaining of struvite. Chemistry and Chemical Technology 2017;11(4):463-8.

Vaverková M, Elbl J, Koda E, Adamcová D, Bilgin A, Lukas V, et al. Chemical composition and hazardous effects of leachate from the active municipal solid waste landfill surrounded by farmlands. Sustainable Chemical Engineering and Technology, Sustainability 2020;12(11):4531-51.

Voytovych I, Malovanyy M, Zhuk V, Mukha O. Facilities and problems of processing organic wastes by family-type biogas plants in Ukraine. Journal of Water and Land Development 2020;45(4-6):185-9.

Wang K, Li L, Tan F, Wu D. Treatment of landfill leachate using activated sludge technology: A review. Archaea 2018;2018: Article No. 1039453.

Wei M, Zhang R, Zhou M, Yuan Z, Yuan H, Zhu N. Treatment of fresh leachate by microaeration pretreatment combined with IC-AO^2 process: Performance and mechanistic insight. Science of the Total Environment 2021;789:Article No. 147939.

Yang Y, Ricoveri A, Demeestere K, Van Hulle S. Advanced treatment of landfill leachate through combined Anammox-based biotreatment, O_3/H_2O_2 oxidation, and activated carbon adsorption: Technical performance, surrogate-based control strategy, and operational cost analysis. Journal of Hazardous Materials 2022;430:Article No. 128481.

Zamri M, Kamaruddin M, Yusoff M, Aziz H, Foo K. Semi-aerobic stabilized landfill leachate treatment by ion exchange resin: Isotherm and kinetic study. Applied Water Science 2017;7(2):581-90.

The Investigation on Mineral Wool Performance as a Potential Filter to Remove TSS in Cikapayang River, East Jawa, Indonesia

Wisnu Prayogo[1*], Januar Parlaungan Siregar[2], Prayatni Soewondo[3], Zulkifli Nasution[4], Zarah Arwieny Hanami[5], M. Faisi Ikhwali[6], Abentin Estim[7], and I Wayan Koko Suryawan[8]

[1]Department of Civil Engineering, Universitas Negeri Medan, Medan, Indonesia
[2]Department of Mechanical Engineering, Universiti Malaysia Pahang, Gambang, Malaysia
[3]Department of Environmental Engineering, Institut Teknologi Bandung, Bandung, Indonesia
[4]Department of Regional Planning, Universitas Sumatera Utara, Medan, Indonesia
[5]Department of Environmental Engineering, Universitas Hasanuddin, Makassar, Indonesia
[6]Department of Environmental Engineering, UIN Ar-Raniry, Banda Aceh, Indonesia
[7]Borneo Marine Research Institute, Universiti Malaysia Sabah, Sabah, Malaysia
[8]Department of Natural Resources and Environmental Studies, National Dong Hwa University, Hualien, Taiwan

ARTICLE INFO

Received: 28 May 2022
Received in revised: 12 Aug 2022
Accepted: 22 Aug 2022
Published online: 5 Oct 2022
DOI: 10.32526/ennrj/21/202200118

Keywords:
On-site treatment/ Total suspended solids/ Supporting material

*** Corresponding author:**
E-mail:
wisnuprayogo@unimed.ac.id

ABSTRACT

Mineral wool has been used as a filter medium that reaches approximately 95% removal efficiency of total suspended solids (TSS) on a laboratory scale. However, there is no research available has been applied on a larger scale. Hence, this study investigated the ability of mineral wool to remove TSS in two separate segments of the Cikapayang River at different seasons. This analysis utilizes a mineral wool type I, with a dimension of 180×30×120 cm placed in segment 2, and a mineral wool type II with a dimension of 325×30×100 cm placed in segment 9. Samples were taken using the grab sampling method to analyze the TSS concentration before and after being filtered by mineral wool. This investigation concluded that mineral wool could reduce the TSS concentration by up to 65%, and the removal capacity increased by about 6.82% during the dry season. The concentration of TSS in the dry season positively correlates with the increase in the removal capacity of the media. Mineral wool of type I in segment 2 had a better removal ability (31.43%) than type II in segment 9 (14.71%). This research shows that mineral wool can be used as a support material in sanitation sites in large cities experiencing quality degradation in their water bodies.

1. INTRODUCTION

Surrounded by the most developed area with the most populous in Indonesia (Pynkyawati et al., 2020), Bandung, Cikapayang River is used to dispose of domestic wastewater. The current condition shows that the amount of pollutants contaminating has exceeded the carrying capacity and cannot be assimilated naturally, especially the TSS as a dominant pollutant, according to Prayogo et al. (2020) and Yacub et al. (2022). The water becomes turbid and filled with mud, especially during the dry season. Domestic wastewater contains TSS with concentrations varying from 77-382 mg/L (Widyarani et al., 2022) depending on the population and its activities. TSS is the concentration of suspended and insoluble material in the river that can be trapped by filter media (Gong et al., 2016; Butler and Ford, 2018). TSS includes various types of material, such as decomposed mud, plants, and animals (Gong et al., 2016). The transfer of TSS in the water flow is a crucial part of the material cycle, especially for carbon and nitrogen (Doxaran et al., 2009). Therefore, the increasing TSS concentration leads to increased pollution. This topic has received significant attention worldwide, such as Citarum River (Marselina et al., 2022), Elemi River (Folorunso, 2018), Nomi River (Miura et al., 2019), Pará River (Carneiro et al., 2020), Hau River (Nguyen et al., 2020), and Nakdong River (Kwon et al., 2021). Many experiments had been carried out in the laboratory simulating TSS removal in water streams. However, it could not be compared to field-scale.

Citation: Prayogo W, Siregar JP, Soewondo P, Nasution Z, Hanami ZA, Ikhwali MF, Estim A, Suryawan IWK. The investigation on mineral wool performance as a potential filter to remove TSS in Cikapayang River, East Jawa, Indonesia. Environ. Nat. Resour. J. 2023;21(1): 9-18. (https://doi.org/10.32526/ennrj/21/202200118)

Mineral wool is a 100% natural and environmentally friendly media derived from volcanic lava that can filter TSS on a laboratory scale (Hao et al., 2019). It has a high adsorption capacity, material surface contact, low density, is easy to set in the river, and the water saturation content was twice as high as other granular media. Aphirta et al. (2020) tested 27 cm^3 mineral wool to determine the capacity of TSS removal on a laboratory scale using the Plug Flow Reactor (PFR) system to simulate the Cikapayang River condition with a volume of 10.78 L. The study resulted in the highest removal of 95%. Based on various existing problems and previous mineral wool studies, they were able to eliminate TSS. So, this study aimed to investigate the ability of mineral wool to remove TSS in a field scale in the Cikapayang River, which is influenced by seasons.

2. METHODOLOGY

2.1 Materials

This study used two types of mineral wool from Drainblock B.V. Netherlands as a filter media (Table 1). These two types have been claimed to increase water quality (Merola, 2018; Aphirta et al., 2020; van Jaarsveld, 2020). They were tested to determine the success rate of each product with different Indonesian surface water conditions compared to the Netherlands and to find the best product that can be applied from both. Mineral wool type I was placed in segment 2, while type II is placed in segment 9 as shown in Figure 1. In its application, the length and depth of the mineral wool was adjusted for each segment and is inserted into a supporting frame made of steel.

Table 1. Two types of the characteristic of mineral wool used in this study

Mineral wool	Type I	Type II
Picture		
Density	80 kg/m^3	120 kg/m^3
Water retention capacity	95%	92%
Hydraulic conductivity	6 mm/s	7 mm/s

2.2 Study area and time

The study was located in Cikapayang River, West Java, Indonesia. It is in a tropical area and has an average annual atmospheric temperature of 22.63°C and rainfall of 189.02 mm (Jaya et al., 2020). As a result of restoration, the Cikapayang River at City Hall Bandung has 12 segments with different lengths, widths, and depths. Each segment is limited by a plunge with a height varying from 15-100 cm. Due to field-scale experiments, segment selection in this study is influenced by many factors such as approval by the government, security considerations, and ease of installation. This collection point serves around 35,000 people and includes some small industrial wastewater. The study was conducted in January-March 2019 (rainy season period), followed by April-August 2019 (dry season period). One period of sampling was conducted consecutively for seven days. River water samples were taken before and after through each mineral wool type using the grab sampling method at 9:00 a.m. to represent the peak of domestic activity.

2.3 Data collection

Water samples were taken manually from the middle at a depth of 50 cm below the water surface using a plastic scoop with a handle (Suriadikusumah et al., 2021). River discharge was measured by determining the water velocity (m^2/s) and multiplying it with the height of the water surface (m). The sample container was a polyethylene-type plastic. Labeled samples in airtight bottles were put into boxes containing ice blocks and transported to the laboratory for storage at 4°C before analysis. River discharge (Q, m^3/s), water temperature (T, °C), and dissolved oxygen (DO, mg/L) were measured in situ. Turbidity (mg/L) and TSS (mg/L) were measured directly after sampling

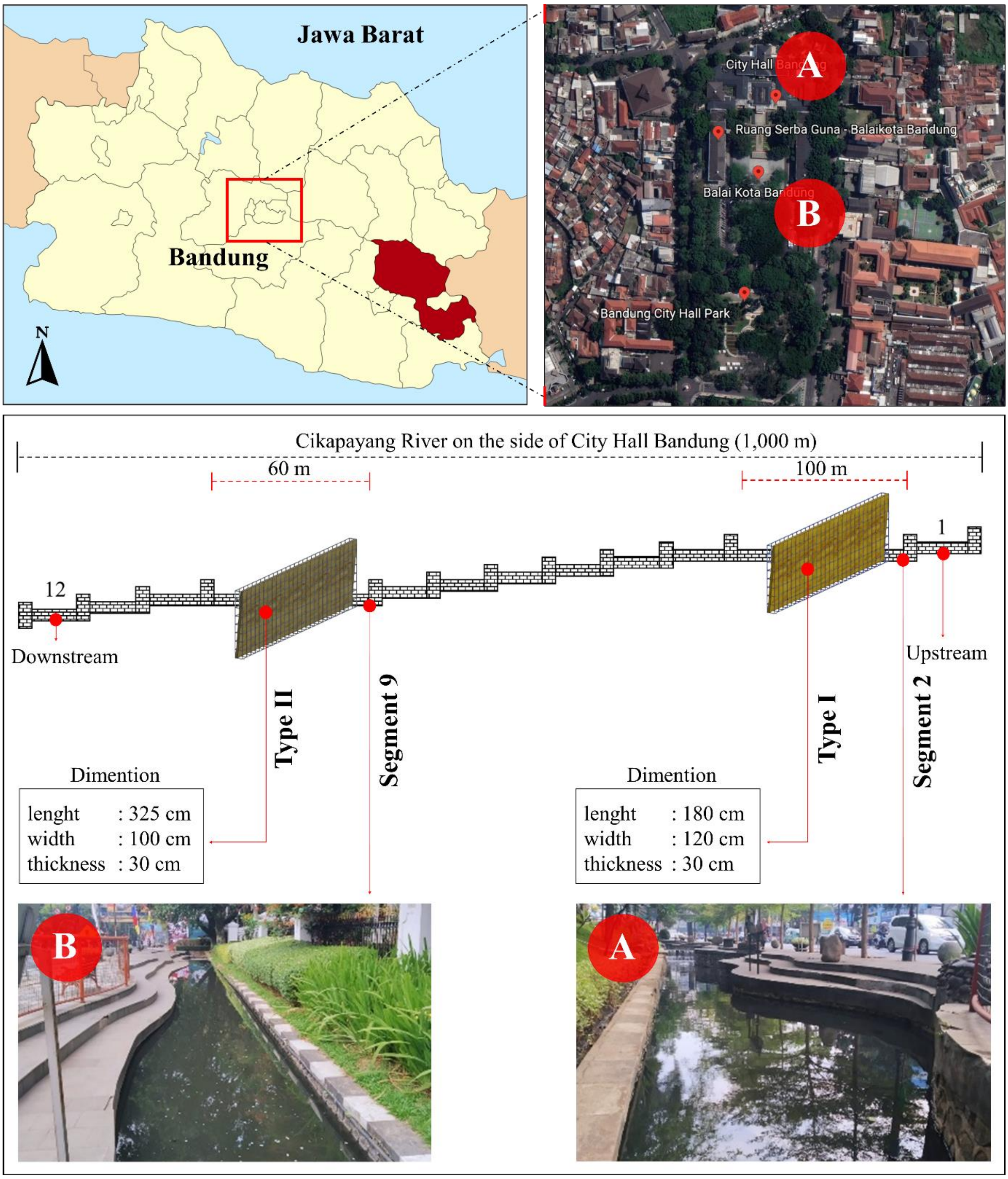

Figure 1. Research location: mineral wool type I at segment 2 (107º36′37.8″E 6º54′37.5″S) and mineral wool type II at segment 9 (107º36′37.3″E 6º54′44″S)

in the laboratory. The temperature was measured using the Water Analyzer Meter EZ-9908, DO using the DO Meter Digital HACH HQ40D, and turbidity using Turbidity Portable Meter WTW 355IR, while TSS used the SMEWW 2540 B method with gravimetric principle. A sample of 250 mL was filtered using Whatman filter paper (no. 42) 2.5 µm pore size with diameter of 125 mm and a vacuum pump. Then, a Memmert Oven UN55 53 L was used to dry the filter and placed in a 90 mm porcelain bowl for 60 min at 105ºC. The bowl was dried in the same oven to get the original weight. TSS concentration was calculated by weighing the solids in a dry bowl. The filter paper depicted the total solids representing the TSS concentration of the water sample (mg/L). Samples were analyzed in duplicate.

2.4 Data analysis

The measurements of TSS were compared with the river water quality standard by Indonesian Government Regulation 81 of 2001, Class II. TSS removal efficiency in Cikapayang River (%) by mineral wool was determined using the Equation (1). Here, RE is the removal efficiency (%), $C_{influent}$ is the initial TSS concentration (mg/L), an $C_{effluent}$ is the TSS concentration after the treatment using mineral wool (mg/L).

$$RE = \left(\frac{C_{influent} - C_{effluent}}{C_{influent}}\right) \times 100\% \qquad (1)$$

Scanning Electron Microscope Energy Dispersive X-Ray (SEM-EDX) was used to identify and characterize materials to observe reactions around interfaces and the elemental composition of mineral wool specimens. The One Way ANOVA is used in this study to test the differences in TSS concentrations in different seasons using the RStudio Cloud software.

3. RESULTS AND DISCUSSION

3.1 River water quality

In this study, Q, T, DO, and turbidity data could identify the TSS concentration affecting aquatic conditions. A total of 19 samples of 10 sampling periods resulted in high concentrations of TSS, which exceeded the standard (50 mg/L). Eighty-nine percent of them were the result of measurements in the dry season. Suspended solids distribution in the Cikapayang River in this season increased by 41%. In comparison, the turbidity in the rainy season ranges from 7-121 mg/L (average of 28 mg/L). The increase in turbidity is the impact of increasing the concentration of TSS from non-natural sources (Hern et al., 2014). The change of seasons causes the water turbidity to increase by 14%. The average water temperature is reduced by 2% during the rainy season. Table 2 presents the range of parameters values and standard deviations of the TSS and other related parameters based on the analysis results on segments 2 and 9 before passing through the mineral wool.

Table 2. Water quality characteristics of Cikapayang River

Parameter	Unit	Standard[a]	Sampling result				Deviation (%)	Annual average
			Rainy season		Dry season			
			Range	Average	Range	Average		
Q	m^3/s	-	0.15-1.56	0.40	0.09-0.67	0.24	15	0.31
T	ºC	25-27	21.12-25.85	24.21	21.98-25.24	23.72	2	23.95
Turbidity	NTU	-	7-121	28	11-150	32	14	27
DO	mg/L	>4	0.5-5.1	2.6	0.1-0.9	0.2	92	2.3
TSS	mg/L	50	7-121	27	10-118	58	41	35

[a]Government of the Republic of Indonesia (2001)

The average DO concentration in the dry season decreased significantly from 2.6 mg/L to only 0.2 mg/L. In other words, DO has declined by 92% compared to the rainy season. Water plants and algae produce oxygen during the daytime photosynthetic process, and this cycle occurs every day, while the oxygen is used for organic matter decomposition by microbial communities. Hence, dead aquatic plants and the increasing amount of pollutants in the water cause a massive reduction of DO (Zhang et al., 2018). Water temperature decrease is significant in June-July, even though this period shows no rain. The average air temperature increased by 4ºC from 21ºC, but the water temperature decreased (0.2-1.5ºC). Shinohara et al. (2021) reveal that surface water temperature is more sensitive to changes in shortwave radiation. Still, this theory does not occur in the Cikapayang River, whose conditions have changed significantly due to input from outside the system. Other factors such as groundwater ingress and heat conduction absorption by the system may affect the surface water temperature. However, in this case, suspended solids that block solar radiation appear to be the main factor responsible for the decrease in surface water temperature. The water temperature decreases significantly when the water discharge shrinks by 15%.

3.2 Effects of seasons and mineral wool types in TSS removal

TSS concentrations in both segments correlated with mineral wool's TSS removal capability in each segment, shown in Figures 2(a) and 2(b). River water quality in the dry season showed a narrower range of parameter values than during the rainy season, but the concentration of pollutants increased. Rainwater entering the river has a conductivity lower than 100 s/cm (Makineci et al., 2015) and is diluted due to mixing with polar ions and molecules so that the TSS concentration measured in the rainy season tends to produce a lower average.

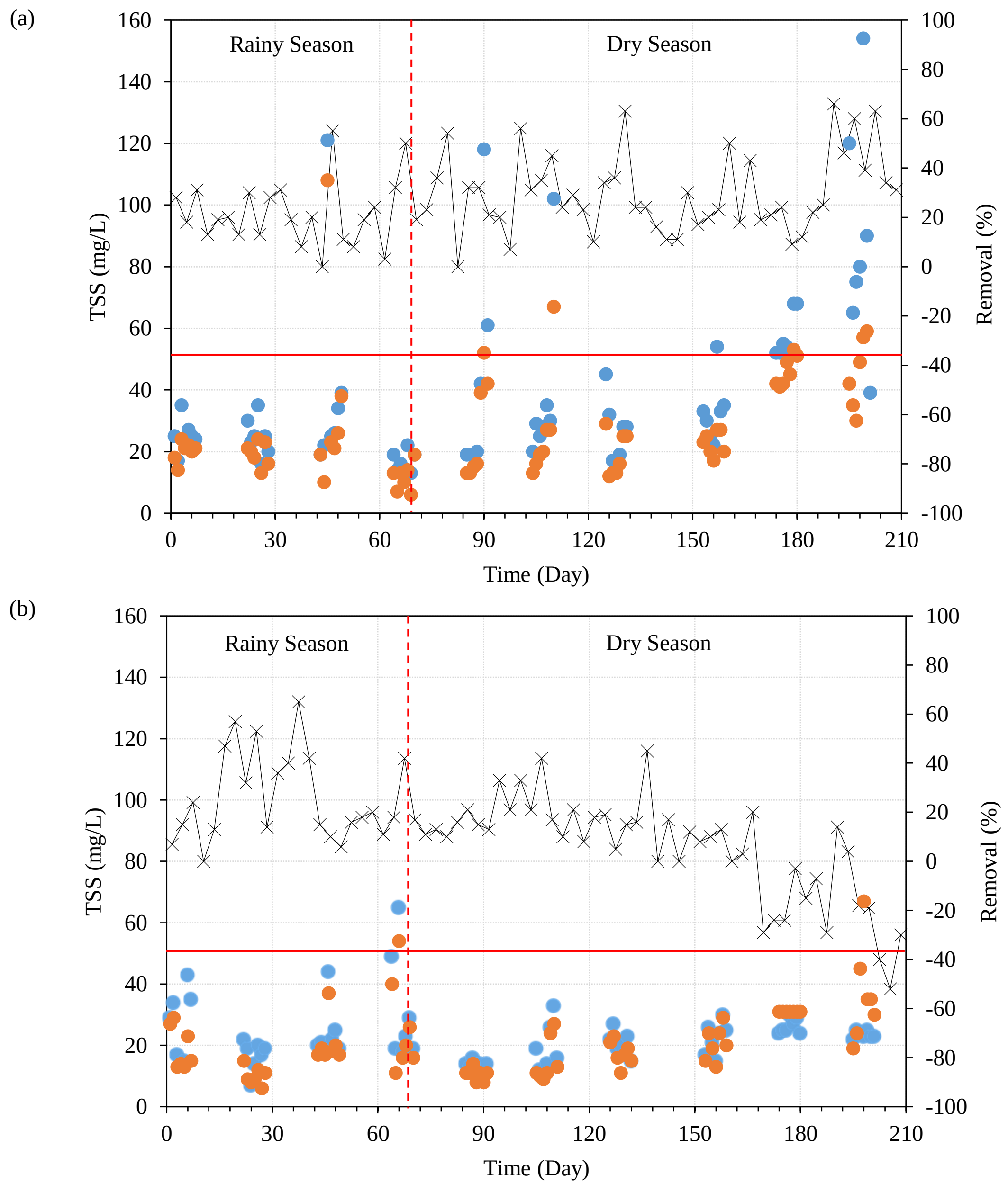

Figure 2. Concentrations of TSS before and after passing mineral wool (a) type I and (b) type II

The average TSS removal efficiency for type I was 31.43% and 14.71% for type II. The best efficiency reached 65% filtered by mineral wool type I. The high concentration of TSS before passing through the media during the dry season caused the removal ability by type I mineral wool in segment 2 to increase by 6.82%. The slowing flow velocity influenced this medium's increase in removal capacity, which caused the contact between suspended solids and the fibers' media to be more optimum. The efficiency of removal by small media in segment 9 was affected by any limiting factors. Suspended solids with a specific gravity higher than the density of water settled and collected on the surface. The solids could then be pulled up during sampling. This then caused the TSS removal ability by type II mineral wool to be lower when compared to type I (Figure 3).

Land-use change in Bandung City causes the terrestrial runoff coefficient on Cikapayang River to have increased from 70.98 mm to 72.04 mm over the last two decades (Atharinafi et al., 2021). As a result, surface terrestrial runoff increased from 48.98 mm in 1999 to 51.8 mm in 2018. Terrestrial runoff permeates into the river, causing the measured water level upstream to increase, while in the downstream (segment 9), the water level tends to be consistent due to the presence of manual discharge control by the presence of bulkheads between segments. The new water flow would run over after reaching the maximum height limit on the insulating wall. The water level in the rainy and dry seasons had a difference of 50 cm in the upstream area. However, the water level in the dry season was mixed with solid particles, so measuring the water volume in segment 2 was complicated. Figure 3 depicts the difference between the minimum, maximum, and average values from two seasons before and after flowing through mineral wool. The concentration of TSS is higher during the dry season, in contrast to Leong et al. (2017), who said that more solids would be found during the rainy season. Based on this fact, domestic wastewater has a more significant influence on TSS concentration in Cikapayang River than the solids contained in the terrestrial runoff. As illustrated in Figure 4, the water velocity significantly affects the media's ability to remove TSS. The river elevation as a restoration result makes this more likely, where the large volume of water creates a downstream push so that the velocity naturally increases. Suspended solids that do not get a strong push by the flow will be held by the media and make it trapped on the surface of the media. In the rainy season, some suspended solids are resuspended due to the impulse by the water velocity that suddenly increases when it rains. It is why the dry season removal efficiency shows higher efficiency.

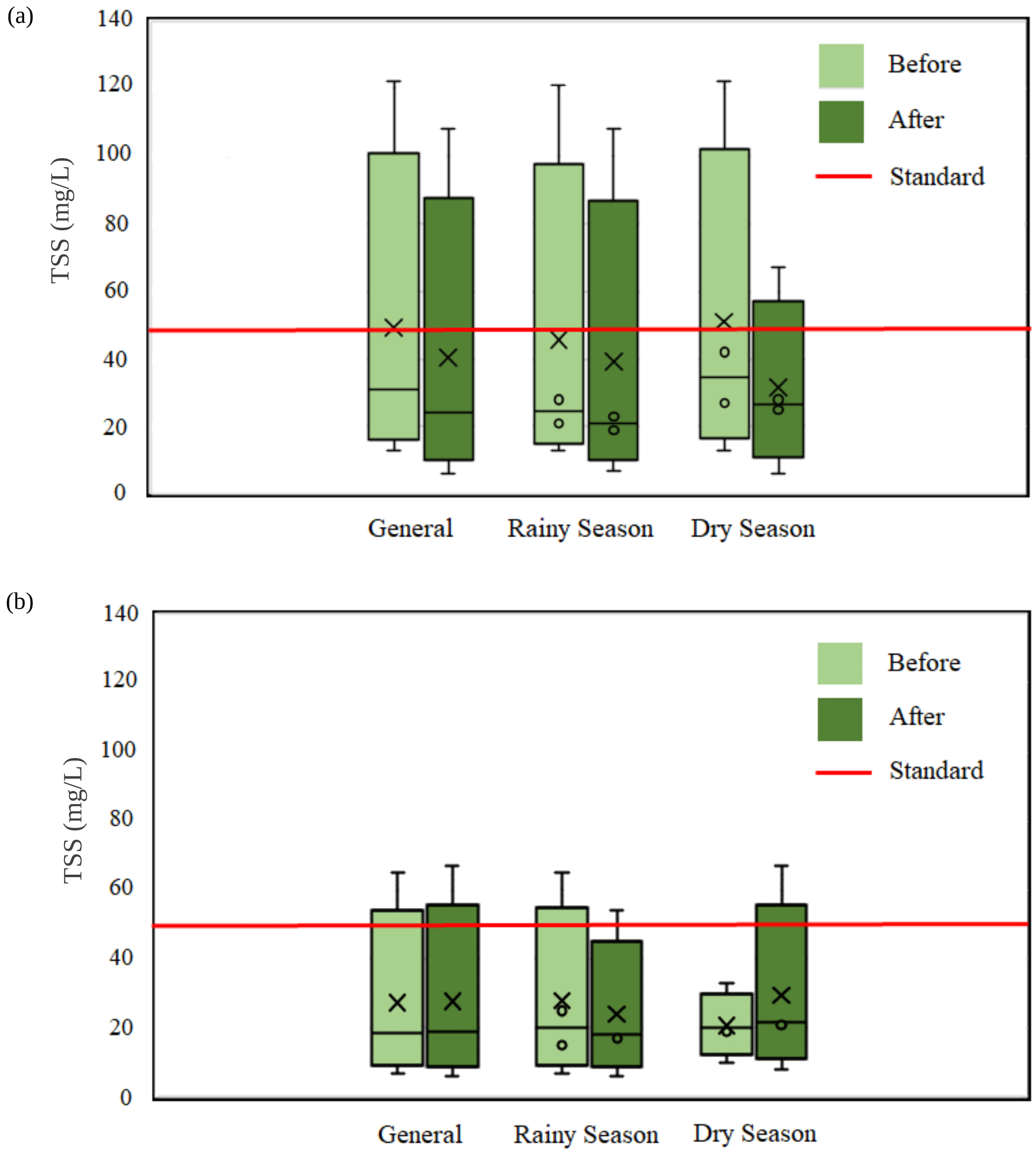

Figure 3. Concentrations of TSS before-after passing mineral wool (a) type I and (b) type II in rainy and dry seasons

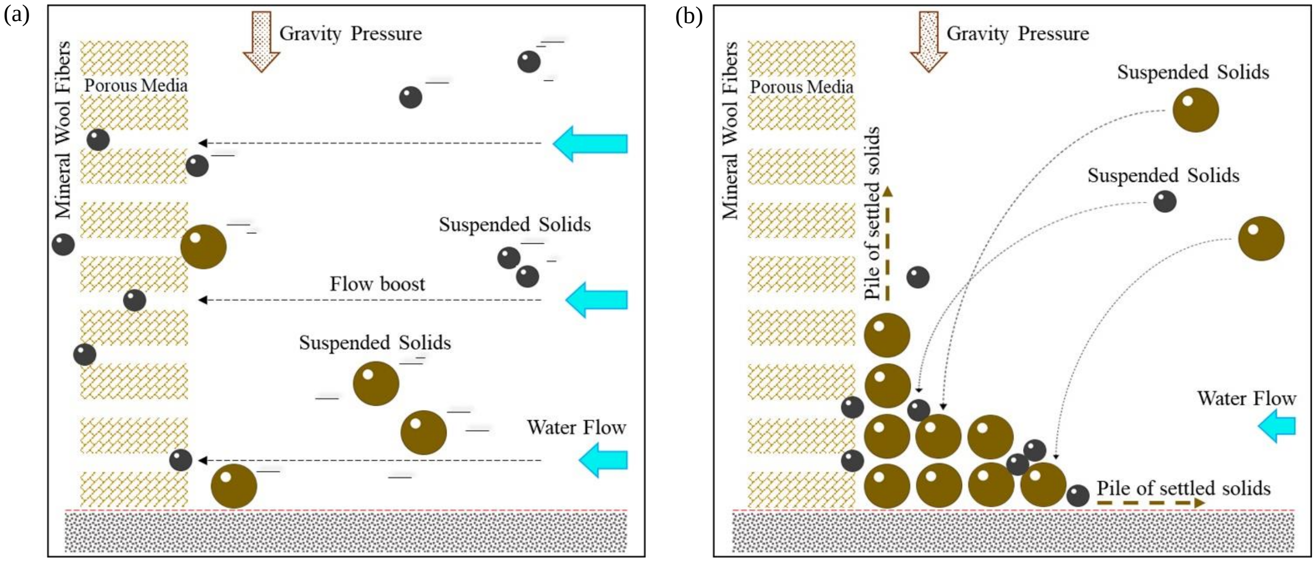

Figure 4. (a) The large volume of the river in the rainy season causes the velocity to increase significantly, and suspended solids resuspension due to a strong push from water flow (b) Slow water flow in the dry season causes suspended solids to accumulate

The ANOVA test results to see the differences in TSS concentrations in different seasons is presented in Table 3. In segment 2, using mineral wool type I, the probability value of F is 0.0000104, where this value is smaller than 0.05. So, it can be concluded that there is a difference in the TSS concentration value in different seasons. However, as for mineral wool type II, the probability value of F obtained is 0.91 (>0.05), which means that it can be concluded that there is no statistical difference between TSS concentrations in different seasons. This is because there is a different pattern in each mineral wool type, as seen in Figure 4, whereas in mineral wool type II, the TSS removal is lower. It the more stable in both seasons because the flow in segment 2 is only affected from upstream. Measured debits are not much different between seasons (only 5%). While segment 2, which is the upstream part of the river, is strongly influenced by fluctuations in various previous flows. The difference in flow rate is very visible, where there is a decrease of 31% during the dry season. Even this value is not the real value because when measuring the water depth, the physical river tends to be filled with piles of mud more than the flow of water.

Table 3. TSS concentrations in different seasons by ANOVA test

Mineral wool	Pr (>F)	Significance level (α)	Conclusion
Type I	0.0000104	0.05	H_0 rejected
Type II	0.921	0.05	H_0 accepted

3.3 SEM-EDX analysis of mineral wool

Two forms of fiber make up mineral wool, namely dangling lacunar and spherical fibers. The spherical shape is formed when the fiber formation is not perfect during production process (Wanko et al., 2016). Based on Figure 5, the morphological spectrum in type I illustrated that the constituent fibers were more systematic than in type II, while the constituent fibers of type II were shorter in size. The more regular and perfect shape caused the gaps between the fibers to widen, allowing more solids in the flow to get caught in the lacunar yarn cavities. SEM analysis showed that the lacunar fiber size in type I had a diameter of 10-20 µm and a spherical shape with a diameter of 75-100 µm. Type II lacunar fibers were 5-15 µm in diameter, while spherical fibers were 80-200 µm in diameter.

The main compounds of mineral wool fibers consist of SiO_2 and Al_2O_3 (Chen et al., 2017). Differences in the chemical composition of the surface of the degraded media correlated with the different TSS removal capabilities between the types. Inorganic elements such as Mg, Al, Si, Ca, and Fe are the main constituents of mineral wool with a total composition of 98%. The high content of Mg, Al, Ca, and Fe from media caused it to be different from other types of wool, such as rock wool, where 59-64% Si is the main constituent element (Yliniemi et al., 2021). The high mineral content makes this type of wool called mineral wool. The TSS analysis showed a correlation between the composition of the media and the removal efficiency, as shown in Figure 6. The high element of carbon (C) in mineral wool type I indicated the optimal ability of the media to remove organic matter. Type I mineral wool that had been set up until the 201st day had an elemental C of 34.81%. The high content of carbon gives an idea of the high level of roughness of the media, thus making the substrate in the water body easily attached due to the large frictional force. Mineral wool type II consisted of 3.61% Mg; 2.84% Al; 10.40% Ca; and 4.86% Fe. The Si content in this type reaches 7.17%, while it is only 5.80% in type I. The results of the SEM EDX test found that the total difference in mineral composition in type I was 13.36% lower than in type II. This phenomenon indicates that the mineral content in the media should give more optimal results. Still, very high solids in the upstream resulted in the removal rate as if the mineral wool type I was better.

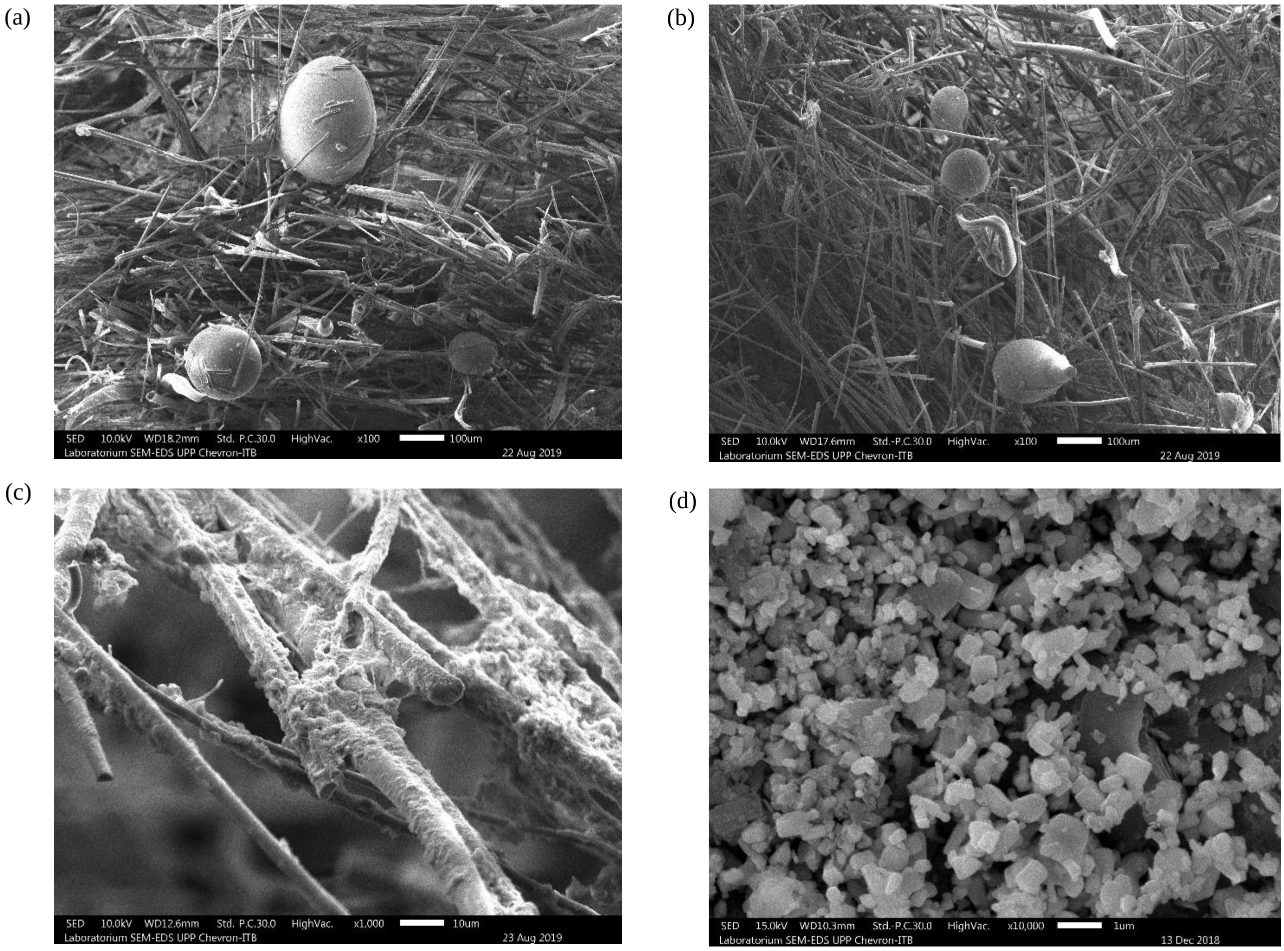

Figure 5. SEM images of mineral wool (a) type I before used, (b) type II before used, (c) after used at 1,000x magnification, and (d) after used at 10,000x magnification

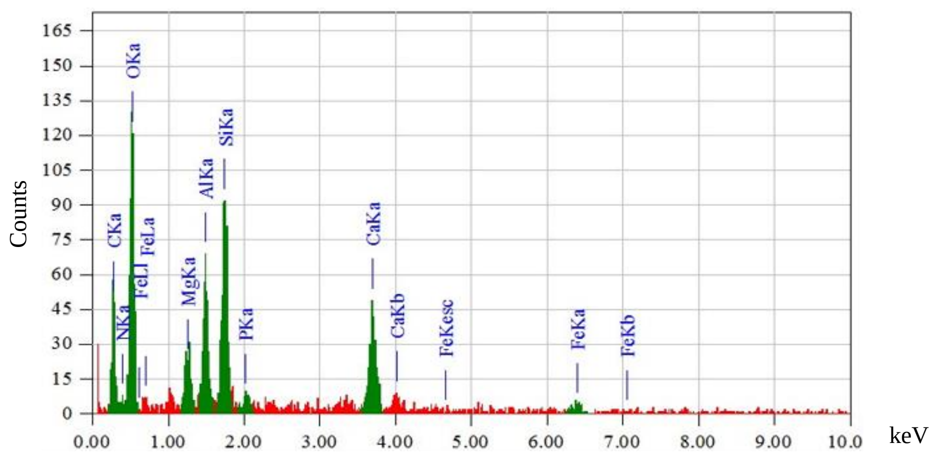

Figure 6. Composition of mineral wool (a) type I and (b) type II, after 201 days

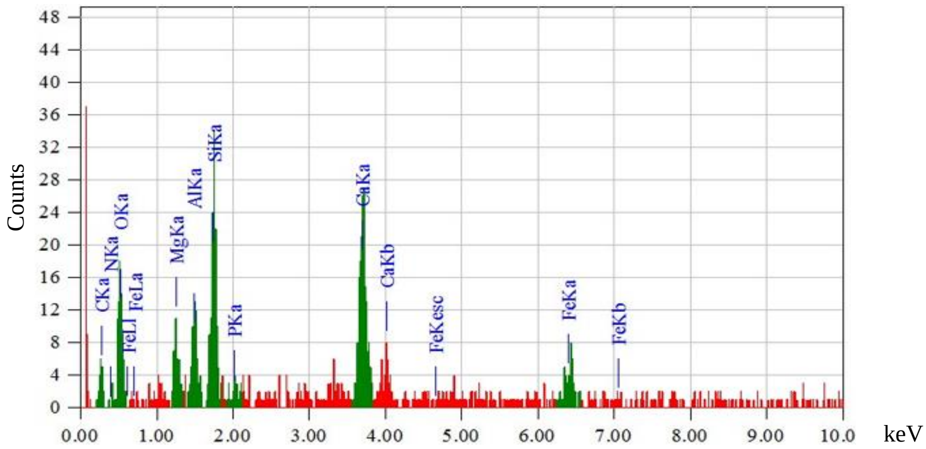

Figure 6. Composition of mineral wool (a) type I and (b) type II, after 201 days (cont.)

4. CONCLUSION

Mineral wool as a filter medium has proven to reduce some TSS concentration in Cikapayang River. The broader surface of the filter media is very relevant for optimal removal of TSS because its surface interacts with suspended solids in the water flow and the number of lacunar fibers that absorb solids increases. The higher mineral concentration as the composition of the constituent elements of each type was positively correlated with the ability of the media to remove TSS material in water bodies. The high concentration of TSS in segment 2 as the upstream of Cikapayang River at City Hall Bandung made it challenging to identify the effect of mineral composition on the media on the TSS removal ability. The environment of the river system between segment 2 and 9, including the difference in TSS concentration in each segment, made it tough to compare the capabilities of the media with each other. However, based on this experiment, mineral wool could be applied as an on-site supporting material to address river pollution in urban areas prone to urbanization due to the lack of domestic wastewater treatment facilities and public awareness. There are quite a lot of studies on mineral wool, but studies in water treatment applications are still very limited. In the future, removal of chemical and biological parameters, kinetics modeling, and economic analyses of the mineral wool use are priorities to analyze the feasibility of this medium comprehensively.

REFERENCES

Aphirta S, Soewondo P, Zakiyya NM, Putri DW, Muntalif BS. The effect of artificial support material existence on removal of organic and nutrient in laboratory scale using plug flow reactor (PFR). E3S Web of Conferences 2020;148:Article No. 01003.

Atharinafi Z, Wijaya N. Land use change and its impacts on surface runoff in rural areas of the upper citarum watershed (case study: Cirasea subwatershed). Journal of Regional and City Planning 2021;32:36-55.

Butler BA, Ford RG. Evaluating relationships between total dissolved solids (TDS) and total suspended solids (TSS) in a mining-influenced watershed. Mine Water and the Environment 2018;37:18-30.

Carneiro AG, Prestes YO, Rollnic M. Estimates of suspended solid transport in the Pará River Estuary. Ocean and Coastal Research 2020;68:1-8.

Chen X, Zhang Y, Huo H, Wu Z. Improving the tensile strength of continuous basalt fiber by mixing basalts. Fibers and Polymers 2017;18:1796-803.

Doxaran D, Froidefond JM, Castaing P, Babin M. Dynamics of the turbidity maximum zone in a macrotidal estuary (the Gironde, France): Observations from field and MODIS satellite data. Estuarine Coastal and Shelf Science 2009;81:321-32.

Folorunso OP. Variations of turbidity (NTU) and suspended solid concentrations (SSC) in Elemi River, Ado-Ekiti, Nigeria. International Journal of Environmental Sciences and Natural Resources 2018;9:63-6.

Gong Y, Liang X, Li X, Li J, Fang X, Song R. Influence of rainfall characteristics on total suspended solids in urban runoff: A case study in Beijing, China. Water 2016;8:Article No. 278.

Government of the Republic of Indonesia. Government Regulation No. 82/2001 on Management of Water Quality and Control over Water Pollution. Jakarta, Indonesia: Government of the Republic of Indonesia; 2001.

Hao W, Xu J, Li R, Zhao X, Qiu L, Yang W. Developing superhydrophobic rock wool for high-viscosity oil/water separation. Chemical Engineering Journal 2019;368:837-46.

Hern TK, Hin LS, Ibrahim S, Sulaiman NMN, Sharifi M, Abe S. Impact of fine sediment on tss and turbidity in retention structure. Journal of Geoscience and Environment Protection 2014;2:1-8.

Jaya IGNM, Ruchjana BN, Abdullah AS, Toharudin T. A relationship between temperature and precipitation over the contiguous Bandung City, Indonesia. Communications in Mathematical Biology and Neuroscience 2020;63:1-14.

Kwon S, Seo IW, Donghae B. Development of suspended solids concentration measurement technique based on multi-spectral satellite imagery in Nakdong River using machine learning model. Journal of Korea Water Resources Association 2021;54:121-33.

Leong JYC, Chong MN, Poh PE, Hermawan A, Talei A. Longitudinal assessment of rainwater quality under tropical climatic conditions in enabling effective rainwater harvesting and reuse schemes. Journal of Cleaner Production 2017; 143:64-75.

Makineci E, Demir M, Kartaloglu M. Acidity (pH) and electrical conductivity changes in terrestrial runoff water from ditches of paved and unpaved forest roads. Baltic Forestry 2015;21: 170-5.

Marselina M, Wibowo F, Mushfiroh A. Water quality index assessment methods for surface water: A case study of the Citarum River in Indonesia. Heliyon 2022;8(7):e09848.

Merola C. Performance of Mineralwool as Filter Medium for the Treatment of Contaminated Drain Water in the Urban Context of Delhi, India [dissertation]. Delft, TU Delft; 2018.

Miura S, Ishikawa T, Yamamoto R. Field study of suspended solid discharge from combined sewerage system of a highly urbanized area: Case study in the watershed of Nomi River in Tokyo. Journal of Japan Society of Hydrology and Water Resources 2019;32:8-22.

Nguyen THD, Phan KD, Nguyen HTT, Tran SN, Tran TG, Tran BL, et al. Total suspended solids distribution in hau river using sentinel 2a satellite imagery. ISPRS Annals of the Photogrammetry, Remote Sensing and Spatial Information Science 2020;6:91-7.

Prayogo W, Soewondo P, Zakiyya NM, Putri DW, Muntalif BS. The removal of organic materials and nutrients with addition of artificial supporting materials in the water body (a case study of Cikapayang River, City Hall Bandung). Proceedings of the 1st International Conference on Urban Design and Planning; 2019 Sep 10; Semarang: Indonesia; 2020.

Pynkyawati T, Yulinda FH, Nurdarajat F, Septiyagi Y. Revitalizing environment order against spatial outside in Cikapayang River Park area. International Journal of Built Environment and Scientific Research 2020;4:11-22.

Shinohara R, Tanaka Y, Kanno A, Matsushige K. Relative impacts of increases of solar radiation and air temperature on the temperature of surface water in a shallow, eutrophic lake. Hydrology Research 2021;52:916-26.

Suriadikusumah A, Mulyani O, Sudirja R, Sofyan ET, Maulana MHR, Mulyono A. Analysis of the water quality at Cipeusing River, Indonesia using the pollution index method. Acta Ecologica Sinica 2021;41:177-82.

van Jaarsveld N. Phosphate Removal from Wastewater by Mineral Wool Filters [dissertation]. Delft, TU Delft; 2020.

Wanko A, Laurent J, Bois P, Mosé R, Wagner-Kocher C, Bahlouli N, et al. Assessment of rock wool as support material for on-site sanitation: Hydrodynamic and mechanical characterization. Environmental Technology 2016;37:369-80.

Widyarani, Wulan DR, Hamidah U, Komarulzaman A, Rosmalina RT, Sintawardani N. Domestic wastewater in Indonesia: Generation, characteristics and treatment. Environmental Science and Pollution Research 2022;29:32397-414.

Yacub M, Prayogo W, Fitria L, Yusrina A, Marhamah F, Fauzan HA. Kajian penggunaan metode IP, STORET, dan CCME WQI dalam menentukan status mutu Sungai Cikapayang, Jawa Barat. Jurnal Teknologi Lingkungan Lahan Basah 2022;10:111-120. (in Indonesian).

Yliniemi J, Ramaswamy R, Luukkonen T, Laitinen O, de Sousa ÁN, Huuhtanen M, et al. Characterization of mineral wool waste chemical composition, organic resin content and fiber dimensions: Aspects for valorization. Waste Management 2021;131:323-30.

Zhang L, Zhang S, Lv X, Qiu Z, Zhang Z, Yan L. Dissolved organic matter release in overlying water and bacterial community shifts in biofilm during the decomposition of *Myriophyllum verticillatum*. Science of the Total Environment 2018;633:929-37.

Determination of Heavy Metal Residues in Tropical Fruits near Industrial Estates in Rayong Province, Thailand: A Risk Assessment Study

Amara Apilux[1], Thitiporn Thongkam[1], Thitaporn Tusai[2], Phasit Petisiwaveth[3], and Sumana Kladsomboon[3*]

[1]*Department of Clinical Chemistry, Faculty of Medical Technology, Mahidol University, Nakhon Pathom 73170, Thailand*
[2]*Community Health Care Service, Faculty of Medical Technology, Mahidol University, Bangkok 10700, Thailand*
[3]*Department of Radiological Technology, Faculty of Medical Technology, Mahidol University, Nakhon Pathom 73170, Thailand*

ARTICLE INFO

Received: 3 Jul 2022
Received in revised: 20 Sep 2022
Accepted: 26 Sep 2022
Published online: 31 Oct 2022
DOI: 10.32526/ennrj/21/202200146

Keywords:
Heavy metals/ Tropical fruits/ Health risk assessment/ Atomic Absorption Spectrometry/ Inductively Coupled Plasma-Mass Spectrometry/ Rayong Province

*** Corresponding author:**
E-mail: sumana.kla@mahidol.edu

ABSTRACT

This study determined the extent of heavy metal contamination of local fruit in Rayong, Thailand, an area where an industrial base is adjacent to agricultural areas. Dietary exposure to agricultural products grown in contaminated areas can cause multiple adverse effects to the human body. In order to avoid such undesirable effects, concentrations of heavy metals [arsenic (As), cadmium (Cd), copper (Cu), mercury (Hg), lead (Pb), and zinc (Zn)] were investigated in popular tropical fruits from three districts of Rayong, namely Wang Chan, Klang and Mueang. The levels of heavy metals were determined by inductively coupled plasma- mass spectrometry (ICP-MS) and cold vapor-atomic absorption spectrometry (CV-AAS). Levels of the six heavy metals in sampled fruits (durian, jackfruit, pineapple, rambutan, long kong, and mangosteen) were in the range of 0.0004-6.7095 mg/kg; 16.7% of fruit samples exceeded maximum permissible limits of Pb. Based on health risk assessments, values of estimated daily intake (EDI) were less than those of maximum tolerable daily intake. However, for non-carcinogenic risks, high hazard index (HI) values were found in some markets while for carcinogenic risks (CRs), CR values of three fruits (durian, jackfruit, and mangosteen) exceeded acceptable levels. Therefore, long-term fruit consumption could impact health of local consumers. These results provided insight into the need for regular monitoring of heavy metal concentrations in potentially contaminated fruits and for prevention of its potential effects.

1. INTRODUCTION

Fruits are rich sources of important nutrients including folate, magnesium, potassium, calcium, and vitamins A and C (Striegel et al., 2018; Wanwimolruk et al., 2015; Swami et al., 2012; Ketsa et al., 2020). Thus, fruit consumption helps to maintain nutritional health and prevent illness (including cancers, and cardiovascular, neurological and gastrointestinal diseases) (Hurst and Hurst, 2012). Due to these benefits, fruits are increasingly recommended for daily consumption by the World Health Organization (FAO/WHO, 2003). But these health benefits may be overwhelmed when the fruits are contaminated.

Heavy metals are widely used in several aspects of agriculture and in a number of industries, and so may be parts of emissions into the environment (soil, water, or air) (Kinuthia et al., 2020; Lorestani et al., 2020; Ojekunle et al., 2022). In general, plants absorb metals essential for growth from cultivated soil, water, and even air. However, plants can also absorb toxic metals from contaminated environments (Lactusu et al., 1996; Big et al., 2012). These metals may not be biodegradable and have long biological half-lives, making them prone to accumulation in fruits and human consumers, potentially leading to adverse health effects (Kim et al., 2015; Dorsey et al., 2004). For example, vomiting, abdominal pain, dehydration,

Citation: Apilux A, Thongkam T, Tusai T, Petisiwaveth P, Kladsomboon S. Determination of heavy metal residues in tropical fruits near Industrial Estates in Rayong Province, Thailand: A risk assessment study. Environ. Nat. Resour. J. 2023;21(1): 19-34. (https://doi.org/10.32526/ennrj/21/202200146)

lung irritation, liver damage, and neurological problems were found to occur with long-term heavy metal consumption (Järup, 2003; Kim et al., 2015; FAO/WHO, 2011). Thus, heavy metal contamination of fruit is an important concern in the maintenance of human health and greater monitoring of heavy metal contamination is needed.

Thailand is a developing country in which expansion of industrial facilities is often in close proximity to agriculture. The number of industrial estates and parks has increased in each province, especially in the central and eastern parts of the country (such as Ayutthaya, Pathumthani, Samut Sakhon, Bangkok, Samut Prakan, Chonburi, Saraburi, and Rayong). Along with this industrialization, contamination of the environment and of agricultural products has been reported repeatedly [For example, in Ayutthaya (Kladsomboon et al., 2020; Klinsawathom et al., 2017), Loei (Pamonpol and Tokhun, 2019), Nakhon Pathom (Choprathumma et al., 2019), Pathumthani (Jankeaw et al., 2015), and Rayong (Kerdthep et al., 2009; Simasuwannarong et al., 2012; Nilkarnjanakul et al., 2022)].

Rayong Province lies in eastern Thailand, adjacent to major economic provinces (Chonburi and Chachoengsao). The Eastern Economic Corridor project (Dunseith, 2018) has transformed Rayong into Thailand's hub for manufacturing, research, and service support to export-oriented industries. However, 65.8% of its total area is still agricultural and many popular tropical fruits (such as durian, mangosteen, jackfruit, mango, pineapple, rambutan, and long kong) are grown mainly in this area (Rayong Provincial Government Center, 2020). As a result of these changes, fruits are often grown near the industrial development zone and are at risk of contamination. Despite these risks, heavy metal contamination in Rayong fruits has not been investigated.

Therefore, this study was designed to investigate possible heavy metal (Cu, Zn, As, Cd, Pb, and Hg) contamination of popular tropical fruits (durian, mangosteen, jackfruit, pineapple, rambutan, and long kong) of Rayong Province. Residue levels of heavy metals found in fruits were compared with permissible limits set by the Ministry of Public Health of Thailand (MoPH), the Food and Agriculture Organization (FAO) of the United Nations, the World Health Organization (WHO) and the European Union (EU). Furthermore, health risk assessment which is an essential tool for evaluating the possible health effects caused by contaminants was evaluated using estimated daily intake (EDI), target hazard quotient (THQ), hazard index (HI), and cancer risk (CR) (Xiao et al., 2017; Radfard et al., 2018). This work describes the methods and results of the study, providing useful information for health management and policy-making for prevention of heavy metal contamination and improved public health.

2. METHODOLOGY

2.1 Sampling

Six Thai fruits were targeted for study: durian (*Durio zibethinus* L.), jackfruit (*Artocarpus heterophyllus* Lam.), mangosteen (*Garcinia mangostana* L.), pineapple (*Ananas comosus* (L.) Merr.), rambutan (*Nephelium lappaceum* L.), and long kong (*Lansium parasiticum* (Osbeck) K.C.Sahni and Bennet). Fresh samples of these fruits were collected from three public markets located in the Rayong Districts of Wang Chan, Klang and Mueang. Market locations where samples were collected: Wang Chan is located at 12°57′35″ North latitude and 101°30′12″ East longitude, Klang is located at 12°46′48″ North latitude and 101°39′5″ East longitude, and Mueang is located at 12°38′46″ North latitude and 101°20′49″ East longitude (Figure 1). In this work, the identity of the three markets were concealed by using the pseudonyms market A, market B, and market C. Based on the sampling methods recommended for the determination of pesticide residues (FAO/WHO, 1999; Ministry of Agriculture and Cooperatives, 2008), fruits were classified using the average weight of each fruit type. Thus, three groups of fruit type were defined as: (1) average weight per fruit less than 25 g, (2) average weight per fruit 25-250 g, and (3) average weight per fruit greater than 250 g. Samples for analysis [one kilogram (or ten fruits) (for Groups 1 and 2); two kilograms (or five fruits) (for Group 3)] of each fruit type were randomly collected from different sellers at each market. All samples were kept in clean, zip-lock polythene bags and transported to the Mahidol University laboratory within 48 h.

2.2 Sample preparation

Samples were washed with deionized distilled water. Then edible parts of the fruits were collected, cut into small pieces, and dried in a hot air oven at 80ºC for 24 h (Islam and Hoque, 2014). These samples were weighed before and after drying. The dried samples were powdered by mortar, collected in polythene screw cap tubes and stored at 4ºC until subsequent digestion.

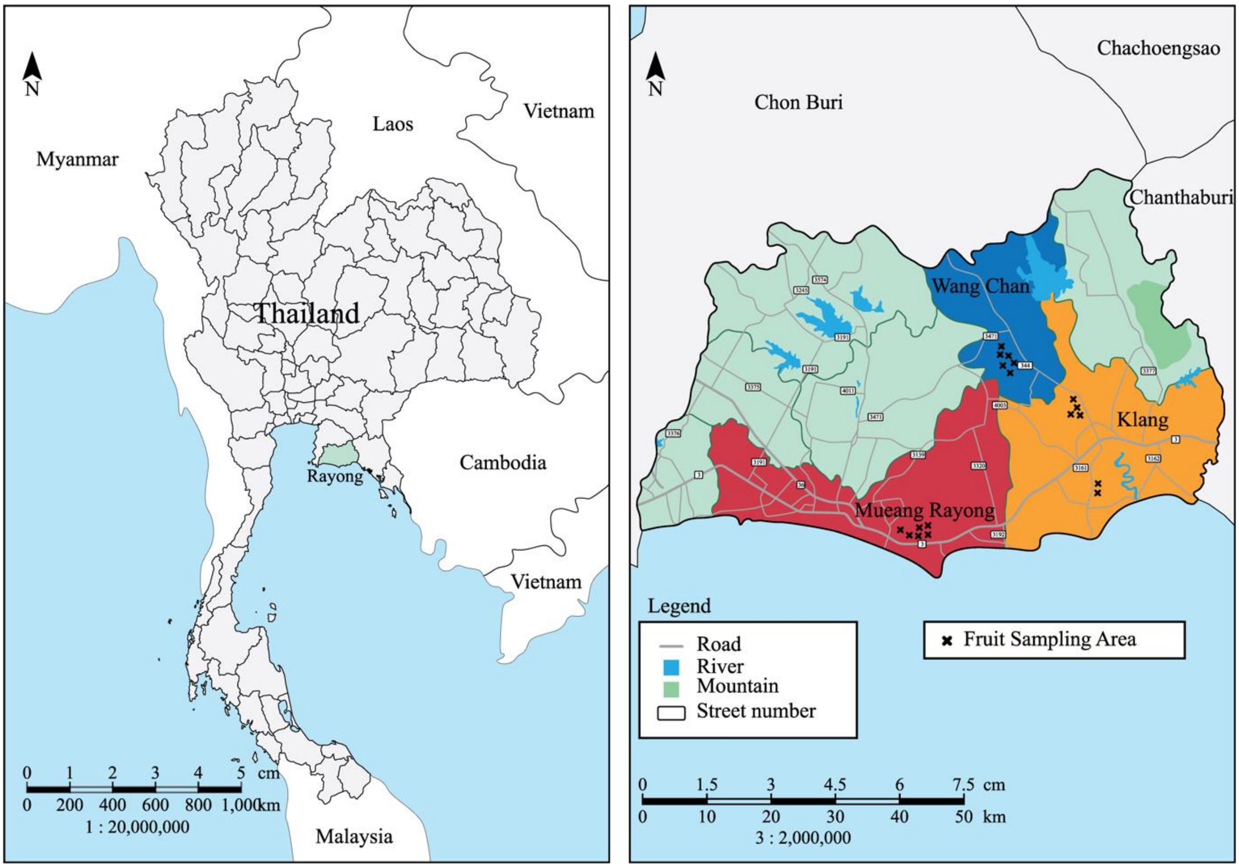

Figure 1. Map showing location of Rayong Province, Thailand (Left), and of study areas within Rayong (Right) where fruits were sampled (in Wang Chan, Klang and Mueang Districts).

2.3 Reagents and materials

Analytical reagents, namely, hydrochloric acid (HCl), nitric acid (HNO_3), hydrogen peroxide (H_2O_2), and stannous chloride ($SnCl_2$) were purchased from Merck (Darmstadt, Germany). A mercury standard (1,000 µg/mL) was purchased from SCP Science (Montreal, QC, Canada), while an ICP multi-element calibration standard of Ag, Al, As, Ba, Be, Bi, Ca, Cd, Co, Cr, Cs, Cu, Fe, Ga, In, K, Li, Mg, Mn, Na, Ni, Pb, Rb, Se, Sr, Ti, U, V, and Zn (10 mg/mL), and internal calibration standard solutions of Bi, Ge, In, Li, Sc, Tb, and Y (10 mg/mL), were purchased from Perkin Elmer (Waltham, MA, USA). Milli-Q water was used to prepare all stock solutions. Nitric acid and hydrogen peroxide were used for digestion of the dried samples. $SnCl_2$ and HCl were the reducing agents for Hg analyses. The calibration curves and quality control analyses for As, Cd, Cu, Pb, and Zn were prepared by multi-element and internal calibration standard solutions, respectively. All standards and sample solutions were diluted with 1% (v/v) nitric acid solution in Milli-Q water before analysis.

2.4 Hg analysis

A cold vapor-atomic absorption spectrophotometer (Flow Injection Mercury Systems 100 and 400; FIMS series; PerkinElmer) was used for Hg analysis. Sample solutions (500 µL each) were prepared in a mixture of 1.1% (v/v) $SnCl_2$ and 3% (v/v) HCl. The prepared samples were pumped through the reactor with the aid of a peristaltic pump. Then, elemental mercury vapor was generated and entered into a quartz cell for analysis of Hg. A Hg standard curve was established by standard Hg solutions at concentrations of 5, 10, and 20 µg/L. To confirm that the CV-AAS system was working accurately, internal quality control of Hg based on standard Hg solutions (2 and 15 µg/L) were run with every 10 samples. The percentage relative standard deviation (%RSD) value was maintained in the range of 10% to verify precision according to previous research that the acceptable values of RSD for the level analyte of 10 µg/L is 32% (González and Herrador, 2007). In case of Hg analysis, maximum absorbance was obtained by adjusting the Cathode lamps at 253.7 nm, then the absorbance value was converted to a concentration of Hg (with units of mg/kg). Finally, concentration values were compared with maximum permissible limits to detect contamination in fruit samples.

2.5 As, Cd, Cu, Pb, and Zn analyses

An inductively coupled plasma-mass spectrometer (NexION 300 ICP-MS) was used for As, Cd, Cu, Pb, and Zn analyses. Based on NexION® Software Reference Guide, version 1.3, for ICP-MS Instrument Control (PerkinElmer, CT, USA) (Bass and Jones, 2010), standard curves were established using multi-element standard solutions at concentrations of 25, 50, 75, and 100 µg/L. The internal standard solution contained 10 mg/L of Bi, Ge, In, Sc, Li, Tb, and Y. Standards and digested sample solutions were prepared in 1% (v/v) HNO_3. The optimized conditions for As, Cd, Cu, Pb, and Zn analyses were 1.05 L/min of nebulizer gas flow, 1.35 L/min of auxiliary gas flow, 18 L/min of plasma gas flow, and 1,600 W of radio-frequency (RF) in an ICP system. The readings were taken from the equipment as µg/L and then the results were converted to mg/kg (the actual concentration of heavy metal in a sample) using Equation (1).

$$C_i = 0.1 \times A \times \frac{W_D}{W_W} \quad (1)$$

Where; C_i is the concentration of heavy metal in a sample (mg/kg). A is the concentration of the heavy metal in digested solution (µg/L). W_D is dry weight of the sample (g) and W_w is its wet weight (g). Similar to Hg measurements, concentrations were compared with the appropriate maximum permissible limits.

2.6 Validation and quality control

For validation of the quantitative analyses of heavy metals in fruit samples and their aqueous extracts, evaluation of multiple parameters was performed. The limit of detection (LOD) and limit of quantification (LOQ) were obtained using blank samples (for ICP-MS) and a calibration approach (for CV-AAS) (Wenzl et al., 2016). Moreover, linear range, accuracy, repeatability, and reproducibility (precision) were investigated. To monitor reliability of the results, internal quality control was conducted every 10 samples. Average recoveries were determined for the different heavy metals. In addition, appropriate quality assurance procedures and precautions were taken and all samples were handled carefully to avoid cross-contamination.

2.7 Statistical data analysis

Statistical analyses were performed using SPSS Statistical Package, version 18 (SPSS, Chicago, IL, USA) to assess the influence of sources of variance (fruit type and location) on each heavy metal. Data from each heavy metal in the six fruit types from the three different local markets were included. Descriptive statistics and one-way ANOVA tests were performed. Post hoc comparisons using Tukey HSD test were used to determine differences among the heavy metal concentrations and fruit types. Statistical significance was defined at the 95% confidence level ($^*p < 0.05$).

2.8 Health risk assessment

In this study, to assess the human health risks for non-carcinogenic and carcinogenic metals associated with fruit consumption, four approaches were used: (1) estimated daily intake (µg/kg bw/day), (2) target hazard quotient, (3) non-carcinogenic hazard index or total target hazard quotient, and (4) carcinogenic risk.

2.8.1 Estimated daily intake

The estimated daily intake (EDI) of heavy metals was calculated as follows:

$$EDI = \frac{C_i \times F_{IR}}{W_{AB}} \quad (2)$$

Where; C_i is the concentration of a heavy metal in fruit (mg/kg), F_{IR} is the average daily ingestion rate (g/day) of fruit, and W_{AB} is average body weight (kg). Based on the Thailand National Health Examination Survey (Satheannoppakao et al., 2009), the average daily consumption of durian and jackfruit is 116.8 g/person/day. Based on WHO data, the average daily consumption of pineapple is 9.75 g/person/day, and the average daily consumption of stone fruits (such as mangosteen, rambutan, and long kong) is 7.3 g/person/day (WHO, 2003). Average body weights in the Thai population are 68.5±12.1 kg for males and 54.5±9.8 for females (Lim et al., 2009).

2.8.2 Tolerable daily intake

Tolerable daily intake (TDI) or provisional tolerable daily intake (PTDI) are estimates of the amount of a substance in food that can be taken daily over a lifetime without significant risk to health

(Hashemi et al., 2019). The EDI values in the present study were compared with TDI or PTDI for each heavy metal. Table 1 shows the current provisional tolerable weekly intake (PTWI) or provisional tolerable monthly intake (PTMI) values for Cd, Cu, Hg, Pb, and Zn, and the lower limit of the benchmark dose ($BDML_{0.5}$) value for As based on the Codex Alimentarius (FAO/WHO, 2018) and the calculated TDI values based on PTWI, PTMI, or $BDML_{0.5}$.

Table 1. Provisional tolerable weekly/monthly intake (PTWI /PTMI) and calculated TDI based on the PTWI/PTMI (FAO/WHO, 2018; Mohamed et al., 2019; Bamuwamye et al., 2015)

Heavy metal	PTWI or PTMI (mg/kg bw)	TDI value (mg/kg bw)
As	NA	0.003[a,b]
Cd	0.025 (PTMI)	0.00083[b]
Cu	3.5 (PTWI)	0.5[c]
Hg	0.0016 (PTWI)	0.00023[b]
Pb	NA	NA[b]
Zn	7 (PTWI)	1[c]

NA: not applicable; [a]Based on Joint FAO/WHO Expert Committee on Food Additives (JECFA) (FAO/WHO, 2018); [b]Based on Codex Alimentarius International Food Standard (FAO/WHO, 2019); [c]Based on Joint FAO/WHO Expert Committee on Food Additives (JECFA) (FAO/WHO, 1982)

2.8.3 Target hazard quotient

Target hazard quotient (THQ) is a complex parameter derived from the ratio between the reference dose (R_{FD}) and estimated dose of a contaminant, to estimate the potential health risk associated with chronic exposure to that contaminant. It is calculated as follows (Ogwok et al., 2014):

$$\mathrm{THQ} = \left(\frac{(E_F \times E_D \times F_{IR} \times C)}{(R_{FD} \times W_{AB} \times T_A)}\right) \times 10^{-3} \qquad (3)$$

Where; E_F is the frequency of exposure from consumption of heavy metal contaminated fruits (365 days/year), E_D is the duration of human exposure or the average lifetime of humans (71.8 years for males and 78.6 years for females) (Institute for Population and Social Research, 2016), F_{IR} is the average daily ingestion rate (g/day) of fruit, C is the concentration of a heavy metal in fruits (mg/kg), R_{FD} is the oral reference dose (mg/kg/day) which indicates the daily exposure to which humans can be exposed continually over a lifetime without appreciable risk of deleterious effects, R_{FD} (based on USEPA and CalEPA) for As, Cd, Cu, Hg, Pb, and Zn are 3.0×10^{-4} (IRIS, 2022), 1.0×10^{-3} (IRIS, 2022; Harmanescu et al., 2011), 4.0×10^{-2} (Ogwok et al., 2014; Harmanescu et al., 2011), 1.6×10^{-4} (Zeng et al., 2015), 3.5×10^{-3} (Harmanescu et al., 2011), and 0.3 (IRIS, 2022; Harmanescu et al., 2011) mg/kg/day, respectively, W_{AB} is average body weight which for Thais is 68.5±12.1 kg for males and 54.5±9.8 for females (Lim et al., 2009), T_A is the average time of human exposure to non-carcinogens (365 days/year × 70 years), and 10^{-3} is the unit conversion factor. In case of THQ<1, adverse effects are unlikely to occur; whereas, if THQ≥1, there is a high risk that the toxin induces adverse effects over a lifetime of exposure (Song et al., 2009; Zeng et al., 2015).

2.8.4 Non-carcinogenic hazard index or total target hazard quotient (TTHQ)

The hazard index (HI) was calculated for multiple heavy metals to estimate the total potential non-carcinogenic health impact on the human body caused by the combined exposure to them (Mohammadi et al., 2019). The HI is determined as the sum of all THQs calculated for individual heavy metals using Equation (4):

$$\text{Total THQ (HI)} = \sum_{k=1}^{n} \begin{matrix} \mathrm{THQ} = \mathrm{THQ}_{As} + \mathrm{THQ}_{Cd} + \mathrm{THQ}_{Cu} \\ + \mathrm{THQ}_{Hg} + \mathrm{THQ}_{Pb} + \mathrm{THQ}_{Zn} \end{matrix} \qquad (4)$$

When; HI<1, chronic risks are unlikely; whereas when HI≥1, chronic non-carcinogenic risks are likely (Cao et al., 2015).

2.8.5 Carcinogenic risk

The carcinogenic risk (CR) is calculated as an estimation of the incremental probability of an individual developing cancer as a result of exposure to a potential carcinogen. According to the International Agency for Research on Cancer, As and Cd are categorized in Group 1 carcinogens: chemicals which are definite human carcinogens; Pb is categorized in Group 2B: chemicals which are possible human carcinogens. CR, defined as the risk generated by a lifetime of average exposure to carcinogenic chemicals (Zeng et al., 2015), is calculated using the cancer slope factor (CSF). In the present study, the CR values due to As, Cd, and Pb were each calculated using Equation (5):

$$\mathrm{CR} = \left[\frac{E_F \times E_D \times F_{IR} \times C \times CSF}{W_{AB} \times T_A}\right] \qquad (5)$$

Where; E_F is the frequency of exposure from consumption of heavy metal-contaminated fruits (365-day/year), E_D is the duration of exposure or the average lifetime of humans, F_{IR} is the average daily ingestion rate (kg/day) of fruit, C is the concentration of heavy metals in fruits (mg/kg), CSF is the cancer slope factor which is provided by IRIS and CALEPA [1.50 mg/kg/day for As (Hashemi et al., 2019; IRIS, 2022); 15 mg/kg/day for Cd (Zeng et al., 2015); 0.0085 mg/kg/day for Pb (Hashemi et al., 2019)], W_{AB} is average body weight, for adult Thais, this is 68.5±12.1 kg for males and 54.5±9.8 for females (Lim et al., 2009), and T_A is the average time of human exposure to non-carcinogens (365 days/year × 70 years).

When multiple carcinogenic elements were present, the total carcinogenic risk (CR_{Total}) (Zeng et al., 2015) was described using Equation (6):

$$CR_{Total} = \sum CR \tag{6}$$

Where; CR is the carcinogenic risk associated with each heavy metal.

Based on the USEPA, a CR value of 1×10^{-6} is considered the point of excess carcinogenic risk. This value indicates a probability of 1/1,000,000 for an individual to develop cancer (based on g/day for 70 years). For each heavy metal, a CR value less than 1×10^{-6} is considered insignificant and cancer risk can be neglected; a CR value above 1×10^{-4} is considered as significant and that there is a cancer risk. CR_{Total} values of 1.0×10^{-6} to 1.0×10^{-4} are considered acceptable (Cao et al., 2015); we chose a CR_{Total} of 1.0×10^{-5} as the cut-off of acceptable levels as did by Mohammadi et al. (2019).

3. RESULTS AND DISCUSSION

In this study, levels of As, Cd, Cu, Pb, and Zn were determined by ICP-MS, and of Hg by CV-AAS. The analytical performance of these methods was investigated and the results are shown in Table 2. A calibration curve was established for each heavy metal (data not shown). Plots of intensity and absorbance against spiked standards were linear and in the range of 0.01-100 µg/L and 0.001-0.040 mg/kg for ICP-MS and CV-AAS, respectively. Established calibration curves had correlation coefficients of 0.9979-0.9997. Limits of detection and quantification were 0.001-0.440 and 0.005-0.500 mg/kg, respectively. The recovery of different heavy metals was within the range of 70-120%, with %RSD ≤ 20% consistent with SANTE/11813/2017 documentation (European Commission, 2017).

3.1 Heavy metal concentrations

Concentrations of heavy metals contaminating the fruits collected from three markets in Rayong, namely market A, market B, and market C, are presented in Table 3. The metals varied in concentration among the different fruits. A high content of essential micronutrients (Cu and Zn) was found, ranging from 0.2926 to 6.7095 mg/kg. Concentrations of toxic metals (As, Cd, Hg, and Pb) ranged from 0.0004 to 0.4625 mg/kg. Additionally, the concentrations of individual heavy metals were investigated. The order of metal concentrations was: for As, jackfruit > durian > mangosteen > long kong > pineapple > rambutan; for Cd, mongosteen > jackfruit > durian > rambutan > long kong > pineapple; for Cu, jackfruit > durian > rambutan > mangosteen > long kong > pineapple; for Hg, jackfruit > durian > pineapple > mangosteen/rambutan > long kong; for Pb, long kong > jackfruit > durian > rambutan > pineapple > mangosteen; for Zn, jackfruit > durian > rambutan > long kong > mangosteen > pineapple.

The level of Pb in 16.7% of fruit samples exceeded the permissible level of contamination (0.1 mg/kg) [durian in market B (0.1427±0.0635 mg/kg), jackfruit in market B (0.2949±0.0763 mg/kg), and long kong in market A (0.4625±0.0604 mg/kg)]. Based on these results, consumption of fruits collected in these areas should raise concern for Pb contamination. Its presence might be due to phosphate fertilizer application as described in reports from Cakmak et al. (2010) and Satachon et al. (2019), or derived from the heavy metal-related industries which contribute to cultivated area contamination (via soil and water) (Kumar et al., 2020). Several studies on heavy metal contamination have been reported from Thai provinces where many industrial estates are located, for example Pathumthani and Ayutthaya Provinces (Jankeaw et al., 2015; Kladsomboon et al., 2020). Given the lead results from this study in Rayong, concentrations should be periodically monitored and actions taken to prevent potential harm. Moreover, more in-depth studies should be conducted to inform future public health strategies.

Cadmium was also found in fruit samples collected in this study. Although the concentrations of Cd did not exceed permissible limits, accumulation of Cd is an important issue and needs to be monitored due to its carcinogenic potential. There are updates of

Table 2. Coefficient of determination (R^2), calibration range, %recovery, relative standard deviations (%RSD), LOD, and LOQ of ICP-MS and CV-AAS in analyses of fruit samples

Heavy metals	R^2 value	Calibration range (µg/L)	Calibration range (mg/kg)	%Recovery (Mean±SD)	%RSD	LOD (mg/kg)	LOQ (mg/kg)
As*	0.9992	0.55-100	0.055-10	106.00±0.34	3.2020	0.055	0.010
Cd*	0.9986	0.01-100	0.001-10	104.70±0.69	6.6186	0.001	0.010
Cu*	0.9996	4.40-100	0.440-10	99.97±0.04	0.3530	0.440	0.500
Hg**	0.9997	0.01-0.40	0.001-0.04	93.5000±0.0007	3.7813	0.001	0.005
Pb*	0.9993	0.01-100	0.001-10	106.55±0.16	1.5264	0.001	0.010
Zn*	0.9979	2.40-100	0.240-10	106.50±0.13	1.1951	0.240	0.270

* measured by ICP-MS; ** measured by CV-AAS

guidelines for soil Cd concentration (Six and Smolders, 2014) aimed to avoid net Cd accumulation (Smolders and Six, 2013). Based on our results, Cd concentrations in fruits were low enough for safe consumption.

Arsenic and mercury were found in small amounts in sampled fruits. As and Hg contamination of fruits may occur through the absorption of these heavy metals after pesticide application and contamination of cultivated areas as described by Li et al. (2016). For example, As-containing pesticides (with lead arsenate, copper arsenate and calcium arsenate) were extensively used on some fruits to control cattle ticks and pests, leading to accumulation in plant tissue (Madejón et al., 2006). Hg is a toxic metal which has effects on the nervous, digestive and kidney systems. It is considered by WHO as one of the top ten chemicals of major public health concern (WHO, 2020). Similar to the sources of Pb contamination, Hg often enters the environment via pesticide application and emission from heavy metal-related industries (Turull et al., 2018; Li et al., 2017). A report from Ecological Alert and Recovery-Thailand (EARTH) warned of Hg contamination in industrial sites in Rayong Province (EARTH, 2016) and its spread to farmland and orchards with potential contamination of fruits. However, concentrations of mercury in our study samples were below the maximum permissible limit from the Ministry of Public Health, Thailand, suggesting that fruit from this study area are safe for consumption.

Copper and zinc are essential micronutrients for plant growth, participating in several processes including photosynthetic electron transport, cell wall and nitrogen metabolism, and protein regulation (Shabbir et al., 2020; Liščáková et al., 2022). However, in agriculture, Cu is also considered an antifungal agent usually used as copper sulphate and copper oxychloride. Extensive application of this agent can lead to Cu release into the environment (Seeda et al., 2020). In this study, results demonstrated that all fruit samples were rich in Cu and Zn, especially the jackfruit and durian. However, the concentrations of Cu and Zn were less than the permissible limits and the fruits considered safe for consumption.

According to the statistical plan, one-way analysis of variance was used to compare heavy metal (As, Cd, Cu, Hg, Pb, and Zn) residues in the fruits collected in each location (market A, B, and C).

Table 3. Mean concentrations (mg/kg)±S.D. of heavy metals in Rayong fruits and their maximum permissible limits

Samples	Market	As	Cd	Cu	Hg	Pb	Zn
Durian	A	0.0183±0.0009	0.0078±0.0016	0.9276±0.0470	0.0026±0.0003	0.0944±0.0023	2.1634±0.2499
	B	0.0049±0.0000	0.0112±0.0002	2.2244±0.0238	0.0045±0.0009	0.1427±0.0635	2.0812±0.0596
	C	0.0177±0.0016	0.0062±0.0002	1.7258±0.1296	0.0058±0.0006	0.0611±0.0053	2.5706±0.2659
Jackfruit	A	0.0038±0.0001	0.0060±0.0003	2.4548±0.0364	0.0046±0.0002	0.0869±0.0179	1.8466±0.0024
	B	0.0241±0.0013	0.0274±0.0046	5.5860±0.0043	0.0144±0.0042	0.2949±0.0763	6.7095±1.3070
	C	0.0142±0.0007	0.0035±0.0003	1.9873±0.0914	0.0013±0.0001	0.0213±0.0021	1.3915±0.1091
Mangosteen	A	0.0102±0.0010	0.0073±0.0007	1.2953±0.2125	0.0023±0.0001	0.0096±0.0002	0.7796±0.0436
	B	0.0016±0.0001	0.0119±0.0000	0.9383±0.0361	0.0023±0.0001	0.0333±0.0086	0.9097±0.0111
	C	0.0043±0.0003	0.0192±0.0021	0.5860±0.0520	0.0020±0.0001	0.0078±0.0004	0.7260±0.0735
Pineapple	A	0.0045±0.0004	0.0005±0.0001	0.6374±0.0100	0.0024±0.0001	0.0273±0.0078	0.7659±0.0265
	B	0.0023±0.0002	0.0004±0.0000	0.2926±0.0036	0.0020±0.0002	0.0113±0.0007	0.3325±0.0044
	C	0.0041±0.0012	0.0011±0.0001	0.5043±0.1894	0.0026±0.0001	0.0173±0.0051	0.9092±0.2915
Rambutan	A	0.0036±0.0020	0.0033±0.0006	1.2471±0.1288	0.0029±0.0003	0.0289±0.0024	2.2017±0.2091
	B	0.0019±0.0001	0.0026±0.0002	1.0895±0.0910	0.0014±0.0010	0.0272±0.0032	1.3416±0.0877
	C	0.0037±0.0005	0.0033±0.0013	0.8838±0.1167	0.0023±0.0003	0.0566±0.0608	1.1674±0.1796
Long kong	A	0.0046±0.0004	0.0014±0.0001	1.5142±0.2333	0.0008±0.0002	0.4625±0.0604	1.2572±0.1891
	B	0.0035±0.0001	0.0019±0.0000	0.6639±0.0373	0.0010±0.0001	0.0097±0.0002	1.0441±0.0514
	C	0.0036±0.0001	0.0021±0.0003	0.4628±0.0165	0.0020±0.0004	0.0188±0.0019	0.9153±0.0069
Maximum permissible limits (mg/kg)		2[a]	0.05[a,b]	20[c]	0.02[a]	0.1[a,b]	99.4[d]

[a]Based on Standard for Contaminants in Food (MoPH, 2020).
[b]Based on Codex Alimentarius International Food Standard (FAO/WHO, 2019).
[c]Based on EU Pesticides database (EU, 2022).
[d]Based on Joint FAO/WHO Joint Expert Committee on Food Additives (JECFA) (FAO/WHO, 1996; Mensah et al., 2009).

The analyses revealed that there were no statistically significant differences of the As [F(2.33=0.167), p=0.847], Cd [F(2.33=1.341), p=0.276], Cu [F(2.33=1.272), p=0.294], Hg [F(2.33=1.203), p=0.313], Pb [F(2.33=1.748), p=0.190], nor Zn [F(2.33=1.000), p=0.379] levels among locations at the 95% confidence level. However, concentrations of metals were significantly different with regard to type of fruit. Significant differences of As [F(5.30=6.721), p^*=0.000], Cd [F(5.30=5.863), p^*=0.001], Cu [F(5.30=9.825), p^*=0.000], Hg [F(5.30=3.112), p^*=0.022], and Zn [F(5.30=4.787), p^*=0.002] were found, while differences of Pb [F(5.30=1.903), p=0.123] were not significant.

To determine the source of differences, post hoc tests were used to discriminate and explain heavy metal concentrations among the six fruit types (comparing each to the other five fruit types for each heavy metal). The analyses revealed statistically significant differences among the heavy metal concentrations. In detail, there were statistically significant differences among seven pairs (durian and pineapple, durian and rambutan, durian and long kong, jackfruit and pineapple, jackfruit and rambutan, jackfruit and long kong, jackfruit and mangosteen) for As, five pairs (jackfruit and pineapple, jackfruit and long kong, pineapple and mangosteen, rambutan and mangosteen, long kong and mangosteen) for Cd, five pairs (durian and jackfruit, jackfruit and pineapple, jackfruit and rambutan, jackfruit and long kong, jackfruit and mangosteen) for Cu, one pair (jackfruit and long kong) for Hg, and three pairs (jackfruit and pineapple, jackfruit and long kong, jackfruit and mangosteen) for Zn.

However, the different concentrations of detected metals in each fruit type might be due to differing causes, such as physiology of the fruits, status of heavy metal contamination, proximity to industrial areas, type of industrial activity, agricultural activities (for example, fertilizer application), transportation, sample storage and preparation for assay (Taiwo et al., 2022; Ghasemidehkordi et al., 2018).

Given the results of this study, long- term consumption of some fruit posed the potential for adverse health effects. Therefore, health risk assessments were carried out in this study area.

3.2 Risk assessments of heavy metals

To assess the human health risks from both non-carcinogenic and carcinogenic metals associated with fruit consumption, four approaches were utilized: (1) estimated daily intake, (2) target hazard quotient, (3) non-carcinogenic hazard index or total target hazard quotient, and (4) carcinogenic risk.

A dietary exposure approach was used for evaluation of ingestion levels of nutrients and even contaminants. Estimated daily intake of individual heavy metals through fruit consumption are shown in Table 4. High EDI values were found for jackfruit and durian with all heavy metals, for both males and females. The EDIs were, in descending order, Zn>Cu>Pb>As>Cd>Hg for both genders for market A and C, and Zn>Cu>Pb>Cd>As>Hg for both genders in market B. These results were in agreement with a 2006 report from Egypt (Radwan and Salama, 2006) that Cu and Zn are the metals most frequently found in fruits and vegetables. Moreover, these EDI values were below the maximum tolerable daily intake (MTDI) and calculated TDI from PTWI/PTMI as recommended in the FAO/WHO guideline (see in Table 1). Thus, there appeared to be no or little possibility of adverse health effects from Cu or Zn through fruit consumption by either gender.

Target health quotient, non-carcinogenic hazard index, and carcinogenic risk were also used for estimation of the potential health risks associated with chronic exposure to heavy metals. Values were calculated using the heavy metal concentrations found in fruits from the three sampled Rayong markets and the estimated average fruit consumption by the local population. The THQ and HI values, obtained using fruit samples, are shown in Tables 5 and 6 for males and females, respectively. The average THQs of each heavy metal through fruit ingestion by males were Cu (0.2269), As (0.1682), Hg (0.1280), Pb (0.1244), Cd (0.0384), and Zn (0.0341). Results were similar for females: Cu (0.3122), As (0.2315), Hg (0.1761), Pb (0.1712), Cd (0.0528), and Zn (0.0469). All calculated THQs were < 1, suggesting that adverse effects would be unlikely. The average HI values of the six heavy metals for males and females were 0.7202 and 0.9909, respectively. Since these HI values were less than 1, chronic health risks were unlikely to occur. However, the risk was somewhat higher in females due to longer duration of exposure than in males. In addition, HI values were estimated for each market. The calculated HI values were, in descending order, market B (1.0797) > market A (0.5439) > market C (0.5370) for males, and market B (1.4855) > market A (0.7484) > market C (0.7389) for females. It was the high

Table 4. Estimated daily intake (μg/kg bw/day) and tolerable daily intake of heavy metals

Fruit	FIR (g/day)	Market	Male (BW=68.5 kg)						Female (BW=54.5 kg)					
			As	Cd	Cu	Hg	Pb	Zn	As	Cd	Cu	Hg	Pb	Zn
Durian	116.8	A	0.0313	0.0133	1.5818	0.0045	0.1610	3.6889	0.0393	0.0168	1.9881	0.0056	0.2024	4.6366
		B	0.0084	0.0191	3.7928	0.0077	0.2434	3.5487	0.0106	0.0240	4.7671	0.0096	0.3059	4.4604
		C	0.0302	0.0106	2.9427	0.0099	0.1042	4.3831	0.0379	0.0133	3.6986	0.0125	0.1309	5.5091
Jackfruit	116.8	A	0.0065	0.0103	4.1857	0.0078	0.1481	3.1487	0.0082	0.0130	5.2609	0.0099	0.1862	3.9575
		B	0.0412	0.0467	9.5248	0.0246	0.5028	11.440	0.0518	0.0588	11.971	0.0309	0.6320	14.379
		C	0.0243	0.0059	3.3885	0.0023	0.0363	2.3727	0.0306	0.0075	4.2590	0.0028	0.0456	2.9822
Mangosteen	7.3	A	0.0010	0.0007	0.1380	0.0002	0.0010	0.0830	0.0013	0.0009	0.1735	0.0003	0.0012	0.1044
		B	0.0001	0.0012	0.1000	0.0002	0.0035	0.0969	0.0002	0.0016	0.1256	0.0003	0.0044	0.1218
		C	0.0004	0.0020	0.0624	0.0002	0.0008	0.0773	0.0005	0.0025	0.0784	0.0002	0.0010	0.0972
Pineapple	9.75	A	0.0006	0.0000	0.0907	0.0003	0.0038	0.1090	0.0008	0.0001	0.1140	0.0004	0.0048	0.1370
		B	0.0003	0.0000	0.0416	0.0002	0.0016	0.0473	0.0004	0.0000	0.0523	0.0003	0.0020	0.0594
		C	0.0005	0.0001	0.0717	0.0003	0.0024	0.1294	0.0007	0.0002	0.0902	0.0004	0.0031	0.1626
Rambutan	7.3	A	0.0003	0.0003	0.1329	0.0003	0.0030	0.2346	0.0004	0.0004	0.1670	0.0003	0.0038	0.2949
		B	0.0002	0.0002	0.1161	0.0001	0.0029	0.1429	0.0002	0.0003	0.1459	0.0001	0.0036	0.1797
		C	0.0003	0.0003	0.0941	0.0002	0.0060	0.1244	0.0005	0.0004	0.1183	0.0003	0.0075	0.1563
Long Kong	7.3	A	0.0004	0.0001	0.1613	0.0000	0.0492	0.1339	0.0006	0.0001	0.2028	0.0001	0.0619	0.1683
		B	0.0003	0.0002	0.0707	0.0001	0.0010	0.1112	0.0004	0.0002	0.0889	0.0001	0.0013	0.1398
		C	0.0003	0.0002	0.0493	0.0002	0.0020	0.0975	0.0004	0.0002	0.0619	0.0002	0.0025	0.1226
Sum of EDI (All 6 fruits)		A	0.0404	0.0251	6.2906	0.0133	0.3665	7.3984	0.0508	0.0315	7.9065	0.0168	0.4606	9.2989
		B	0.0507	0.0677	13.646	0.0331	0.7553	15.387	0.0638	0.0851	17.151	0.0416	0.9494	19.340
		C	0.0564	0.0194	6.6090	0.0133	0.1518	7.1846	0.0709	0.0244	8.3067	0.0167	0.1908	9.0302
Calculated TDI			$3^{a,b}$	0.83^{b}	500	0.23^{b}	NA^{b}	1,000	$3^{a,b}$	0.83^{b}	500	0.23^{b}	NA^{b}	1,000
Maximum tolerable daily intake (MTDI) (Hashemi et al., 2019; FAO/WHO, 2002)			1.8	0.8	166.7	1.3	3	300	1.8	0.8	166.7	1.3	3	300

[a]Based on Joint FAO/WHO Expert Committee on Food Additives (JECFA) (FAO/WHO, 2018)
[b]Based on Codex Alimentarius International Food Standard (FAO/WHO, 2019)

Table 5. Target hazard quotient and non-carcinogenic hazard index by metal and fruit in males

Fruit	Market	THQ of individual heavy metals (For 68.5 kg male)						∑ THQ HI	HI Average
		As	Cd	Cu	Hg	Pb	Zn		
Durian	A	0.1070	0.0137	0.0405	0.0289	0.0471	0.0126	0.2500	0.2760
	B	0.0288	0.0196	0.0972	0.0494	0.0713	0.0121	0.2786	
	C	0.1033	0.0109	0.0754	0.0640	0.0305	0.0149	0.2992	
	Average	0.0797	0.0147	0.0710	0.0474	0.0496	0.0132		
Jackfruit	A	0.0223	0.0106	0.1073	0.0504	0.0434	0.0107	0.2449	0.4108
	B	0.1410	0.0479	0.2442	0.1579	0.1473	0.0391	0.7777	
	C	0.0833	0.0061	0.0868	0.0147	0.0106	0.0081	0.2098	
	Average	0.0822	0.0215	0.1461	0.0744	0.0671	0.0193		
Mangosteen	A	0.0037	0.0008	0.0035	0.0015	0.0003	0.0002	0.0102	0.0083
	B	0.0006	0.0013	0.0025	0.0016	0.0010	0.0003	0.0074	
	C	0.0015	0.0021	0.0016	0.0014	0.0002	0.0002	0.0072	
	Average	0.0019	0.0014	0.0025	0.0015	0.0005	0.0002		
Pineapple	A	0.0022	0.0000	0.0023	0.0022	0.0011	0.0003	0.0083	0.0069
	B	0.0011	0.0000	0.0010	0.0018	0.0004	0.0001	0.0047	
	C	0.0020	0.0001	0.0018	0.0024	0.0007	0.0004	0.0076	
	Average	0.0018	0.0001	0.0017	0.0021	0.0007	0.0003		
Rambutan	A	0.0013	0.0003	0.0034	0.0019	0.0009	0.0008	0.0088	0.0076
	B	0.0007	0.0002	0.0029	0.0009	0.0008	0.0004	0.0062	
	C	0.0013	0.0003	0.0024	0.0015	0.0017	0.0004	0.0079	
	Average	0.0011	0.0003	0.0029	0.0015	0.0011	0.0005		
Long kong	A	0.0016	0.0001	0.0041	0.0006	0.0144	0.0004	0.0214	0.0104
	B	0.0012	0.0002	0.0018	0.0007	0.0003	0.0003	0.0047	
	C	0.0013	0.0002	0.0012	0.0013	0.0005	0.0003	0.0051	
	Average	0.0014	0.0002	0.0024	0.0009	0.0051	0.0003		
Calculated THQ	A	0.1383	0.0257	0.1613	0.0858	0.1074	0.0252	0.5439	0.7202
	B	0.1736	0.0695	0.3499	0.2126	0.2213	0.0526	1.0797	
	C	0.1929	0.0199	0.1694	0.0856	0.0445	0.0245	0.5370	
Average THQ		0.1682	0.0384	0.2269	0.1280	0.1244	0.0341		

Table 6. Target hazard quotient and non-carcinogenic hazard index by metal and fruit in females

Fruit	Market	THQ of individual heavy metals (For 54.5 kg female)						∑ THQ HI	HI average
		As	Cd	Cu	Hg	Pb	Zn		
Durian	A	0.1472	0.0188	0.0558	0.0398	0.0649	0.0173	0.3440	0.3797
	B	0.0396	0.0270	0.1338	0.0680	0.0981	0.0166	0.3834	
	C	0.1421	0.0150	0.1038	0.0881	0.0420	0.0206	0.4117	
	Average	0.1097	0.0203	0.0978	0.0653	0.0683	0.0182		
Jackfruit	A	0.0307	0.0146	0.1476	0.0694	0.0597	0.0148	0.3370	0.5652
	B	0.1940	0.0660	0.3360	0.2173	0.2027	0.0538	1.0700	
	C	0.1146	0.0084	0.1195	0.0203	0.0146	0.0111	0.2887	
	Average	0.1131	0.0297	0.2011	0.1023	0.0923	0.0265		
Mangosteen	A	0.0051	0.0011	0.0048	0.0021	0.0004	0.0003	0.0140	0.0114
	B	0.0008	0.0018	0.0035	0.0022	0.0014	0.0004	0.0103	
	C	0.0021	0.0028	0.0022	0.0019	0.0003	0.0003	0.0099	
	Average	0.0027	0.0019	0.0035	0.0021	0.0007	0.0004		
Pineapple	A	0.0030	0.0001	0.0032	0.0031	0.0015	0.0005	0.0115	0.0095
	B	0.0015	0.0000	0.0014	0.0025	0.0006	0.0002	0.0065	
	C	0.0028	0.0002	0.0025	0.0033	0.0009	0.0006	0.0105	
	Average	0.0024	0.0001	0.0024	0.0030	0.0010	0.0004		
Rambutan	A	0.0018	0.0005	0.0046	0.0027	0.0012	0.0011	0.0121	0.0105
	B	0.0009	0.0003	0.0040	0.0013	0.0011	0.0006	0.0086	
	C	0.0018	0.0005	0.0033	0.0021	0.0024	0.0005	0.0108	
	Average	0.0015	0.0004	0.0040	0.0020	0.0016	0.0007		
Long kong	A	0.0023	0.0002	0.0056	0.0008	0.0198	0.0006	0.0295	0.0143
	B	0.0017	0.0002	0.0024	0.0010	0.0004	0.0005	0.0065	
	C	0.0018	0.0003	0.0017	0.0018	0.0008	0.0004	0.0070	
	Average	0.0019	0.0002	0.0033	0.0012	0.0070	0.0005		
Calculated THQ	A	0.1902	0.0354	0.2219	0.1181	0.1477	0.0348	0.7484	0.9909
	B	0.2389	0.0956	0.4814	0.2925	0.3045	0.0723	1.4855	
	C	0.2654	0.0274	0.2331	0.1178	0.0612	0.0337	0.7389	
Average THQ		0.2315	0.0528	0.3122	0.1761	0.1712	0.0469		

concentrations of heavy metals (see Table 3) which led to the high HI values. High HI values (>1) indicated a possibility of chronic non-carcinogenic risk to humans in the case of long-term fruit consumption. Therefore, these results can be used in warning farmers to be aware of the heavy metal-contaminated fruits and consumers of the health risk.

3.3 Carcinogenic assessment

As, Cd, and Pb are classified as being carcinogenic by the International Agency for Research on Cancer (IARC, 2018). We therefore calculated and estimated their carcinogenic risk (CR) values. This was assessed based on intake levels and the cancer slope factor (CSF) of the specified heavy metal. The calculated values are shown in Table 7. The average CR values by fruit, in descending order were: jackfruit > durian > mangosteen > pineapple > long kong > rambutan for As; jackfruit > durian > mangosteen > rambutan > long kong > pineapple for Cd; jackfruit > durian > long kong > rambutan > pineapple > mangosteen for Pb (in both males and females). Individual CR values for As, Cd, and Pb in all fruits sampled ranged from 0.007-990.657 ($\times10^{-6}$), Thus, all CR values were less than 1×10^{-4}, except Cd in durian (all market sites) and jackfruit (market A and B). Of all CR values, 10.2% were higher than the acceptable range. This suggested that prolonged consumption of durian or jackfruit from these areas carried a cancer risk related to cadmium but not to arsenic nor lead.

Total CRs were also estimated using the sum CRs (ΣCR) of As, Cd, and Pb. As shown in Table 7, total CR values were in the range of 1.56×10^{-6} to 1.08×10^{-3}. Total CR values above the acceptable level (1×10^{-5}) were found with durian, jackfruit and mangosteen: 2.58×10^{-4}, 3.62×10^{-4}, and 2.19×10^{-5} for males; 3.56×10^{-4}, 4.99×10^{-4}, and 3.02×10^{-5} for females. These results suggested that there was a carcinogenic risk to consumer health with the long-term consumption of these fruits.

Table 7. Carcinogenic risks associated with local fruit consumption ($\times10^{-6}$)

Fruits	Market	Male (BW=68.5 kg)			∑ CR	Female (BW=54.5 kg)			∑ CR
		As	Cd	Pb		As	Cd	Pb	
Durian	A	48.158	205.776	1.404	255.339	66.261	283.131	1.931	351.325
	B	12.981	294.576	2.122	309.680	17.861	405.313	2.919	426.094
	C	46.502	163.858	0.908	211.269	63.983	225.454	1.250	290.688
	Average	35.880	221.403	1.478	258.762	49.368	304.633	2.033	356.036
Jackfruit	A	10.047	159.384	1.291	170.723	13.825	219.299	1.777	234.901
	B	63.455	719.997	4.384	787.837	87.309	990.657	6.032	1,083.998
	C	37.486	92.071	0.316	129.875	51.578	126.683	0.435	178.697
	Average	36.996	323.818	1.997	362.812	50.904	445.546	2.748	499.199
Mangosteen	A	1.673	12.075	0.008	13.757	2.303	16.614	0.012	18.929
	B	0.278	19.623	0.030	19.933	0.383	27.000	0.042	27.426
	C	0.712	31.518	0.007	32.238	0.980	43.366	0.009	44.357
	Average	0.888	21.072	0.015	21.976	1.222	28.993	0.021	30.237
Pineapple	A	0.996	1.291	0.033	2.322	1.371	1.777	0.046	3.195
	B	0.516	1.032	0.014	1.562	0.710	1.420	0.019	2.150
	C	0.917	2.595	0.021	3.534	1.261	3.571	0.029	4.862
	Average	0.810	1.639	0.023	2.473	1.114	2.256	0.031	3.402
Rambutan	A	0.602	5.570	0.026	6.199	0.828	7.664	0.036	8.530
	B	0.325	4.338	0.025	4.689	0.447	5.969	0.034	6.451
	C	0.613	5.488	0.052	6.154	0.843	7.551	0.072	8.467
	Average	0.513	5.132	0.034	5.681	0.706	7.061	0.048	7.816
Long Kong	A	0.756	2.381	0.429	3.568	1.040	3.277	0.591	4.909
	B	0.581	3.244	0.009	3.834	0.799	4.463	0.012	5.276
	C	0.593	3.497	0.017	4.107	0.815	4.811	0.024	5.651
	Average	0.643	3.041	0.152	3.836	0.885	4.184	0.209	5.279

4. CONCLUSION

In this study, the levels of heavy metals (As, Cd, Cu, Hg, Pb, and Zn) in fresh fruit samples did not exceed the permissible limits, except for lead in durian (market B), jackfruit (market B), and long kong (market A). No significant differences in heavy metal concentration were found related to sampling location. On the other hand, the levels of As, Cd, Cu, Hg, and Zn were significantly different among fruit types. Based on the THQ calculations, consumption of these fruits in this area was safe from heavy metal accumulation when fruit types were estimated individually. But collectively, consumption of all these fruits was associated with chronic non-carcinogenic risk in some market sites (market B: HI=1.0797 and 1.4855 for males and females, respectively). Carcinogenic risk was highest in relation to cadmium ingestion (average CR value 3.44×10^{-4}), while less so in relation to lead and arsenic. Furthermore, consumption of three of the six fruit types (durian, jackfruit, and mangosteen) carried some carcinogenic risk based on total CR assessment. This study may be helpful in decreasing health risks associated with fruit consumption, encouraging the monitoring of fruits for heavy metals, and informing future remediation strategies.

ACKNOWLEDGEMENTS

This research project is supported by Mahidol University. This research and innovation activity is funded by National Research Council of Thailand (NRCT).

REFERENCES

Bamuwamye M, Ogwok P, Tumuhairwe V. Cancer and non-cancer risks associated with heavy metal exposures from street foods: Evaluation of roasted meats in an urban setting. Journal of Environment Pollution and Human Health 2015;2(3):24-30.

Bass D, Jones D. The determination of trace metals in human urine using the NexION 300 ICP-MS. Atomic Spectroscopy 2010;31(5):165-9.

Big CL, Lacatusu R, Damian F. Heavy metals in soil-plant system around Baia Mare City, Romania. Carpathian Journal of Earth and Environmental Sciences 2012;7(3):219-30.

Cakmak D, Saljnikov E, Mrvic V, Jakovljevic M, Marjanovic Z, Sikiric B, et al. Soil properties and trace elements contents following 40 years of phosphate fertilization. Journal of Environmental Quality 2010;39(2):541-7.

Cao S, Duan X, Zhao X, Wang B, Ma J, Fan D, et al. Health risk assessment of various metal (loid) s via multiple exposure pathways on children living near a typical lead-acid battery plant, China. Environmental Pollution 2015;200:16-23.

Choprathumma C, Thongkam T, Jaiyen C, Tusai T, Apilux A, Kladsomboon S. Determination of toxic heavy metal contaminated in food crops in Nakhon Pathom Province, Thailand. Khon Kaen Agriculture Journal 2019;7(1):83-94.

Dorsey A, Ingerman L, Swarts S. Toxicological Profile for Copper. USA: U.S. Department of Health and Human Services and Agency for Toxic Substances and Disease Registry; 2004.

Dunseith B. Thailand's Eastern Economic Corridor - What You Need to Know [Internet]. 2018 [cited 2022 Aug 23]. Available from: https://www.aseanbriefing.com/news/thailand-eastern-economic-corridor/.

Ecological Alert and Recovery-Thailand (EARTH). Heavy metals in water: Serious pollution concentration found near industrial areas in Thailand [Internet]. 2016 [cited 2021 Jul 16]. Available from: https://english.arnika.org/press-releases/thailand-high-concentration-of-heavy-metals-found-in-water.

European Union (EU). EU pesticides database [Internet]. 2022 [cited 2022 May 21]. Available from: https://ec.europa.eu/food/plant/pesticides/eu-pesticides-database/mrls/?event=search.pr.

European Commission. Analytical Quality Control and Method Validation Procedures for Pesticide Residues Analysis in Food and Feed: SANTE/11813/2017. Brussels, Belgium: European Commission; 2017.

Food and Agriculture Organization of the United Nations/World Health Organization (FAO/WHO). Codex Alimentarius - General Standards for Contaminants and Toxins in Food. Schedule 1: Maximum and Guideline Levels for Contaminants and Toxins in Food. Reference CX-FAC 02/16. Rotterdam, Netherland: Joint FAO/WHO Food Standards Programme, Codex Committee; 2002.

Food and Agriculture Organization of the United Nations/World Health Organization (FAO/WHO). Codex Alimentarius - General Standard for Contaminants and Toxins in Food and Feed. (Last amended 2019). CODEX STAN. 193-1995. Geneva, Switzerland: Joint FAO/WHO Food Standard Programme, Codex Committee; 2019.

Food and Agriculture Organization of the United Nations/World Health Organization (FAO/WHO). Diet, Nutrition and the Prevention of Chronic Diseases. Geneva, Switzerland: Joint FAO/WHO Expert Consultation; 2003.

Food and Agriculture Organization of the United Nations/World Health Organization (FAO/WHO). Evaluation of Certain Food Additives and Contaminants. Geneva, Switzerland: Joint FAO/WHO Expert Committee on Food Additives; 1982.

Food and Agriculture Organization of the United Nations/World Health Organization (FAO/WHO). Recommended Methods of Sampling for the Determination of Pesticide Residues for Compliance with MRLs (CAC/GL 33-1999). Rome, Italy: Joint FAO/WHO Food standards Programme; 1999.

Food and Agriculture Organization of the United Nations/World Health Organization (FAO/WHO). Safety Evaluation of Certain Contaminants in Food. Geneva, Switzerland: Joint FAO/WHO Expert Committee on Food Additives; 2011.

Food and Agriculture Organization of the United Nations/World Health Organization (FAO/WHO). The List of Maximum Levels for Contaminatants and Toxins in Foods. Utrecht, Netherland: Joint FAO/WHO Expert Committee on Food Additives; 2018.

Food and Agriculture Organization of the United Nations/World Health Organization (FAO/WHO). Toxicological Evaluation of Certain Food Additives and Contaminants in Food/Prepared by the Forty-Fourth Meeting of the Joint FAO/WHO Expert Committee on Food Additives. Rome, Italy: Joint FAO/WHO Expert Committee on Food Additives; 1996.

Ghasemidehkordi B, Malekirad AA, Nazem H, Fazilati M, Salavati H, Shariatifar N, et al. Concentration of lead and mercury in collected vegetables and herbs from Markazi province, Iran: A non-carcinogenic risk assessment. Food and Chemical Toxicology 2018;113:204-10.

González AG, Herrador MÁ. A practical guide to analytical method validation, including measurement uncertainty and accuracy profiles. TrAC Trends in Analytical Chemistry 2007;26(3):227-38.

Harmanescu M, Alda LM, Bordean DM, Gogoasa I, Gergen I. Heavy metals health risk assessment for population via consumption of vegetables grown in old mining area: A case study: Banat County, Romania. Chemistry Central Journal 2011;5(1):1-10.

Hashemi M, Sadeghi A, Saghi M, Aminzare M, Raeisi M, Rezayi M, et al. Health risk assessment for human exposure to trace metals and arsenic via consumption of hen egg collected from largest poultry industry in Iran. Biological Trace Element Research 2019;188(2):485-93.

Hurst R, Hurst S. Fruits and vegetables as functional foods for exercise and inflammation. In: Bioactive Food as Dietary Interventions for Arthritis and Related Inflammatory Diseases. Academic Press; 2012. p. 319-36.

Institute for Population and Social Research. Population of Thailand: Volume 25. Mahidol Population Gazette; 2016.

International Agency for Research on Cancer (IARC). Agents classified by the IARC monographs, Volumes 1-123 [Internet]. 2018 [cited 2021 Jul 1]. Available from: https://monographs.iarc.who.int/wp-content/uploads/2018/09/ClassificationsAlphaOrder.pdf.

Islam MS, Hoque MF. Concentrations of heavy metals in vegetables around the industrial area of Dhaka city, Bangladesh and health risk assessment. International Food Research Journal 2014;21(6):2121-6.

Jankeaw M, Tongphanpharn N, Khomrat R, Iwai CB, Pakvilai N. Heavy metal contamination in meat and Crustaceans products from Thailand local markets. International Journal of Environmental and Rural Development 2015;6(2):153-8.

Järup L. Hazards of heavy metal contamination. British Medical Bulletin 2003;68(1):167-82.

Kerdthep P, Tongyonk L, Rojanapantip L. Concentrations of cadmium and arsenic in seafood from Muang District, Rayong Province. Journal of Health Research 2009;23(4): 179-84.

Ketsa S, Wisutiamonkul A, Palapol Y, Paull RE. The durian: Botany, horticulture, and utilization. Horticultural Reviews 2020;47:125-211.

Kim NH, Hyun YY, Lee KB, Chang Y, Rhu S, Oh KH, et al. Environmental heavy metal exposure and chronic kidney disease in the general population. Journal of Korean Medical Science 2015;30(3):Article No. 272.

Kinuthia GK, Ngure V, Beti D, Lugalia R, Wangila A, Kamau L. Levels of heavy metals in wastewater and soil samples from open drainage channels in Nairobi, Kenya: Community health implication. Scientific Reports 2020;10(1):1-13.

Kladsomboon S, Jaiyen C, Choprathumma C, Tusai T, Apilux A. Heavy metals contamination in soil, surface water, crops, and resident blood in Uthai District, Phra Nakhon Si Ayutthaya, Thailand. Environmental Geochemistry and Health 2020; 42(2):545-61.

Klinsawathom T, Songsakunrungrueng B, Pattanamahakul P. Heavy metal concentration and risk assessment of soil and rice in and around an open dumpsite in Thailand. EnvironmentAsia 2017;10(2):53-64.

Kumar A, Kumar A, Cabral-Pinto M, Chaturvedi AK, Shabnam AA, Subrahmanyam G, et al. Lead toxicity: Health hazards, influence on food chain, and sustainable remediation approaches. International Journal of Environmental Research and Public Health 2020;17(7):Article No.2179.

Lactusu R, Rauta C, Carstea S, Ghelase I. Soil-plant-man relationships in heavy metal polluted areas in Romania. Applied Geochemistry 1996;11(1-2):105-7.

Li R, Wu H, Ding J, Fu W, Gan L, Li Y. Mercury pollution in vegetables, grains and soils from areas surrounding coal-fired power plants. Scientific Reports 2017;7(1):1-9.

Li Y, Ye F, Wang A, Wang D, Yang B, Zheng Q, et al. Chronic arsenic poisoning probably caused by arsenic-based pesticides: Findings from an investigation study of a household. International Journal of Environmental Research and Public Health 2016;13(1):Article No.133.

Lim LLY, Seubsman SA, Sleigh A. Validity of self-reported weight, height, and body mass index among university students in Thailand: Implications for population studies of obesity in developing countries. Population Health Metrics 2009;7:Article No. 15.

Liščáková P, Nawaz A, Molnárová M. Reciprocal effects of copper and zinc in plants. International Journal of Environmental Science and Technology 2022;19:9297-312.

Lorestani B, Merrikhpour H, Cheraghi M. Assessment of heavy metals concentration in groundwater and their associated health risks near an industrial area. Environmental Health Engineering and Management Journal 2020;7(2):67-77.

Madejón P, Marañón T, Murillo JM. Biomonitoring of trace elements in the leaves and fruits of wild olive and holm oak trees. Science of the Total Environment 2006;355(1-3):187-203.

Mensah E, Kyei-Baffour N, Ofori E, Obeng G. Influence of Human Activities and Land Use on Heavy Metal Concentrations in Irrigated Vegetables in Ghana and their Health Implications. Appropriate Technologies for Environmental Protection in the Developing World: Springer; 2009. p. 9-14.

Ministry of Public Health, Thailand (MoPH). Standard for Contaminants in Food: Volume 137. Bangkok: The Government Gazette; 2020.

Ministry of Agriculture and Cooperatives. Method of Sampling for the Determination of Pesticide Residues. Thai agricultural standard, TAS 9025-2008. Bangkok, Thailand: National Bureau of Agricultural Commodity and Food Standards; 2008.

Mohamed H, Haris PI, Brima EI. Estimated dietary intake of essential elements from four selected staple foods in Najran City, Saudi Arabia. Chemistry Central Journal 2019;13: Article No. 73.

Mohammadi AA, Zarei A, Majidi S, Ghaderpoury A, Hashempour Y, Saghi MH, et al. Carcinogenic and non-carcinogenic health risk assessment of heavy metals in drinking water of Khorramabad, Iran. MethodsX 2019;6: 1642-51.

Nilkarnjanakul W, Watchalayann P, Chotpantarat S. Spatial distribution and health risk assessment of As and Pb contamination in the groundwater of Rayong Province, Thailand. Environmental Research 2022;204:Article No. 111838.

Ogwok P, Bamuwamye M, Apili G, Musalima JH. Health risk posed by lead, copper and iron via consumption of organ meats in Kampala City (Uganda). Journal of Environment Pollution and Human Health 2014;2(3):69-73.

Ojekunle OZ, Rasaki A, Taiwo AM, Adegoke KA, Balogun MA, Ojekunle OO, et al. Health risk assessment of heavy metals in drinking water leaching through improperly managed dumpsite waste in Kurata, Ijoko, Sango area of Ogun State, Nigeria. Groundwater for Sustainable Development 2022; 18:Article No. 100792.

Pamonpol K, Tokhun N. Heavy metal contamination at highland agricultural soil at Dan Sai District, Loei Province, Thailand. Journal of Public Health and Development 2019;17(3):13-22.

Radfard M, Yunesian M, Nabizadeh R, Biglari H, Nazmara S, Hadi M, et al. Drinking water quality and arsenic health risk assessment in Sistan and Baluchestan, Southeastern Province, Iran. Human and Ecological Risk Assessment 2018;24:1-17.

Radwan MA, Salama AK. Market basket survey for some heavy metals in Egyptian fruits and vegetables. Food and Chemical Toxicology 2006;44(8):1273-8.

Rayong Provincial Government Center. Information of Rayong Province [Internet]. 2020 [cited 2021 Jun 23]. Available from: http://www.rayong.doae.go.th/eco%20province%2063.pdf. (in Thai).

Satachon P, Keawmoon S, Rengsungnoen P, Thummajitsakul S, Silprasit K. Source and health risk assessment of some heavy metals in non-certified organic rice farming at Nakhon Nayok Province, Thailand. Applied Environmental Research 2019;41(3):Article No. 8.

Satheannoppakao W, Aekplakorn W, Pradipasen M. Fruit and vegetable consumption and its recommended intake associated with sociodemographic factors: Thailand National Health Examination Survey III. Public Health Nutrition 2009;12(11):2192-8.

Seeda A, Abou El-Nour EZ, Mervat G, Zaghloul S. Interaction of copper, zinc, and their importance in plant physiology: Review, acquisition and transport. Middle East Journal of Applied Sciences 2020;10(3):407-34.

Shabbir Z, Sardar A, Shabbir A, Abbas G, Shamshad S, Khalid S, et al. Copper uptake, essentiality, toxicity, detoxification and risk assessment in soil-plant environment. Chemosphere 2020;259:Article No. 127436.

Simasuwannarong B, Satapanajaru T, Khuntong S, Pengthamkeerati P. Spatial distribution and risk assessment of As, Cd, Cu, Pb, and Zn in topsoil at Rayong Province, Thailand. Water, Air, and Soil Pollution 2012;223(5):1931-43.

Six L, Smolders E. Future trends in soil cadmium concentration under current cadmium fluxes to European agricultural soils. Science of the Total Environment 2014;485:319-28.

Smolders E, Six L. Revisiting and Updating the Effect of Phosphate Fertilizers to Cadmium Accumulation in European Agricultural Soils. Heverlee, Belgium: Division of Soiland Water Management; 2013.

Song B, Lei M, Chen T, Zheng Y, Xie Y, Li X, et al. Assessing the health risk of heavy metals in vegetables to the general population in Beijing, China. Journal of Environmental Sciences 2009;21(12):1702-9.

Striegel L, Chebib S, Dumler C, Lu Y, Huang D, Rychlik M. Durian fruits discovered as superior folate sources. Frontiers in Nutrition 2018;5:Article No. 114.

Swami SB, Thakor N, Haldankar P, Kalse S. Jackfruit and its many functional components as related to human health: A review. Comprehensive Reviews in Food Science and Food Safety 2012;11(6):565-76.

Taiwo AM, Olowookere ZA, Bada BS, Akinhanmi TF, Oyedepo JA. Contamination and health risk assessments of metals in selected fruits from Abeokuta, Southwestern Nigeria. Journal of Food Composition and Analysis 2022;114:Article No. 104801.

Turull M, Komarova T, Noller B, Fontàs C, Díez S. Evaluation of mercury in a freshwater environment impacted by an organomercury fungicide using diffusive gradient in thin films. Science of the Total Environment 2018;621:1475-84.

USEPA’s Integrated Risk Information System (IRIS). IRIS Asessment [Internet]. 2022 [cited 2021 Jul 2]. Available from: https://www.epa.gov/iris.

Wanwimolruk S, Kanchanamayoon O, Boonpangrak S, Prachayasittikul V. Food safety in Thailand 1: It is safe to eat watermelon and durian in Thailand. Environmental Health and Preventive Medicine 2015;20(3):204-15.

Wenzl T, Haedrich J, Schaechtele A, Piotr R, Stroka J, Eppe G, et al. Guidance Document on the Estimation of LOD and LOQ for Measurements in the Field of Contaminants in Food and Feed. Luxembourg: Publication Office of the European Union; 2016.

World Health Organization (WHO). GEMS/Food Regional Diets: Regional per Capita Consumption of Raw and Semi-Processed Agricultural Commodities: Prepared by the Global Environment Monitoring System/Food Contamination Monitoring and Assessment Programme (GEMS/Food). Geneva, Switzerland: Food Safety Department and World Health Organization; 2003.

World Health Organization (WHO). 10 chemicals of public health concern [Internet]. 2020 [cited 2022 Aug 23]. Available from: https://www.who.int/news-room/photo-story/photo-story-detail/10-chemicals-of-public-health-concern.

Xiao M, Li F, Zhang J, Lin S, Zhuang Z, Wu Z. Investigation and health risk assessment of heavy metals in soils from partial areas of Daye City, China. IOP Conference Series: Earth and Environmental Science 2017;64:Article No. 012066.

Zeng F, Wei W, Li M, Huang R, Yang F, Duan Y. Heavy metal contamination in rice-producing soils of Hunan province, China and potential health risks. International Journal of Environmental Research and Public Health 2015; 12(12):15584-93.

Forecasting Municipal Solid Waste Generation in Thailand with Grey Modelling

Thichakorn Pudcha[1,3], Awassada Phongphiphat[1,3,*], Komsilp Wangyao[1,3], and Sirintornthep Towprayoon[1,2,3]

[1]The Joint Graduate School of Energy and Environment, King Mongkut's University of Technology Thonburi, Bangkok, Thailand
[2]Earth Systems Science Research Cluster, King Mongkut's University of Technology Thonburi, Bangkok, Thailand
[3]Center of Excellence on Energy Technology and Environment, Ministry of Higher Education, Science, Research and Innovation, Bangkok, Thailand

ARTICLE INFO

Received: 28 Apr 2022
Received in revised: 22 Sep 2022
Accepted: 26 Sep 2022
Published online: 30 Nov 2022
DOI: 10.32526/ennrj/21/202200104

Keywords:
Municipal solid waste/ Forecasting model/ Grey forecasting model/ Greenhouse gas/ Waste-to-energy

*** Corresponding author:**
E-mail:
awassada.pho@kmutt.ac.th

ABSTRACT

Forecasting municipal solid waste generation is crucial in planning for effective and sustainable waste management. Where data on waste are limited, the grey model (GM) has proven to be a useful tool for forecasting. This study applied GM for forecasting municipal solid waste generation in Thailand up to 2030, based on a dataset from 2011-2018. Both univariate models and multivariate models with four influencing factors (population density, gross domestic product per capita, household expenditure, and household size) were tested. The GM (1,1)-0.1 and GM (1,3) provided the lowest prediction errors among all models. Based on these models, waste generation in 2030 was projected to be 84,070-95,728 tonnes/day (1.23-1.40 kg/capita/day), an approximately 10-25% increase compared to 2018. In a business-as-usual scenario, there would be 6,404,848 tonnes of improperly treated waste by 2030, resulting in greenhouse gas emissions from its disposal of up to 2,600 GgCO_2e. This amount of waste is equivalent to 380 MWe of electricity; therefore, it should receive more attention. Results show that the improved management of improperly treated waste would help Thailand reach its waste-to-energy production target of 500 MW by 2036. Furthermore, diverting this portion of waste from open dump sites would directly reduce greenhouse gas emissions from the waste sector more than the set target of Thailand's Nationally Determined Contribution Roadmap on Mitigation 2021-2030 (1,300 GgCO_2e).

1. INTRODUCTION

Thailand's municipal solid waste (MSW) generation has grown continuously in the last decade. In contrast, waste collection, transportation services, and sanitary facilities are still limited, leading to illegal waste dumping, open burning, and MSW leakage into the environment (Wichai-utcha and Chavalparit, 2019). Other critical issues related to MSW management in Thailand include the lack of MSW statistics required for effective waste management planning, insufficient budget for operation and maintenance, inefficient waste treatment technology, limitations of laws and regulations, and poor cooperation between local government and private sectors. Thailand is challenged to move forward to zero waste management and achieve sustainable development goals (SDGs) and a circular economy. Forecasting can assist decision-makers and policymakers in projecting future needs and selecting appropriate MSW treatment technologies. A reliable forecast of MSW generation (MSWG) should be made available to create a sustainable solid waste management plan at the city or country level. For example, Johnson et al. (2017) employed a gradient-boosting regression model to predict MSWG across New York City and applied a spatiotemporal model. The models helped improve waste collection and the distribution of waste collecting vehicles and develop waste reduction strategies. An MSWG forecasting model and scenario analysis were applied to investigate the effect of current waste policies up to 2050 in the Balearic Islands. The forecasted and

Citation: Pudcha T, Phongphiphat A, Wangyao K, Towprayoon S. Forecasting municipal solid waste generation in Thailand with grey modelling. Environ. Nat. Resour. J. 2023;21(1):35-46. (https://doi.org/10.32526/ennrj/21/202200104)

scenario results identified that the optimistic scenario decreased the amount of MSW sent to landfills by 40% and increased selective collection by 30% (Estay-Ossandon and Mena-Nieto, 2018). Di-Foggia and Beccarello (2021) used an econometric method based on a regression model to estimate the costs of waste facilities in Italy. The results from the model suggest that Italy could reduce landfill use and raise waste-to-energy capacity leading to a more positive cost-saving impact on waste management.

The selection of an appropriate prediction model depends on the purposes, the duration of prediction (short-, medium-, or long-term), and data availability. Linear regression analysis is a fundamental approach that is helpful in MSW forecasting (Ghinea et al., 2016). However, it requires many input data to produce steady and trustworthy results (Armstrong, 2001). Another model widely used to forecast MSW is the artificial neural network (ANN). ANN is a mathematically based nonlinear model. It has been used to estimate weekly and monthly waste generation and provides good performance and better results than the principal component regression analysis. (Noori et al., 2009). Nevertheless, the ANN model needs many months of waste generation data for long-term forecasting (Ali-Abdoli et al., 2012). Both regression analysis and ANN have limited utility if there is insufficient input information. When using limited data, available forecasting models include system dynamics (SD), grey model (GM), and fuzzy logic.

The SD model provides a viable alternative when there is limited data availability. It has been used for simulating MSWG and evaluating source separation, the capacity of waste treatment, and cost management (Sukholthaman and Sharp, 2016). SD modeling can be beneficial for policymakers and sanitation managers to project a broad view of waste management. However, it is relatively complex and requires advanced software processing (Xiao et al., 2020).

One widely used mathematical model for environmental projection is the GM of grey system theory, introduced by Deng (1982). The advantage of GM is its ability to work with limited data (at least four data points required). Chhay et al. (2018) used the univariate GM with 16 annual datasets to predict MSWG for the next 15 years. Zhang et al. (2019) also used multivariate GM to forecast MSWG for the next five years using nine annual datasets.

In a developing country such as Thailand, publicly available data on MSWG are limited and inconsistent. Intharathirat et al. (2015) applied multivariate GM to forecast Thai MSWG to 2030 using 13 annual datasets from 2000 to 2012, and the results were highly accurate for 18 years. Unfortunately, the methodology for estimating MSWG in national statistics has changed since 2010. Hence, the most recent and continuous dataset on MSWG in Thailand contains only eight annual datasets (2011-2018). The monthly statistics for MSWG of the whole country were not available publicly. As a result, GM is a feasible model for MSWG forecasting, providing solutions that can benefit sustainable MSW management. This study provides updated forecasts of MSWG in Thailand based on GM and presents the estimates for energy potential and GHG emissions from improperly treated waste (impW). The results will aid policymakers and local authorities in planning waste and GHG management policies.

2. METHODOLOGY

2.1 Input data for the models

2.1.1 MSW generation and management in Thailand

The key government offices responsible for analyzing and reporting the waste situation in Thailand are the Pollution Control Department (PCD) and the Department of Local Administration (DLA). The annual MSWG data during 1993-2018 is available publicly on the state report of pollution and solid waste in the country by the PCD (PCD, 2022a) and online database (PCD, 2022b). However, the MSWG data is inconsistent due to the data collection system and estimation method leading to limited available MSWG data for the forecast. Details of MSWG during 1993-2018 are shown in Supplementary data: Supplement S1-S2.

The PCD also reports on various types of waste disposal and waste utilization. To estimate the energy potential and GHG emissions, this study focused on the collected waste that is improperly treated; this includes open dumping (OD), controlled dumping (CD) of waste of more than 50 tonnes/day, incineration (IN) without proper pollution control, and open burning (OB). When this study was conducted, the most recent year for which information was available was 2017. MSW data of 2,441 municipalities were analyzed by Phongphiphat et al. (2019) and found that proportions of OD, IN, CD, and OB were 16.4%, 0.6%, 0.9%, and 0.4%, respectively. This study used these proportions to estimate GHG emissions and energy potential for impW in all future years.

2.1.2 Factors influencing MSWG

Selected current studies on MSWG forecasting are summarized in Table 1. Social and economic factors are frequently used in forecasting models, particularly population and GDP. This study considered the potential drivers by focusing on data availability, statistical significance, and the relationship between drivers and waste quantity at the national level. Four drivers, including population density, household size, gross domestic product (GDP) per capita, and household expenditure were selected for the model. Population density represents urban morphology and it is beneficial when one needs to compare countries or cities (Oribe-Garcia et al., 2015). Household size is the number of people per household, which is related to household solid waste in an econometric model (Beigl et al., 2004). GDP/capita was trained and tested in a regression model and provided high coefficient of determination (R^2) results (Ceylan, 2020). Household expenditure represents the potential for goods consumption by a household. According to Weng et al. (2010), there is a statistically significant and positive association between consumption expenditure and the amount of garbage discarded.

The data sources of selected drivers were as follows: the number of registered populations, number of houses, and country area were from DOPA (2018), the GDP statistics were from NESDB (2018), and the average household expenditures were from NSO (2018). The population density, household size, and GDP/capita were calculated. The 2019-2030 population projections were from NESDB (2013). Other future values were from the projections calculated using GM (1,1). These drivers were used as independent variables in the multivariate GM.

2.1.3 Dataset selected for model training and testing

The annual data for MSWG in tonnes/day and the selected factors during 2011-2018 were used for model training and testing with the GM models. This study used an ex-pose forecast. The model was built using the training data, while the test data were preserved to estimate forecast accuracy. Hyndman and Athanasopoulos (2018) suggested that the test data typically comprise about 20% of the total data. However, due to the limited data availability, only the last two values of the MSW sequence (data from 2017 and 2018) were used for model testing. The preceding values in the sequence stood for model training.

2.2 Forecasting using the grey model

After data collection, six steps of work were carried out to forecast MSWG: (1) preliminary analysis of collected data; (2) analysis of variable correlations by using Pearson correlation (R) and GRA; (3) training of the data in univariate and multivariate GM models; (4) model validation by using four error measures (described in section 2.3) to select a suitable model for MSWG forecast; (5) using the selected model to forecast; and (6) analysis of the prediction interval to evaluate the uncertainty of forecasting.

GM models are mathematical approaches operating based on two sequences, including a sequence of raw data and its accumulation-generated sequence. The univariate GM models, such as GM (1,1) and GM (1,1)-α, are first-order grey differential equations with one variable and without influencing factors forms (Sifeng and Yi, 2010). The multivariate GM models or GM (1,n) include influencing factors that relate to waste quantity, where n-1 equals the influencing factors number. Both differential equations in GM (1,1) and GM (1,n) can be estimated by the least square method to generate the forecasted data. All GM equations used for forecasting in this study are explained in Supporting Information 2.

2.3 Model validation and prediction intervals

To validate and compare the forecasts, four error measures, including the mean absolute percentage error (MAPE), mean absolute error (MAE), mean squared error (MSE), and root mean squared error (RMSE), were calculated. Their equations were explained in Chhay et al. (2018), Kannangara et al. (2018), and Zhang et al. (2019).

The best-fit model was used to forecast MSWG from 2019 to 2030 with the prediction interval (PI) of 95%, assuming that the forecast errors were normally distributed. Details and the equation were explained by Intharathirat et al. (2015).

2.4 Estimation of GHG emissions and energy potential

GHG emissions based on waste disposal activities were estimated following the IPCC guidelines, volume 5 (IPCC, 2006), and applied global warming potentials for CH_4 and N_2O of 28 and 265, respectively (IPCC, 2014). The GHG estimation was conducted from 2017 to 2030. Due to the limited data availability, the shares of impW were assumed to be constant, based on the 2017 data mentioned in section 2.1.1.

Table 1. The literature on the MSW forecasting model including data and driver uses

Modelling methods	Scope	Input data (waste amount)		Forecasting period (year)	Influencing factors			Reference
		Type	No's		Social	Economic	Other	
ANFIS	City	TS-y	41	17	Population, and percentage of urban population	GDP per capita	-	Tiwari et al. (2008)
ANN, RA	City	TS-m	120	22	Population	Household income	Maximum temperature	Ali Abdoli et al. (2012)
ANN	City	TS-y	18	-	Population, number of residents, household, and tourist	Household income	-	Sun and Chungpaibulpatana (2017)
ANN	Municipality	TS-y	13	-	Population, education, owned dwellings, and fraction of one person households	Personal income, employment rate, population worked at usual work place	-	Kannangara et al. (2018)
ANN	Country	TS-y	11	-	Urban population, Human Development Index (HDI), scientists and engineers, life expectancy at birth etc.	GDP, domestic material consumption, health expenditure, etc.	-	Adamović et al. (2018)
ANN, GM	Country	TS-y	16	15	Urban population	GDP, energy consumption	-	Chhay et al. (2018)
EM	City	TS-y	32	-	Population, average household size, population density, infant mortality rate, life expectancy at birth, and overnight stay	GDP, sectoral employment, and unemployment rate	-	Beigl et al. (2004)
FIG-GA-SVR	City	TS-y	21	9	Population	Household income, GDP, and total retail sales of consumer goods	-	Dai et al. (2020)
GM	City	TS-y	9	-	Population	City of GDP, retail sales, consumer spending	-	Zhang (2013)
GM	Country	TS-y	13	18	Population density, urbanization, and household size	Proportion employment, GDP per capita	-	Intharathirat et al. (2015)
GM, RA	City	TS-y	9	5	Population, tourists, and education	Retail sales of social consumer goods, urban per capita consumption expenditure	-	Zhang et al. (2019)
GM	City	TS-y	13	15	Population density	Household income	-	Duman et al. (2019)
RA	City	TS-y	15	-	Population density, average surface of family dwelling, education, etc.	Population employed, total personal income, tourist activity, density of retail outlet, etc.	-	Oribe-Garcia et al. (2015)
RA	City	TS	1	10	Number of residents, population (aged 15-59 years), and urban life expectancy	-	-	Ghinea et al. (2016)
RA	City	TS-w	8	1	Population density, age, education	Earning	Season and weather	Johnson et al. (2017)
RA	City	CS	50	-	Household size, education, occupation	Household income, energy consumption	-	Kumar and Samadder (2017)
RA	City	CS	580	-	Population, education, and culture	Household income and expenditure, energy and fuel structure and industry types	Climate and geography	Han et al. (2018)

Abbreviations: ANFIS=modeling methods include adaptive neuro-fuzzy inference system; ANN=artificial neural network; EM=econometric model; FIG=fuzzy information granulation; GM=grey model; RA=regression analysis; GA-SVR=support vector regression model optimized by genetic algorithm; SD=system dynamic; TSA=time series analysis; TS=time-series data; CS=cross-sectional data; -w=weekly; -m=monthly; -y=yearly

Table 1. The literature on the MSW forecasting model including data and driver uses (cont.)

Modelling methods	Scope	Input Data (waste amount)		Forecasting period (year)	Influencing factors			Reference
		Type	No's		Social	Economic	Other	
RA	Country	TS-y	8	-	Human Development Index	GDP and unemployment rate	Total CO_2 emissions	Namlis and Komilis (2019)
RA	Country	TS-y	24	-	Population	GDP per capita, inflation rate, unemployment rate	-	Ceylan (2020)
SD	Municipality	CS	3	11	Population, average household size,	Household income, and income of municipality	-	Dyson and Chang (2005)
TSA	Region	TS-y	29	29	Population	GDP per capita	-	Chung (2010)
TSA	City	TS-w	417	10	Population, average household size, infant mortality rate, and life expectancy at birth,	Sectoral employment, and GDP per capita	-	Rimaityte et al. (2012)

Abbreviations: ANFIS=modeling methods include adaptive neuro-fuzzy inference system; ANN=artificial neural network; EM=econometric model; FIG=fuzzy information granulation; GM=grey model; RA=regression analysis; GA-SVR=support vector regression model optimized by genetic algorithm; SD=system dynamic; TSA=time series analysis; TS=time-series data; CS=cross-sectional data; -w=weekly; -m=monthly; -y=yearly

Waste composition is an essential part of estimating accurate GHG emissions from impW. This study used created a proxy waste composition (Figure 1) by averaging the results of waste sampling from previous studies conducted by Phongphiphat et al. (2019) and Towprayoon and Phongphiphat (2013) at the MSW landfills of three large municipalities of Thailand, namely, Chiang Mai, Chonburi, and Khon Kaen. The waste sampling and quartering followed the procedures outlined in ASTM (2016). Waste samples were then classified into eleven components according to the IPCC guidelines.

According to DEDE (2020), the target of alternative energy from MSW would increase by 80% from DEDE (2015). Waste-to-energy (WtE) incineration plants are widely encouraged to reduce waste mass with electricity generation. Thus, this study estimated the energy potential in MWe by assuming impW was sent to WtE incineration. The average net calorific value used for unsorted MSW was 7.82 MJ/kg, and the efficiency capacity of the power plant was 20% and 16% of downtime per year (Towpayoon and Phongphiphat, 2013).

3. RESULTS AND DISCUSSION

3.1 Relationship between MSWG and selected drivers

The Pearson correlation coefficient (r) of all variables from 2011 to 2016 was examined as preliminary analysis. Results showed that household size had the strongest inverse relationship with MSWG, at 0.82, followed by population density (r=0.81), GDP/capita (r=0.75), and household expenditure (r=0.70). These results indicated that all drivers were related to waste quantity because the correlation values were higher than 0.70 (Asuero et al., 2006). Moreover, all factors were investigated in GRA, and the results were expressed as a grey relational grade. The grey relational grade's closeness to 1 indicates a higher degree of similarity between the two series' geometric patterns (Wu and Chen, 2005). Results showed that population density (γ=0.71) was the most significant driver, followed by GDP/capita (γ=0.70), household expenditure (γ=0.52), and household size (γ=0.49). Population density was also found to be the most influential factor correlated to MSW quantity from GRA in Intharathirat et al. (2015), though the study was based on a different period of data from Thailand. The relationship between MSWG and household size was opposite that of the Pearson correlation and GRA results. Due to its limitations, GRA only works for the sequences with direct relationships (Javed et al., 2019). Thus, the inverse relationship of household size was the lowest grey relational grade.

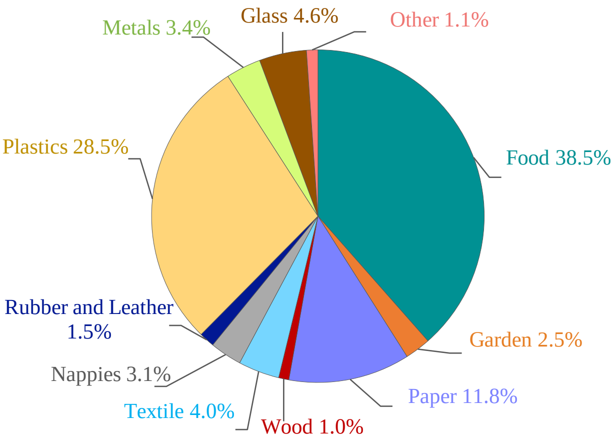

Figure 1. The proxy MSW composition of Thailand for GHG estimation in this study (Adapted by permission from: Springer Nature, Pudcha et al. (2022))

This study used all four factors to train and test the multivariate model. The analysis began with GM (1,5), where all four influencing factors were included. Then, for the following models, the weakest factors from the GRA results were removed one by one. The household size was removed for the GM (1,4). GM (1,3) consisted of two factors, namely population density and household expenditure, and GM (1,2) consisted of only one driver, which was population density.

3.2 Model training and testing

Results from model training using the univariate and multivariate model, based on the data from 2011-2018, are shown in Figures 2(a) and Figure 2(b), respectively. Results from data testing or model validation are shown in Table 2 for Models 1-8. All models yielded MAPE values lower than 10%, indicating a high prediction accuracy (Lewis, 1982). In the univariate models, the forecast errors increased as the α increased. These findings indicated that the old data in the sequence of this study were important to the model. For this reason, predicted values from GM (1,1)-0.1 were closest to the actual values compared to other models, except for one training point in 2013, as shown in Figure 2(a). GM (1,1)-0.5, without preference for old or new data, had the second-best prediction accuracy. Hence, this study used GM (1,1)-0.1 and GM (1,1)-0.5 from the univariate model for further forecasting of MSWG.

The GM (1,n) multivariate models fit the actual data better than the univariate models. The reason was that GM (1,n) models account for multiple factors that influence MSWG; thus, they could capture and predict changes in MSWG better than GM (1,1).

GM (1,3) had the lowest error rate at 0.88%, followed by GM (1,4), GM (1,2), and GM (1,5). It can be concluded that GM (1,3), which was made up of MSWG data, population density, and GDP/capita, provided the best forecasts for existing MSWG data. As seen in Figure 2(b), the trends from GM (1,2) to GM (1,4) increased or slightly increased in their indication of waste projection, while GM (1,5) decreased. GM (1,5) results indicated that conducting the model with a low correlation of influencing factors did not increase the prediction accuracy or yield a reasonable outcome. Moreover, Hyndman and Athanasopoulos (2021) described that the concise time series should be modeled simply because anything with more than one or two parameters will produce poor forecasts due to the estimation error. Therefore, GM (1,5), which had the highest error, was not used to forecast MSWG in this study.

3.3 Forecasts for MSW generation

Five models, GM (1,1)-0.1, GM (1,1)-0.5, GM (1,2), GM (1,3), and GM (1,4), were selected for use in forecasting MSWG to 2030. Figure 3 shows five trend lines for the forecast results. Three of them exhibited an upward trend, while the other two models indicated a downward trend. The results of annual projections are displayed in Table 3.

The projection of MSWG from GM (1,1)-0.5 was the highest among all models. According to GM (1,1)-0.5, MSWG would increase 26% from 2018 to 2030 (PI: 93,922-99,166). The MSWG/capita would increase 23% from 2018 to 2030 (PI: 1.38-1.45). GM (1,1)-0.1 resulted in a slightly lower MSWG forecast, reduced by 0.9% in 2030 compared to GM (1,1)-0.5.

In the case of GM (1,3), the projection of MSWG increased to 10% by 2030 (PI: 83,029-85,110). The projected MSWG/capita increased to 7% by 2030 (PI: 1.22-1.25). The rates of increase in GM (1,3) were lower compared to those of GM (1,1) because although the GDP values increase continuously, Thailand's population will decline slightly (NESDB, 2013). Therefore, GM (1,3) results indicated a balance between the factors influencing MSWG. In addition, GM (1,3) had a narrow PI finding compared to the other models, except for GM (1,4).

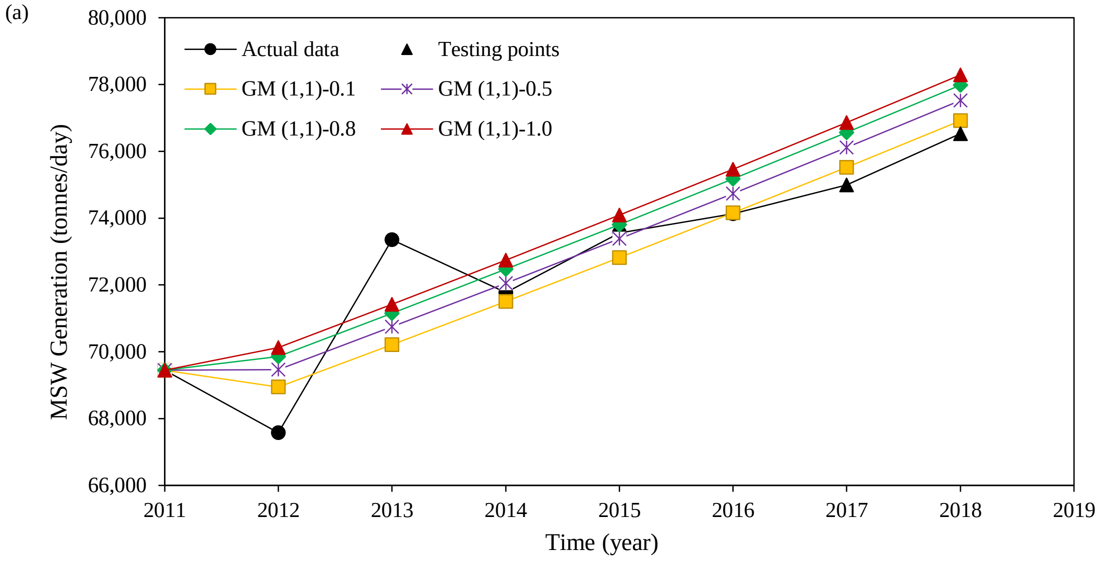

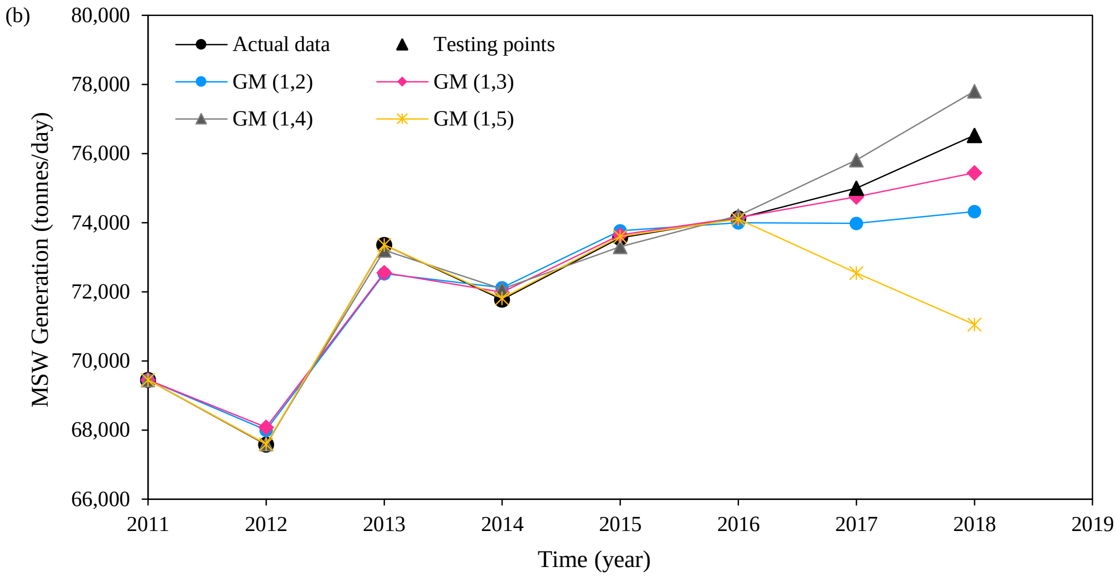

Figure 2. Results of training and testing (a) univariate models, and (b) multivariate models (cont.)

Table 2. Results of model validation using MAPE, MAE, MSE, and RMSE

Classification	No	Model	Average			
			MAPE (%)	MAE	MSE	RMSE
Univariate	1	GM (1,1)-0.1	0.603	456	213,266	462
	2	GM (1,1)-0.5	1.396	1,057	1,120,370	1,058
	3	GM (1,1)-0.8	1.749	1,509	2,279,995	1,510
	4	GM (1,1)-1.0	2.392	1,811	3,283,874	1,812
Multivariate	5	GM (1,2)	2.124	1,615	2,959,891	1,720
	6	GM (1,3)	0.877	669	620,324	788
	7	GM (1,4)	1.378	1,046	1,147,169	1,071
	8	GM (1,5)	5.215	3,966	18,012,534	4,244

Table 3. Forecasts of MSW generation (kt/day), MSW generation rate (kg/capita/day), amount of improperly treated waste (Mt), estimated energy potential (MW), and greenhouse gas emissions ($ktCO_2e$)

Year	MSW generation (kt/day)						Population[a] (Million person)	MSW generation rate (kg/capita/day)						Inappropriately -disposed waste (Mt)		Energy potential (MW)		GHG emissions ($ktCO_{2e}$)	
	Actual data[a]	GM (1,1) -0.1	GM (1,1) -0.5	GM (1,2)	GM (1,3)	GM (1,4)		Actual data[b]	GM (1,1) -0.1	GM (1,1) -0.5	GM (1,2)	GM (1,3)	GM (1,4)	GM (1,1) -0.1	GM (1,3)	GM (1,1) -0.1	GM (1,3)	GM (1,1) -0.1	GM (1,3)
2011	69.450	69.450	69.450	69.450	69.450	69.450	64.076	1.080	1.084	1.084	1.084	1.084	1.084						
2012	67.577	68.944	69.467	68.000	68.079	67.595	64.457	1.050	1.070	1.078	1.055	1.056	1.049						
2013	73.355	70.213	70.749	72.525	72.550	73.202	64.786	1.150	1.084	1.092	1.119	1.120	1.130						
2014	71.779	71.505	72.055	72.119	71.989	72.079	65.125	1.110	1.098	1.106	1.107	1.105	1.107						
2015	73.560	72.820	73.384	73.770	73.646	73.303	65.729	1.130	1.108	1.116	1.122	1.120	1.115						
2016	74.130	74.160	74.738	74.002	74.149	74.203	65.932	1.140	1.125	1.134	1.122	1.125	1.125						
2017	74.998	75.525	76.118	73.976	74.745	75.815	66.189	1.130	1.141	1.150	1.118	1.129	1.145						
2018	76.529	76.915	77.522	74.321	75.444	77.804	66.414	1.150	1.158	1.167	1.119	1.136	1.172						
2019		78.330	78.953	75.963	77.613	75.571	67.990		1.152	1.161	1.117	1.142	1.111	5.241	5.193	311	308	750	749
2020		79.771	80.410	76.246	78.315	75.300	68.128		1.171	1.180	1.119	1.150	1.105	5.337	5.240	317	311	1,039	1,035
2021		81.239	81.894	76.390	78.912	75.182	68.245		1.190	1.200	1.119	1.156	1.102	5.435	5.280	323	313	1,291	1,279
2022		82.734	83.405	76.502	79.499	75.023	68.342		1.211	1.220	1.119	1.163	1.098	5.535	5.319	329	316	1,510	1,488
2023		84.257	84.945	76.588	80.082	74.798	68.417		1.232	1.242	1.119	1.170	1.093	5.637	5.358	335	318	1,704	1,668
2024		85.807	86.512	76.651	80.661	74.501	68.471		1.253	1.263	1.119	1.178	1.088	5.741	5.397	341	320	1,875	1,822
2025		87.386	88.109	76.688	81.237	74.127	68.502		1.276	1.286	1.119	1.186	1.082	5.847	5.435	347	323	2,027	1,956
2026		88.994	89.735	76.700	81.810	73.672	68.511		1.299	1.310	1.120	1.194	1.075	5.954	5.474	353	325	2,164	2,071
2027		90.632	91.391	76.686	82.379	73.130	68.496		1.323	1.334	1.120	1.203	1.068	6.064	5.512	360	327	2,287	2,172
2028		92.300	93.077	76.655	82.954	72.504	68.467		1.348	1.359	1.120	1.212	1.059	6.175	5.550	367	329	2,400	2,259
2029		93.998	94.795	76.578	83.510	71.765	68.394		1.374	1.386	1.120	1.221	1.049	6.289	5.587	373	332	2,504	2,336
2030		95.728	96.544	76.481	84.070	70.928	68.306		1.401	1.413	1.120	1.231	1.038	6.405	5.625	380	334	2,600	2,404

[a]Statistics of registered population during 2011-2018 from the DOPA and the population projection during 2019-2030 from the NESDB; [b]National statistics from the PCD

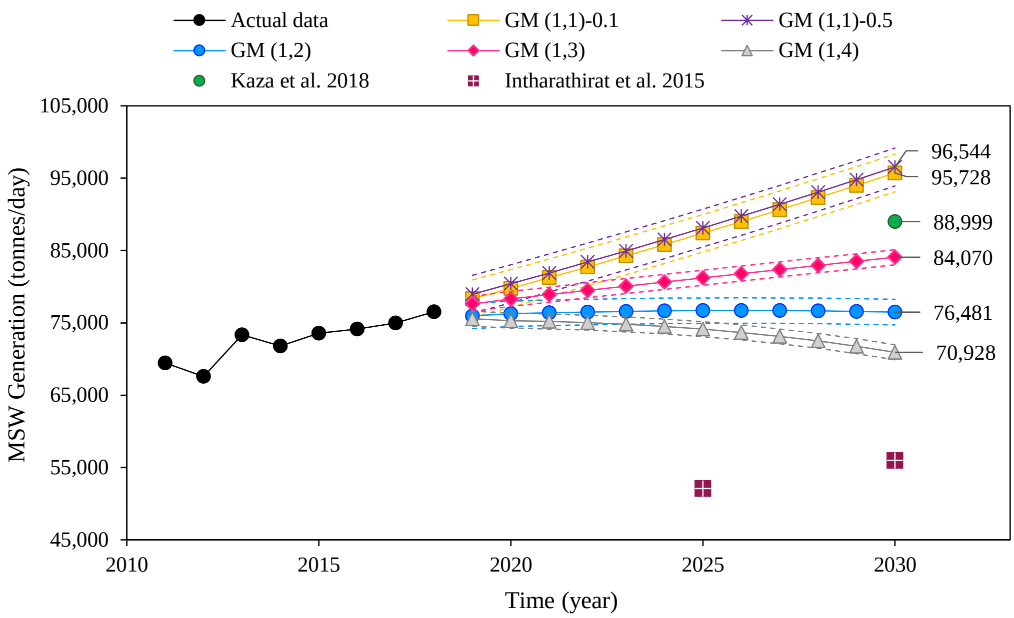

Figure 3. Comparison of forecasts for the MSW generation (tonnes/day) prepared by using five grey models in this study and forecasts conducted by other studies.

GM (1,2) and GM (1,4) showed decreasing trends. The forecasted MSWG for 2030 from GM (1,2) did not differ significantly from 2018 due to the decrease in population. Forecasts from GM (1,4) showed that MSWG would drop by 7% by 2030. Although GM (1,4) had the narrowest PI and the second-highest accuracy from the multivariate model, the downward trend is an unlikely future outcome. Results from these two models indicated that the change of future-influencing factors and model selection had a strong impact on forecasting.

In a previous waste forecast study from Thailand, Kaza et al. (2018) projected waste generation using GDP/capita based on a regression model. Their forecast was in between our results from univariate and multivariate GMs. In another previous study (Intharathirat et al., 2015), the forecasted values for 2025 and 2030 were the lowest (Figure 3) due to the use of a different dataset, as previously mentioned. Kaza et al. (2018) also estimated the average national waste generation rate by region using available data in 2016. The waste generation rate of countries in the East Asia and Pacific region ranged from 0.14 to 3.72 kg/capita/day, with an average of 0.56 kg/capita/day. This study forecasted that the average MSWG/capita for Thais would still be lower than the current rate for East Asia and Pacific countries, even in 2030. Therefore, the forecasting results were reasonable.

Both univariate and multivariate GMs, especially GM (1,1)-0.1 and GM (1,3), performed well although they were modeled with limited data. However, these forecasts are expected to change with the transformation of the population structure, economic factors, consumption trends, and policy and regulation.

3.4 Estimation of GHG emissions and energy potential from improperly treated waste

The presence of impW has negative impacts on both human health and the environment. Sustainable management of MSW inevitably includes eliminating impW. Assuming that MSW disposal would be handled as usual with the rates found in 2017, the amount of impW in 2030, based on GM (1,1)-0.1 and GM (1,3), is shown in Table 3. This impW would lead to uncontrolled GHG emissions estimated to be up to 2,600 $GgCO_2e$ in 2030 (Figure 4). OD of MSW is the biggest GHG emission source through the release of CH_4. The estimated shares of GHG emissions from OD, CD, IN, and OB forecasted for 2030 were 88.3%, 10.1%, 0.4%, and 1.2%, respectively. Thailand's Nationally Determined Contribution Roadmap on GHG Mitigation, launched in 2017, set a target for GHG emission reduction from the waste sector at 1,300 $GgCO_2e$ by 2030. The proposed activities for GHG mitigation included waste reduction at source and waste utilization before final disposal (ONEP, 2017). This study's findings suggest that limiting the MSW, especially organic waste going to open dumpsites, could help the nation mitigate a significant amount of GHG and reach the target. In addition, authorities should also be attentive to the controlled dumpsites across the country, as they can be much deeper or taller than open dumpsites and lead to more CH_4 emissions.

A WTE facility is a type of proper waste disposal that aids in the reduction of MSW mass while also providing an alternative fuel source for energy recovery. Besides the WTE facilities, alternative fuel from MSW has been used continuously instead of fossil fuel in cement industries (Hong et al., 2018). In Thailand, the Alternative Energy Development Plan (AEDP) set a target for energy recovery from MSW of 900 MWe by 2037 (DEDE, 2020). As of 2018, there were 273.4 MWe of WTE facilities installed in Thailand, accounting for almost 30% of the AEDP target (DEDE, 2019). The estimated energy potentials of impW in 2030, based on GM (1,1)-0.1 and GM (1,3) in Table 3, could be part of the fuel for the future WTE facilities to reach the AEDP target. Management of impW as an alternative fuel benefits three sectors: waste management, climate change, and alternative energy. However, fossil CO_2 emissions from burning plastic waste cause concern. The application of CO_2-capture technologies could help mitigate GHG emissions from the processes while avoiding GHG emissions from other fossil fuels (Chandel et al., 2012).

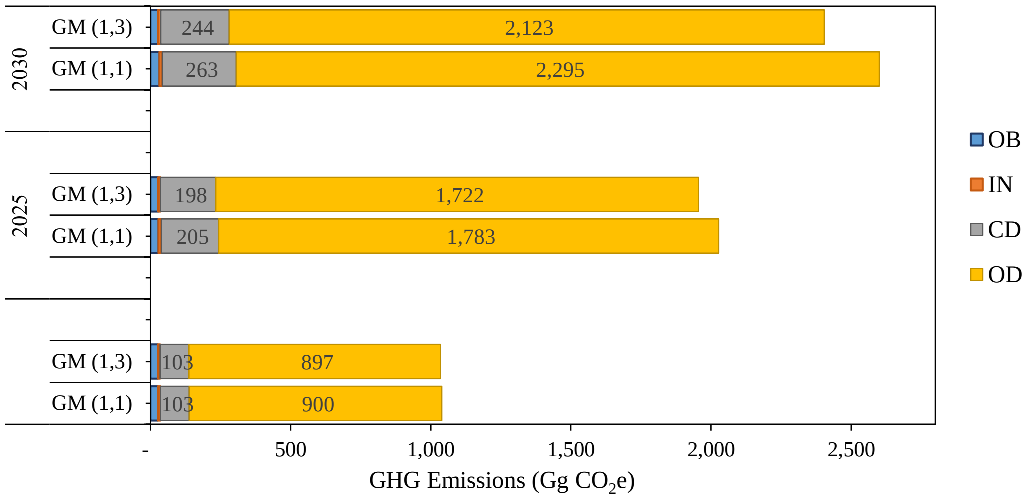

Figure 4. Forecasts of greenhouse gas emissions from improper waste disposal in 2020, 2025, and 2030. (OB=open burning; IN=incineration without pollution prevention; CD=controlled dumping of MSW more than 50 tonnes/day on land; OD=open dumping)

4. CONCLUSION

This study applied univariate and multivariate GMs in forecasting MSWG in Thailand up to 2030, based on the MSW data from 2011-2018. Although GMs can work with limited data, the data stability, the quantity of data, and influencing factors had critical impacts on correlation and forecasting results. The univariate and multivariate models GM (1,1)-0.1 and GM (1,3) offered greater accuracy with a lower error rate than the other six models. As a result, these models were used to forecast MSWG and estimate impW from 2019-2030. Waste generation in 2030 was projected to be 84,070-95,728 tonnes/day (1.23-1.40 kg/capita/day), an approximately 10-25% increase compared to 2018. In a business-as-usual scenario, GHG emission from impW would reach 2,600 $GgCO_2e$ by 2030, with CH_4 emitted from OD accounting for 88.3%. Eliminating dumpsites could help Thailand reach the national GHG mitigation target. The energy potential of impW was projected to be in the range of 334 to 380 MWe. Maximizing the utilization of impW should be prioritized in the future evaluation of national and local policies. In addition, to develop sustainable MSW management in Thailand, it is necessary to increase the efficiency of waste separation at the source and in collection and transportation. Greater attention and further research is needed to investigate the current characteristics of MSW and sorting efficiency, as it affects the design and efficiency of MSW disposal technologies.

ACKNOWLEDGEMENTS

The authors would like to thank Asst. Prof. Dr. Chalor Jarusutthirak, Dr. Rotchana Intharathirat, Dr. Akarapong Untong, and Mr. Supajit Sukkanta for their guidance, and to the Center of Excellence on Hazardous Substance Management, Chulalongkorn University for financial support during the database development. The authors would like to express their gratitude to The Joint Graduate School of Energy and Environment, King Mongkut's University of Technology Thonburi and the Center of Excellence on Energy Technology and Environment, Ministry of Higher Education, Science, Research and Innovation for the financial support provided to perform this study.

REFERENCES

Adamović VM, Antanasijević DZ, Ristić M, Perić-Grujić AA, Pocajt VV. An optimized artificial neural network model for the prediction of rate of hazardous chemical and healthcare waste generation at the national level. Journal of Material Cycles and Waste Management 2018;20:1736-50.

Ali-Abdoli M, Falah-Nezhad M, Salehi-Sede R, Behboudian S. Longterm forecasting of solid waste generation by the artificial neural networks. Environment Progress and Sustainable Energy 2012;31(4):628-36.

Armstrong J. Principles of Forecasting: A Handbook for Researchers and Practitioners. Boston, MA: Kluwer Academic Publishers; 2001.

American Society for Testing and Materials (ASTM). Standard Test Method for Determination of the Composition of Unprocessed Municipal Solid Waste. West Conshohocken, USA: ASTM; 2016.

Asuero AG, Sayago A, González AG. The correlation coefficient: An overview. Critical Reviews in Analysis Chemistry 2006;36(1):41-59.

Beigl P, Wassermann G, Schneider F, Salhofer S. Forecasting municipal solid waste generation in major European cities. Proceedings of the 2nd International Congress on Environmental Modelling and Software; 2004 Jun 1-7; Osnabrück: Germany; 2004.

Ceylan Z. Estimation of municipal waste generation of Turkey using socio-economic indicators by Bayesian optimization tuned Gaussian process regression. Waste Management and Research 2020;38(8):840-50.

Chandel MK, Kwok G, Jackson RB, Pratson LF. The potential of waste-to-energy in reducing GHG emissions. Carbon Management 2012;3(2):133-44.

Chhay L, Reyad MAH, Suy R, Islam MR, Mian MM. Municipal solid waste generation in China: Influencing factor analysis and multi-model forecasting. Journal of Material Cycles and Waste Management 2018;20(3):1761-70.

Chung SS. Projecting municipal solid waste: The case of Hong Kong SAR. Resources, Conservation and Recycling 2010;54(11):759-68.

Dai F, Nie G, Chen Y. The municipal solid waste generation distribution prediction system based on FIG-GA-SVR model. Journal of Material Cycles and Waste Management 2020;22(5):1352-69.

Deng J. Control problems of grey systems. Systems and Control Letters 1982;1(5):288-94.

Department of Alternative Energy Development and Efficiency (DEDE). Alternative Energy Development Plan: AEDP2015. Thailand: Department of Alternative Energy Development and Efficiency; 2015. (in Thai).

Department of Alternative Energy Development and Efficiency (DEDE). Alternative Energy Development Plan: AEDP2018. Thailand: Department of Alternative Energy Development and Efficiency; 2020. (in Thai).

Department of Alternative Energy Development and Efficiency (DEDE). Thailand Energy Efficiency Situation 2018. Thailand: Department of Alternative Energy Development and Efficiency; 2019. (in Thai).

Department Of Provincial Administration (DOPA). Official statistics registration systems [Internet]. 2018 [cited 2018 Jan 30]. Available from: http://stat.dopa.go.th/stat/statnew/upstat_age_disp.php. (in Thai).

Di-Foggia G, Beccarello M. Designing waste management systems to meet circular economy goals: The Italian case. Sustainable Production and Consumption 2021;26:1074-83.

Duman GM, Kongar E, Gupta SM. Estimation of electronic waste using optimized multivariate grey models. Waste Management 2019;95:241-9.

Dyson B, Chang NB. Forecasting municipal solid waste generation in a fast-growing urban region with system dynamics modeling. Waste Management 2005;25(7):669-79.

Estay-Ossandon C, Mena-Nieto A. Modelling the driving forces of the municipal solid waste generation in touristic islands. A case study of the Balearic Islands (2000-2030). Waste Management 2018;75:70-81.

Ghinea C, Drăgoi EN, Comăniţă ED, Gavrilescu M, Câmpean T, Curteanu S, et al. Forecasting municipal solid waste generation using prognostic tools and regression analysis. Journal of Environmental Management 2016;182:80-93.

Han Z, Liu Y, Zhong M, Shi G, Li Q, Zeng D, et al. Influencing factors of domestic waste characteristics in rural areas of developing countries. Waste Management 2018;72:45-54.

Hong GB, Huang CF, Lin HC, Pan TC. Strategies for the utilization of alternative fuels in the cement industry. Carbon Management 2018;9(1):95-103.

Hyndman RJ, Athanasopoulos G. Forecasting: Principles and Practice. 2nd ed. Melbourne, Australia: OTexts; 2018.

Hyndman RJ, Athanasopoulos G. Forecasting: Principles and Practice. 3rd ed. Melbourne, Australia: OTexts; 2021.

Intharathirat R, Abdul-Salam P, Kumar S, Untong A. Forecasting of municipal solid waste quantity in a developing country using multivariate grey models. Waste Management 2015; 39:3-14.

Intergovernmental Panel on Climate Change (IPCC). 2006 IPCC Guideline for National Greenhouse Gas Inventories, Volume 5: Waste. Japan: Institute for Global Environmental Strategies; 2006.

Intergovernmental Panel on Climate Change (IPCC). IPCC. Climate Change 2014: Synthesis Report. Contribution of Working Groups I, II and III to the Fifth Assessment Report of the Intergovernmental Panel on Climate Change. Geneva, Switzerland: IPCC; 2014.

Javed SA, Liu AS. Bidirectional absolute GRA/GIA model for uncertain systems: Application in project management. IEEE Access 2019;7:60885-96.

Johnson NE, Ianiuk O, Cazap D, Liu L, Starobin D, Dobler G, et al. Patterns of waste generation: A gradient boosting model for short-term waste prediction in New York City. Waste Management 2017;62:3-11.

Kannangara M, Dua R, Ahmadi L, Bensebaa F. Modeling and prediction of regional municipal solid waste generation and diversion in Canada using machine learning approaches. Waste Management 2018;74:3-15.

Kaza S, Yao L, Bhada-Tata P, Van-Woerden F. What a Waste 2.0: A Global Snapshot of Solid Waste Management to 2050. Thailand: World Bank Publications; 2018.

Kumar A, Samadder SR. An empirical model for prediction of household solid waste generation rate: A case study of Dhanbad, India. Waste Management 2017;68:3-15.

Lewis CD. Industrial and Business Forecasting Methods. London, United Kingdom: Butterworth Scientific; 1982.

Namlis KG, Komilis D. Influence of four socioeconomic indices and the impact of economic crisis on solid waste generation in Europe. Waste Management 2019;89:190-200.

Noori R, Abdoli MA, Ghazizade MJ, Samieifard R. Comparison of neural network and principal component-regression analysis to predict the solid waste generation in Tehran. Iranian Journal of Public Health 2009;38(1):74-84.

National Statistical Office (NSO). Statistical Data Services: Household-Socio-Economic-Survey [Internet]. 2018 [cited 2018 Jan 30]. Available from: http://www.nso.go.th/sites/2014en/Pages/survey/Social/Household/The-2017-Household-Socio-Economic-Survey.aspx.

Office of Natural Resources and Environmental Policy (ONEP). Thailand's Nationally Determined Contribution (NDC) Roadmap on Mitigation 2021-2030. Thailand: Office of Natural Resources and Environmental Policy; 2017. (in Thai).

Office of The National Economic and Social Development Board (NESDB). Population Projections for Thailand 2010-2040. Thailand: Office of The National Economic and Social Development Board; 2013. (in Thai).

Office of The National Economic and Social Development Board (NESDB). Gross Domestic Product, Chain Volume Measures. Thailand: Office of The National Economic and Social Development Board; 2018.

Oribe-Garcia I, Kamara-Esteban O, Martin C, Macarulla-Arenaza AM, Alonso-Vicario A. Identification of influencing municipal characteristics regarding household waste generation and their forecasting ability in Biscay. Waste Management 2015;39:26-34.

Pudcha T, Phongphiphat A, Towprayoon S. Greenhouse gas mitigation and energy production potentials from municipal solid waste management in Thailand through 2050. Earth Systems and Environment 2022; advance online publication, 13 July 2022 https://doi.org/10.1007/s41748-022-00323-z.

Pollution Control Department (PCD). Publication-annual report [Internet]. 2022a [cited 2022 Jul 17]. Available from: https://www.pcd.go.th/publication. (in Thai).

Pollution Control Department (PCD). State of solid waste in the country [Internet]. 2022b [cited 2022 Jul 17]. Available from: https://thaimsw.pcd.go.th/report_country.php. (in Thai).

Phongphiphat A, Limpiti T, Pudcha T. Thailand's MSW Forecasting Model for Sustainable MSW Management and Utilization. Thailand: Center of Excellence on Hazardous Substance Management; 2019.

Rimaityte I, Ruzgas T, Denafas G, Račys V, Martuzevicius D. Application and evaluation of forecasting methods for municipal solid waste generation in an Eastern-European city. Waste Management and Research 2012;30(1):89-98.

Sifeng L, Yi L. Grey Systems: Theory and Applications. Springer Complexity; 2010.

Sukholthaman P, Sharp A. A system dynamics model to evaluate effects of source separation of municipal solid waste management: A case of Bangkok, Thailand. Waste Management 2016;52:50-61.

Sun N, Chungpaibulpatana S. Development of an appropriate model for forecasting municipal solid waste generation in Bangkok. Energy Procedia 2017;138:907-12.

Tiwari MK, Bajpai S, Dewangan UK. Prediction of industrial solid waste with ANFIS model and its comparison with ANN model: A case study of Durg-Bhilai Twin City India. International Journal of Engineering and Innovative Technology 2008;6(2):192-201.

Towprayoon S, Phongphiphat A. Greenhouse Gas Reduction from Solid Waste Management at Municipality Level of Thailand. Thailand: Thailand Greenhouse Gas Management Organization; 2013.

Weng YC, Fujiwara T, Matsuoka Y. An analysis of municipal solid waste discards in Taiwan based on consumption expenditure and policy interventions. Waste Management and Research 2010;28(3):245-55.

Wichai-utcha N, Chavalparit O. 3Rs Policy and plastic waste management in Thailand. Journal of Material Cycles and Waste Management 2019;21:10-22.

Wu WY, Chen SP. A prediction method using the grey model GMC(1, n) combined with the grey relational analysis: A case study on Internet access population forecast. Applied Mathematics and Computation 2005;169(1):198-217.

Xiao S, Huijuan D, Yong G, Xu T, Chang L, Haifeng L. Policy impacts on municipal solid waste management in Shanghai: A system dynamics model analysis. Journal of Cleaner Production 2020;262:Article No. 121366.

Zhang Y. The prediction of the generation of municipal solid waste based on grey combination model. Advanced Materials Research 2013;807:1479-82.

Zhang Z, Zhang Y, Wu D. Hybrid model for the prediction of municipal solid waste generation in Hangzhou, China. Waste Management and Research 2019;37(8):781-92.

Species Diversity, Aboveground Biomass, and Carbon Storage of Watershed Forest in Phayao Province, Thailand

Sitthisak Pinmongkhonkul[1,4], Warin Boonriam[2*], Warach Madhyamapurush[3,4], Niti Iamchuen[5], Panupong Chaiwongsaen[1], Dej Mann[3], Prathakphong Riyamongkol[3], Kriengkrai Seetapan[6], and Sasitorn Hasin[7]

[1]*Department of Biology, School of Science, University of Phayao, Phayao 56000, Thailand*
[2]*Faculty of Environment and Resource Studies, Mahidol University, Nakhon Pathom 73170, Thailand*
[3]*Innovation and Technology Transfer Institute, University of Phayao, Phayao 56000, Thailand*
[4]*Unit of Excellence for Water Management Research, School of Science, University of Phayao, Phayao 56000, Thailand*
[5]*Research Unit of Spatial Innovation Development, School of Information and Communication Technology, University of Phayao, Phayao 56000, Thailand*
[6]*School of Agriculture and Natural Resources, University of Phayao, Phayao 56000, Thailand*
[7]*Innovation of Environmental Management, College of Innovative Management, Valaya Alongkorn Rajabhat University under the Royal Patronage, Pathum Thani 13180, Thailand*

ARTICLE INFO

Received: 28 Apr 2022
Received in revised: 22 Sep 2022
Accepted: 26 Sep 2022
Published online: 2 Nov 2022
DOI: 10.32526/ennrj/21/202200121

Keywords:
Tree diversity/ Tree biomass/ Carbon sequestration/ Seasonal tropical forest/ Phayao

*** Corresponding author:**
E-mail:
warin.boo@mahidol.ac.th;
waboorin@hotmail.com

ABSTRACT

Restoration of watershed forest ecosystems can perform different disturbance regimes over remnant forests, which can ultimately affect plant diversity, soil formation, and carbon storage. To address an issue, this study assessed tree species diversity, aboveground biomass (AGB), and aboveground carbon (AGC) storage of the watershed forest in Phayao Province, Thailand. Data collection was conducted in 18 plots along nine watersheds along the topographic gradients. Tree height and diameter at breast height (DBH) were collected. AGB of vegetation was estimated by using the allometric equation. Likewise, AGC storage was evaluated from half of AGB. A total of 133 species belonging to 105 genera and 39 families were recorded from the watershed forests (1.8 ha). Mixed deciduous forest (MDF) and dry evergreen forest (DEF) exhibited high density and high diversity index, respectively. The highest value of total AGC storage was found in the MDF with 91.2 ton C/ha, following by DEF (78.3 ton C/ha) and dry dipterocarp forest (DDF) (60.5 ton C/ha). Detrended correspondence analysis (DCA) revealed that the occurrences of *Albizia saman*, *Hopea odorata*, *Lagerstroemia calyculata*, and *Acrocarpus fraxinifolius* related to AGB, AGC, slope, and tree canopy in the DEF. Intensity of slope influenced tree species occurrence in the watershed forest of Phayao.

1. INTRODUCTION

Tropical forests have the greatest biodiversity, which contribute up to 50% of the terrestrial primary production and 25% of global terrestrial carbon. Likewise, the highest biomass stock per hectare (ha) is in tropical forests, with values above 200 ton/ha. (FAO, 2020). Tropical forests are important as a global CO_2 sink (IPCC, 2001) with an estimate of 3.1-3.7×1,016 g of carbon (C) per year (equivalent to 11.4-13.6×1,016 g of CO_2) absorbed and converted into plant materials. (Solomon et al., 2007; Malhi and Grace, 2000). During the twentieth century, biodiversity has been threatened by human activity and climate change which affects primary productivity, carbon sequestration, and species diversity (FAO, 2010). In particular, climate events, such as El Niño, have an impact on biodiversity and the ecosystem that is essential to human life (Sala et al., 2000). Thus, assessing aboveground biomass (AGB) as well as aboveground carbon (AGC) storage precisely helps in moderating the effect of climate change. Also, clarification of biomass and carbon storage of plant diversity could allow us to better understand the function of the forests and ecological services.

Citation: Pinmongkhonkul S, Boonriam W, Madhyamapurush W, Iamchuen N, Chaiwongsaen P, Mann D, Riyamongkol P, Seetapan K, Hasin S. Species diversity, aboveground biomass, and carbon storage of watershed forest in Phayao Province, Thailand. Environ. Nat. Resour. J. 2023;21(1):47-57. (https://doi.org/10.32526/ennrj/21/202200121)

In Thailand, forest cover was estimated to be 43.33% of the country's total area in 1973. Forest cover has declined significantly to 25.1% in 1999 due to expanding agricultural land (RFD, 2016). However, forest cover of Thailand has been approximately stable at 31.57-31.62% from 2014 to 2019 according to the current estimates of forest area by Royal Forest Department (RFD, 2020). Meanwhile, the other land use was about 46% and 22% for agriculture and non-agriculture, respectively. In the north, forests are mainly characterized by the presence of mixed deciduous forest (MDF) and dry dipterocarp forest (DDF) which account for 53.39% and 11.43%, respectively (RFD, 2007; Chaiyo et al., 2011). Deforestation and forest degradation have created serious problems in the forest ecosystem as well as soil and water management problems (Steininger et al., 2001). Erosion of soil due to land use patterns of shifting cultivators in Northern Thailand degrades the watershed area.

Watershed forest plays a significant role in forest hydrology, absorbing rainfall to maintain stream flows, underground waters, and reservoirs (Gilmour, 2014). The fluctuations of warming temperatures and variable precipitation are expected to affect the ecosystem of the watershed forest and also the water situation (Sintayehu, 2018). This issue is the challenge for monitoring forest productivity and function which can approach the conservation and management of natural resource values such as protecting local resources, enhancing biodiversity, and sustaining productive biomass. Previous studies have considered that the increase in plant species diversity will increase AGC storage (Poorter et al., 2015; Mensah et al., 2016). In addition, forest type influences the impact of 12% on AGC storage, which means the relationship between AGC and attributed factors varies across forest types (Jia et al., 2022). In order to support the improvement of the 2006 IPCC rules for national greenhouse gas inventories, Jha et al. (2020) predicted that the rate of AGB and AGC recovery was around 50% greater in 2019 than in the last 20 years for secondary Thai tropical forests.

The watershed forest of Phayao Lake (Kwan Phayao) is the origin of the Ing River Basin as a tributary of the Mekong River. Generally, the forests where the original source of the rivers to Kwan Phayao are mainly the MDF, DDF, dry evergreen forest (DEF), and moist evergreen forest (MEF) (Klaydach and Khunrattanasiri, 2012). However, the Ing Watershed has occurred as the main three-dimensional problem comprising the extreme drought in the dry season, severe flooding in the rainy season, and water quality at the present. Thus, it is essential to observe the characteristics of the watershed forest in Phayao and the situation of the forest. This is one of the best approaches for evaluating forest management problems. Consequently, this study was conducted to determine the tree species diversity, AGB, and AGC storage in a watershed forest in Phayao Province, Thailand.

2. METHODOLOGY

2.1 Study area

The study was performed in a tropical seasonal forest in Phayao Province, Northern Thailand. The study sites were in most of Doi Luang National Park representing the watershed forest of Phayao Lake (Kwan Phayao) and Ing River (19°10´N, 99°80´E; about 500-700 m above sea level) which flows to the Mekong River. In this study, the watershed forest was divided into nine sub-watershed areas based on the main reservoir in each sub-district (Figure 1) as follows; 1) Mae Tam reservoir, Mae Tam Sub-district (P1), Mae Na Ruea reservoir, Mae Na Ruea Sub-district (P2), Ban Ton reservoir; Ban Ton-Ban Sang Sub-district (P3), Huai Thap Chang reservoir, San Pa Muang Sub-district (P4), Huai Luek reservoir, Ban Tom Sub-district (P5), Huai Mae Tum reservoir, Tha Cham Pe Sub-district (P6), Huai Mae Yian reservoir, Ban Mai Sub-district (P7), Mae Chawa reservoir, Mae Suk Sub-district (P8), and Mae Suk reservoir, Mae Suk Sub-district (P9). The total annual rainfall was 1,137 mm with the monthly rainfall less than 90 mm during the dry season from November to April. The mean annual temperature was 25.9ºC (13.7-36.0ºC). The total means of elevation and slope in the study plots (n=18) were 597±69.4 m (508-760 m) and 14.8±8.3% (2.15-32.4%), respectively.

2.2 Data collection on plant diversity, community structure, and topography

A total of 18 main plots (50 m × 20 m in each) were established in the watershed forest of Phayao. Twenty subplots (10 m × 10 m in each) were set up in each sub-watershed area (Figure 2). The surveyed data on plant diversity and community structure were recorded during the period from 2019 to 2020. All trees were identified, with measurement of diameter at breast height (DBH, ≥4.5 cm) at 1.3 m above ground, and height (m) measured by the principle of triangulation with a clinometer. The tree species were identified by using the identification of wild plants Vol. 1 and Vol. 2 (DNP, 2007a; DNP, 2007b).

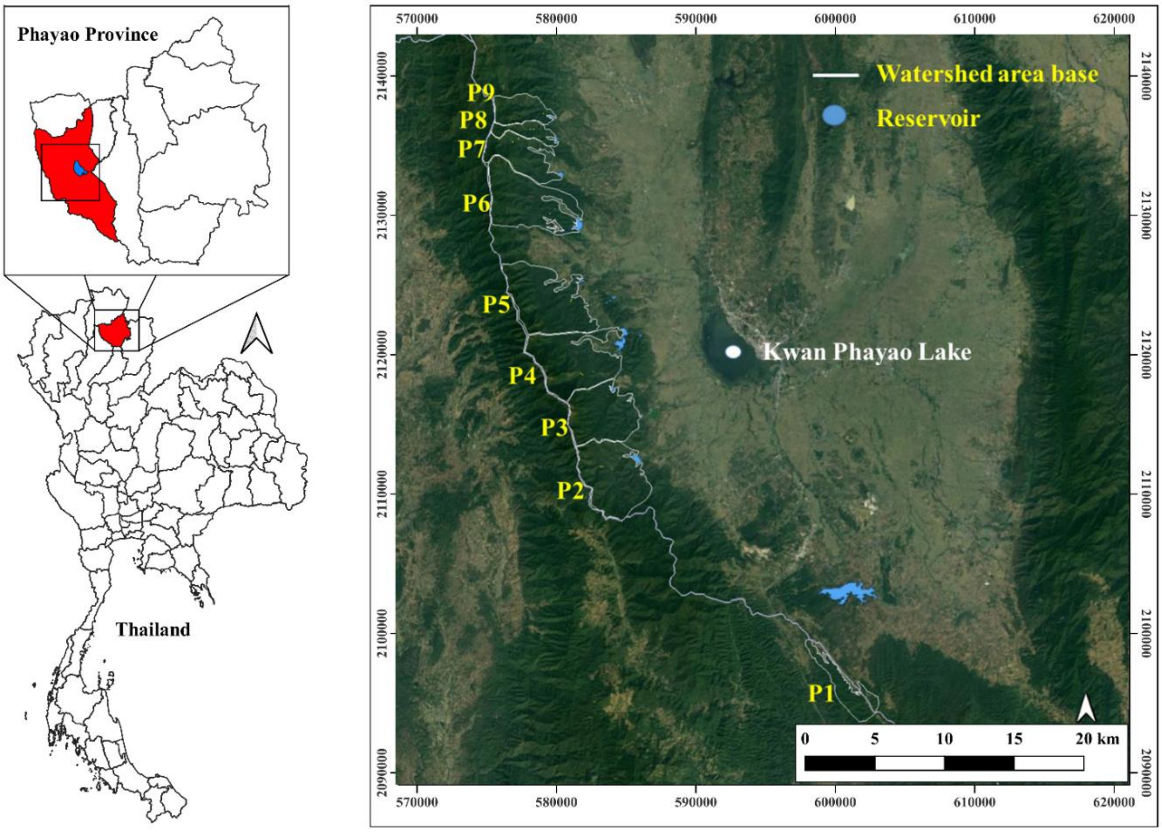

Figure 1. Study area in watershed forest of Phayao Lake (Kwan Phayao) and Ing River

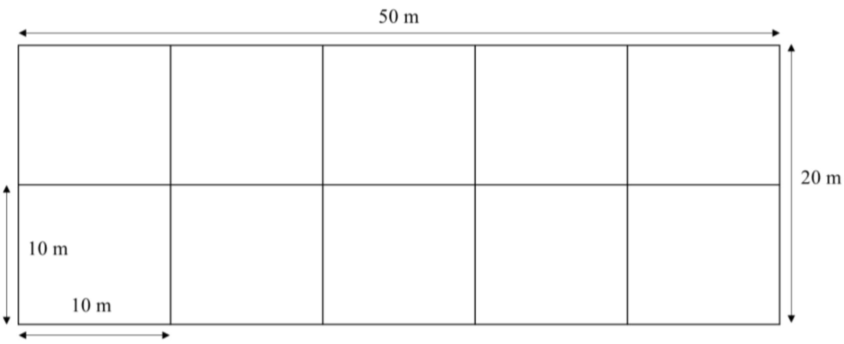

Figure 2. Experiment design of main plot (1,000 m^2) with placement of 100 m^2 in each subplot

Species diversity and community structure of the trees were calculated using the Shannon-Wiener diversity index (H′), Margalef richness (R), and Equitability of Pielou (J´) (Krebs, 1985). These statistical analyses were performed by using PAST statistics software ver. 3.0. The relative ecological importance of each tree species was expressed using the Importance Value Index (IVI), which was calculated as Equation (1):

$$\text{IVI} = \text{RDo} + \text{RD} + \text{RF} \quad (1)$$

Where; RDo is Relative dominance, RD is Relative density, RF is Relative frequency, which was calculated as follow (2),(3),(4):

$$\text{Rdo} = (\text{total basal area of a species}/\text{total basal area of all species}) \times 100 \quad (2)$$

$$\text{RD} = (\text{number of individuals of a species}/\text{total number of individuals}) \times 100 \quad (3)$$

$$\text{RF} = (\text{frequency of a species}/\text{sum frequency of all species}) \times 100 \quad (4)$$

The tree density (Di) in the plots was calculated by using the Equation (5) as follows:

$$\mathrm{Di} = (\mathrm{Xi}/\mathrm{ai}) \tag{5}$$

Where; Di is the tree density, Xi is the total number of species of trees (i), and ai is the study area of the tree (i).

Site-specific elevation, slope, and soil loss were measured at each study site. The elevation of the study area was measured in meters above sea level (m.a.s.l.). Soil loss (A) was evaluated by using a model of Universal Soil Loss Equation (USLE) (Wischmeier and Smith, 1978) which implemented in ArcGIS 10.1 software supposes the multiplication of the five involved factors, at the level of each grid cell with 30 m spatial resolution, using Raster calculator tool (6):

$$\mathrm{A} = \mathrm{R} \times \mathrm{K} \times \mathrm{L} \times \mathrm{S} \times \mathrm{C} \times \mathrm{P} \tag{6}$$

Where; R is the rainfall-runoff erosivity factor, K is a soil erodibility factor, L is the slope length factor, S is the slope gradient factor, C is a cover management factor, and P is a supporting practices factor.

2.3 ABG allometric equation and AGC storage

ABG in the watershed forests was calculated using the specific allometric equation as a function of tree height (H), and DBH (D), including the biomass of stem (Ws)(7), biomass of branch (Wb)(8), and biomass of leaf (Wl)(9). The sum of Ws, Wb, and Wl (Wtc is a total mass of stem and branch) is the total ABG in a tree. The ABG allometric equations were used to analyze for DDF and MDF in this study (Ogawa et al., 1965) as follows:

$$\mathrm{Ws} = 0.0396 \times (\mathrm{D}^2 \times \mathrm{H})^{0.9326} \tag{7}$$

$$\mathrm{Wb} = 0.003487 \times (\mathrm{D}^2 \times \mathrm{H})^{1.0270} \tag{8}$$

$$\mathrm{Wl} = (28.0/\mathrm{Wtc} + 0.025)^{-1} \tag{9}$$

Generally, ABG is considered for an average AGC of approximately 45 to 50% (by oven-dry mass) in all plant species (Schlesinger, 1991). According to various applications, as well as this study, the AGC of vegetation was calculated by multiplying the biomass amounts with the average carbon contents (0.475) in the trees (Solomon et al., 2007).

2.4 Statistical analysis

Pearson’s correlation test was used to examine relationships between AGB and tree sizes (i.e., DBH and height). Tree species were grouped based on the similarity of their attributes by using hierarchical clustering analysis. Based on the ordination analysis, detrended correspondence analysis (DCA) was used to elucidate the relationships between biological assemblages of tree species and environmental factors. All these statistical analyses were performed by using PC-ORD ver. 5.10.

3. RESULTS

3.1 Forest composition and species density

The forest in Phayao watershed had 1,464 tree individuals recorded representing 133 species from 105 genera and 39 families from the total area (1.8 ha). *Lagerstroemia calyculata* and *Gigantochloa albociliata* accounted for the highest number of individuals of wood and bamboo, respectively. The highest number of species was represented by Fabaceae with eight genera and 15 species, while the other families contributed from one to nine species (Supplementary data: Table S1). According to the topographic gradient, the highest number of tree individuals (205 individuals) was found in P2 consisting of 23 families, 35 genera, and 37 species, while the lowest was found in P1 (91 individuals) consisting of 17 families, 24 genera, and 26 species (Table 1). At each site, the forests were dominated by a number of family of Fabaceae, except for the P7. The average tree density was 813 individuals/ha in the watershed forest consisting of the highest and the lowest of the tree densities in P2 and P1, respectively.

3.2 Tree diversity value index and Importance Value Index (IVI)

The highest tree diversity value index was found in P9 with 3.75, 11.56, and 0.77 of Shannon-Wiener diversity index (H′), richness index, and equitability index, respectively. While the watershed forest in P5 showed the lowest of the biodiversity indices except for the richness indices by Margalef index (R) (Table 2). The range of species diversity index (H′) was between 2.75 to 3.75.

Table 1. Species composition, density, total basal of stem, and its topography of watershed forest of Phayao Lake (Kwan Phayao), Thailand

Forest site	Elevation (m)	Slope (%)	Family	Genus	Species	Density (individual/ha)	Basal area of stem (m^2/ha)	USLE (ton/ha/year)
P1	575	20.80	17	24	26	455	26.39	0.65
P2	614	8.06	23	35	37	1,025	32.51	0.61
P3	556	7.69	22	36	38	940	31.05	0.68
P4	667	21.09	21	32	35	815	23.97	2.86
P5	512	7.82	25	34	38	875	28.89	4.76
P6	536	13.05	19	30	31	720	25.23	1.30
P7	701	24.32	24	40	42	1,005	26.40	1.26
P8	584	14.61	25	43	47	730	25.06	0.81
P9	537	16.77	30	53	59	755	28.70	0.69
Mean±SD	597±69.4	14.8±8.4	23±3.8	36±8.3	39±9.5	813±176.4	27.58±2.80	1.51±1.41

Table 2. Species richness and biodiversity index of trees in Phayao Watershed Forest

Forest site	Number of species	Density		Richness indices (Margalef index (R))	Shannon-Wiener diversity index (H′)	Variances (H)	Equitability J. Index (E)
		Wood (tree/ha)	Bamboo (clump/ha)				
P1	26	450	5	5.54	2.96	0.007	0.61
P2	37	1,025	0	6.76	2.95	0.006	0.60
P3	38	940	0	7.06	3.19	0.005	0.65
P4	36	810	5	6.87	2.99	0.008	0.61
P5	38	580	295	7.16	2.75	0.011	0.56
P6	31	555	165	6.03	2.97	0.007	0.61
P7	42	980	25	7.73	3.36	0.004	0.69
P8	47	640	90	9.23	3.35	0.009	0.68
P9	59	685	70	11.56	3.75	0.006	0.77
Average±SD	39±9	741±206	73±100	7.55±1.83	3.14±0.30	0.010±0.002	0.64±0.06

The most important species of the watershed forests were indicated by the Importance Value Index (IVI) as shown in Figure 3. In each forest site, the most important species were *A. saman* (Fabaceae) (36.0%), *Terminalia corticosa* (Combretaceae) (38.6%), *Protium serratum* (Burseraceae) (43.9%), *Shorea siamensis* (Dipterocarpaceae) (45.3%), and *Quercus kerrii* (Fagaceae) (44.3%) in the P1, P2, P5, P6, and P7, respectively. The tree species *Xylia xylocarpa* (Fabaceae) was the most important species at 33.4% and 48.5% in both P3 and P4, respectively, while *L. calyculata* (Lythraceae) the highest important species at 36.2% and 21.9% in P8 and P9, respectively. Based on IVI, the forest sites were classified as DDF in P6 and P7, MDF in P2, P3, P4, and P5, and DEF in P1, P8, and P9. The basal area of tree stem was highest in the MDF at 29.11 m^2/ha, followed by the DEF (26.72) and DDF (25.82).

Overall, this study found that the highest density was 1025 individuals/ha in P2 (MDF) at 614 m and 8.06% of the mean elevation and slope, respectively. This MDF had the most important species of *T. corticosa* (Combretaceae) at 38.6%. In terms of diversity index, the tree biodiversity (diversity, richness, equilibrium indices) along the study areas was highest in P9 (DEF) at 537 m and 16.77% of the mean elevation and slope, respectively. Likewise, this DEF had the most important species of *L. calyculata* (Lythraceae) at 21.9%.

3.3 AGB and AGC storage

The total AGB of living trees (DBH≥4.5) was 1516.58 ton/ha. The highest and the lowest total AGB were estimated at 230 ton/ha in P3 (MDF) and 109 ton/ha in P6 (DDF), respectively (Figure 4). The average AGB (±SD) was 168.51±46.09 ton/ha with the mean per individual of 1.14±2.40 ton/tree/ha. Therefore, the total AGC storage in the watershed forest of this study was 720.58 ton C/ha with an average of 80.04±21.89 ton C/ha. Giving integrative result, there was no a significant different between the DDF (60.5±12.2 ton C/ha), MDF (91.2±21.4 ton C/ha), and DEF (78.3±22.8 ton C/ha) (p=0.299).

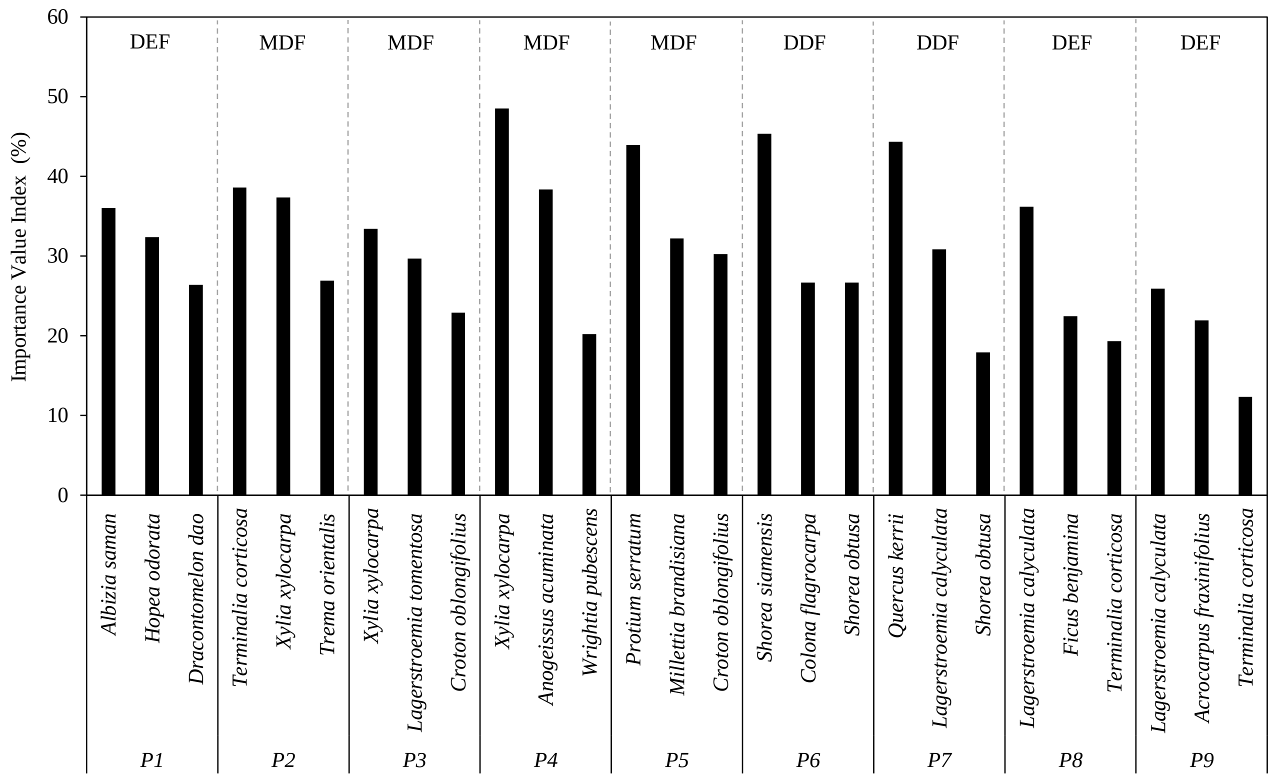

Figure 3. Importance value index (IVI) of dominant tree species (top three species of IVI value) in each forest type of Phayao Watershed Forest

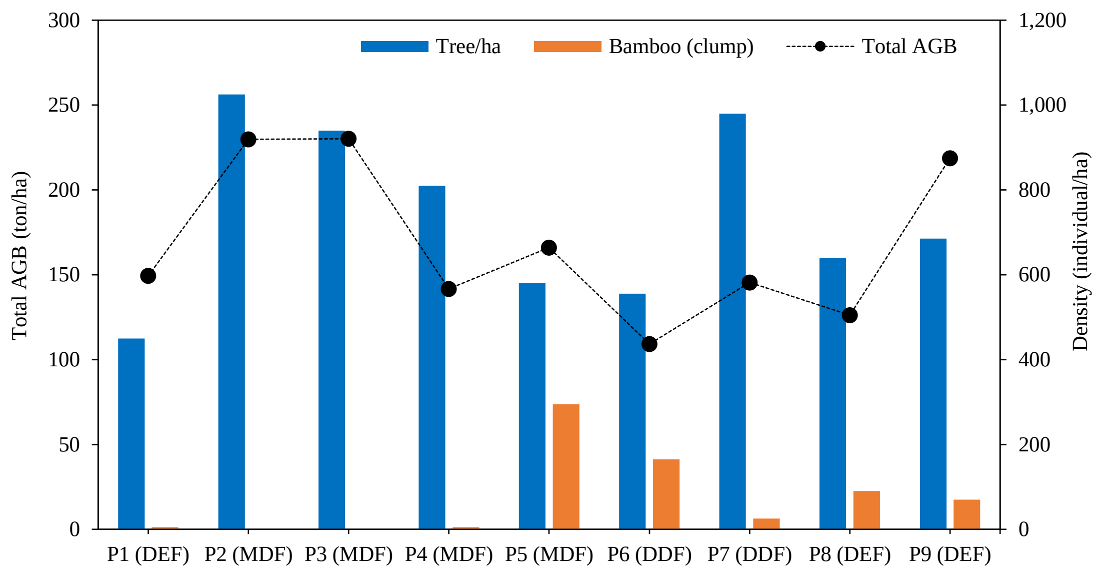

Figure 4. Total AGB and tree density of vegetation in Phayao Watershed Forest

In this study, the bigger trees were relatively high in AGB with the mean (±SD) of DBH and height was 17.7±12.7 cm and 12.8±6.7 cm, respectively. The linear regression analysis showed a significant positive relationship between AGB and both DBH ($p<0.0001$) (regression equation: $Y=0.1655x-1.8056$, $R=0.883$, $R^2=0.779$) and height ($p<0.0001$) (regression equation: $Y=0.2132x-1.6081$, $R=0.596$, $R^2=0.356$) of the trees (Figure 5). Based on family, the highest and lowest mean of the AGB was Irvingiaceae at 6.18 ton/ha and Olacaceae at 0.02 ton/ha, respectively. Based on species, *Ficus benjamina* had the highest AGB in the forest with 29 ton/ha, while *Sterculia guttata* had the lowest AGB with 0.018 ton/ha.

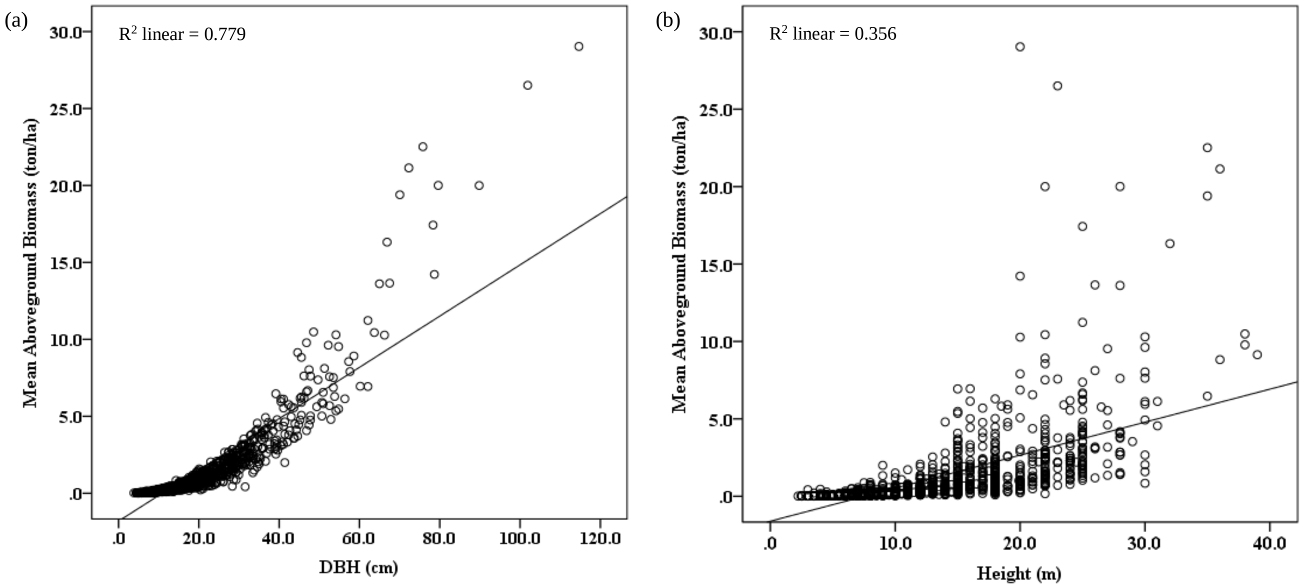

Figure 5. Relationship between aboveground biomass and tree size: DBH (a) and height (b)

3.4 Species distribution on environmental gradients

Based on cluster analysis, the similarity of tree species was grouped from each site using Sorensen (Bray-Curtis) distance technique with information remaining more than 60% as shown in Figure 6. Thus, the tree species in Phayao watershed forest can be divided into five groups as follows:

Group 1 (P1) was distinguished from the others with 100% of dissimilarity. This group was discriminated by composing of the dominant exotic *A. saman*, and native *H. odorata* at an altitude of 575 m and 21% of slope in DEF.

Group 2 (P2 and P5) were found at altitudes ranging from 512 to 614 m and 7.8-8.1% of slope in MDF. The dominant trees belonging to this group were *Millettia brandisiana*, *Croton oblongifolius*, and *Dalbergia cultrata*.

Group 3 (P8 and P9) was found at altitudes ranging from 537 to 584 m and 14.6-16.8% of slope in DEF contributed by the dominance of *L. calyculata*, *T. corticosa*, and *Colona flagrocarpa*.

Group 4 (P6 and P7) was classified as DDF at altitudes of 536-701 m and 13.0-24.3% of slope. The group showed the information remaining almost 100%. It was composed of the dominant tree species *Shorea obtusa*, *S. siamensis*, and *L. calyculata.*

Group 5 (P3 and P4) was located at altitudes ranging from 556 to 667 m and 7.7-21.1% of slope in MDF. This group was dominated by *X. xylocarpa*, *C. oblongifolius*, and *L. calyculata*.

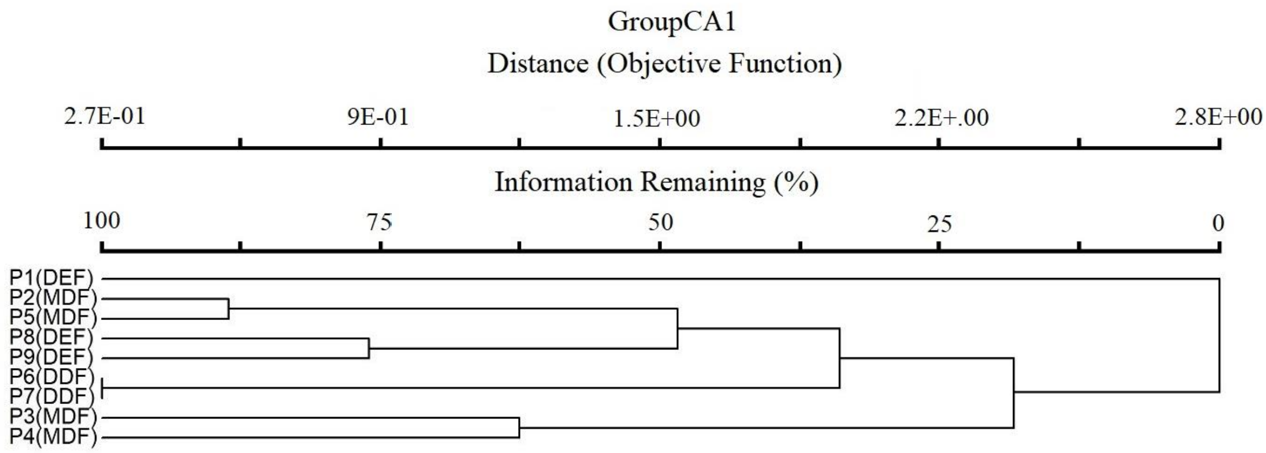

Figure 6. Dendrogram showing a hierarchical relationship among 133 tree species at nine sampling sites in the watershed forest of Phayao.

Correlation among 133 plant species, nine study sites (with vegetation coverage i.e., DDF, MDF, DEF), tree parameters and ecological variables of study sites were illustrated through DCA (Figure 7). In constrained DCA ordination, the maximum explanatory variation was accounted for PC1 axis, in which the maximum explanatory variation was accounted for Axis 1 (0.86) and lower variation on the Axis 2 (0.61). The maximum strength of plant community was represented by specific tree parameters (i.e., tree density and height). The influence of tree parameters and ecological variables (i.e., AGB, slope and tree canopy) were the most representative drive of plant community structure into two community groups along the ecological gradients and tree parameters in watershed forest areas, in which the first group is DEF and MDF, and the second group is DDF. Interestingly, the DCA revealed unique tree species (i.e., *A. saman*, *H. odorata*, *L. calyculata*, and *A. fraxinifolius*) in the DEF, in which its occurrences are related to AGB, slope, and tree canopy. While most tree species in MDF are related to their height and density. Therefore, the slope of the area influenced tree species distribution in the watershed forest.

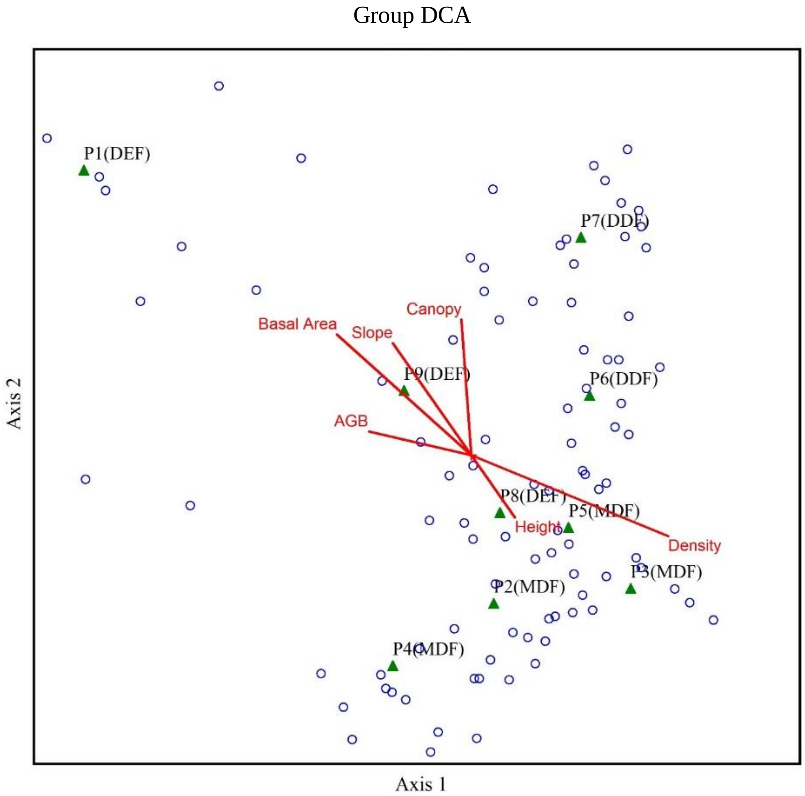

Figure 7. DCA analysis of plant communities in the study area (P1-P9) and environment factors at Phayao Watershed Forest

4. DISCUSSION

Our result showed that the forest types along the watershed area of Phayao Lake (Kwan Phayao) and Ing River can be roughly classified as DEF, MDF, and DDF based on the watershed area. The watershed forest consisted predominantly of Fabaceae (233 individuals), Lythraceae (107 individuals), Euphorbiaceae (98 individuals), Combretaceae (93 individuals), and Dipterocarpaceae (88 individuals) in the study sites. High biodiversity index was found in DEF (P9). The highest density was shown in the MDF (P2 and P3) and DEF (P7), respectively. The highest individual (295 clumps/ha) of Gramineae was found in P5 (MDF). Many previous studies have reported that the important species as well as the dominant species of tree were different in the same forest type of the tropical seasonal forest due to the vegetation structure and composition, topographical gradient, altitude, and disturbance (Marod et al., 1999; Khamyong, 2009; Chaiyo et al., 2012; Liu et al., 2014; Sungpalee et al., 2015). As stated by Liu et al. (2014), the species diversity and composition changed along the topographical gradient as well as the distinction in DEF of group 1 (P1). As in this result, tree diversity was changed by the slope area according to the ordination. However, it was also clear that the spatial distribution of trees was strongly impacted by elevation in mountain ecosystem, northern Thailand (Marod et al., 2019).

According to forest type based on IVI, this study found that the dominant species in DDF were *S. siamensis*, *Q. kerrii*, and *S. obtusa*, mixing with *L. calyculata* and *C. flagrocarpa*. Lamotte et al. (1998) reported that the dominant species were *S. obtusa*, *S. talura*, *Dipterocarpus intricatus*, *Q. kerrii*, *Mitragyna brunonis*, *X. xylocarpa*, *Morinda coreia*, and *Lannea coromandelica* in DDF of northeastern, Thailand. Also, tree species *S. obtusa*, *S. siamensis*, *L. coromandelica*, and *D. Obtusifolius* were important contributors in DDF of western Thailand (Chaiyo et al., 2011). While in DDF in the north of Thailand, the dominant tree species were reported to be *D. obtusifolius*, *D. tuberculatus*, *S. obtusa*, and *S. siamensis* in Doi Suthep-Pui National Park (Khamyong et al., 2018), as well as in the Huai Hong Khrai Royal Development Study Center, and Mae Tha Community Forest, Chiang Mai (Phongkhamphanh et al., 2015).

In the case of MDF, it is well-known that tree species *Tectona grandis* (Teak) is commonly dominant in some other locations in Thailand (Seanchanthong, 2005; Podong et al., 2013; Khamyong et al., 2018). However, *T. grandis* did not appear in some areas (Marod et al., 1999; Phonchaluen, 2009; Chaiyo et al., 2011), that is related to our result, only one individual *T. grandis* was found in P3 (MDF). Our results showed that the MDFs contained mixed stands of important tree species belonging to families such as Fabaceae (*X. xylocarpa* and *M. brandisiana*), Combretaceae (*T. corticosa*), Burseraceae (*P. serratum*), Euphorbiaceae (*C. oblongifolius*), Cannabaceae (*Trema orientalis*), Lythraceae (*Lagerstroemia tomentosa*), and Gramineae (*G. albociliata*).

In the case of DEF, this forest type was composed of dominant tree species *L. calyculata* (Lythraceae), *A. saman* (Fabaceae), *H. odorata* (Dipterocarpaceae), *F. benjamina* (Moraceae), and *A. fraxinifolius* (Fabaceae). Similarly, other reports of DEF had mixed stands of Dipterocarpaceae in Doi Suthep-Pui National Park (Khamyong et al., 2018) as well as in DEF at the Sakaerat Biosphere Reserve, northeastern, Thailand. (Lamotte et al., 1998).

Generally, AGB and AGC storage in the trees increases relatively with increasing density and tree size, and this was seen in the results of this study. Although this study showed a high total AGB of 230 ton/ha in the MDF, it was lower than MDF (311 ton/ha) in Chiang Mai, northern Thailand. In addition, the total average AGB (168.5 ton/ha) of this forest was lower than the total AGB (372.7 ton/ha) in a tropical forest at Doi Inthanon National Park, Chiang Mai, Thailand (Sungpalee et al., 2015). However, this average was higher than in the other sites (MDF) of northern Thailand as follows; Ogawa et al. (1961) showed a total of 49.60 ton/ha in Chiang Mai and 57.50 ton/ha in Lampang, while Kaewkrom et al. (2011) reported that the AGB was 104.59 and 50.95 ton/ha in a primary and secondary MDF in Phetchabun, respectively.

In the DDF, the total AGB ranged from 109 to 145 ton/ha, which was similar to the total AGB of 142.95 ton/ha in northeast Thailand (Senpaseuth et al., 2009). However, the mean AGB (186.4 ton/ha) in DDF at Chaiyaphum, northeast Thailand was higher than this study (Ounkerd et al., 2015). In contrast, there was a much lower AGB of 81.9 (20-40% of slope) and 23.8 ton/ha (<20% of slope) in DDF of western Thailand than this study with 13-24% of slope (Chaiyo et al., 2011).

In the DEF, the total AGB ranged from 129 to 219 ton/ha. This was higher than the AGB in DEF at Thong Pha Phum District, Kanchanaburi Province (140.58 ton/ha) (Terakunpisut et al., 2007), and the north of Thailand (126 ton/ha) (Ogawa et al., 1965). However, the mean of the AGB in this DEF was lower than the mean of DEF (331.75 ton/ha) in Nong Khai Province, northeast, Thailand (Senpaseuth et al., 2009). A result from Sungpalee et al. (2015) reported that a lower tropical montane forest in Doi Inthanon National Park, Chiang Mai, showed a greater AGB value for the middle elevation than at the low and high elevation, while the mean AGB did not significantly differ among the slope aspect and inclination.

Based on DCA, slope area was significantly associated with species distribution, AGB, and AGC storage. According to the results, the relationship between AGB and tree density was negative, while the relationship was positive with tree basal area and canopy cover. On the other hand, Jia et al. (2022) showed that the relationship between stand density and AGC was positive, while the influence of individual tree size variation on AGC storage was negative. However, the occurrences of tree species (1.7-6.6 m^2/ha of basal area), especially *A. saman*, *H. odorata*, *L. calyculata*, and *A. fraxinifolius* were related to AGB and AGC storage in Phayao Watershed Forest. Future studies should further investigate the plant species distribution in enlarged scale areas and spatial factors by using remote sensing in the assessment of AGB and AGC storage covering different forest types.

5. CONCLUSION

Overall, 133 tree species were found in the Phayao Watershed Forest. The study shows the species occurrences are practically related to AGB, AGC, slope, and tree canopy in DEF. Although the AGB and AGC were not related to tree density and height in MDF, there were related to the stand basal area and canopy cover in DEF comprising the highest tree diversity. Therefore, horizontal size variation in tree species could influence the enhancement of AGB as well as AGC storage. Based on the distribution gradient of the tree community, the distribution of tree species in the watershed forest was impacted by slope intensity. This study found that species-specific habitat is essential for improvements and can be applied to watershed forest management in the future. Nevertheless, the study suggests that spatial distribution data (e.g., soil characteristics and streamflow) is necessary for evaluating tree assemblages and diversity patterns.

ACKNOWLEDGEMENTS

This study was financially supported by National Research Council of Thailand (NRCT). The demonstration and laboratory of this work was mainly supported by the Unit of Excellence for Water Management Research (FF64-UoE006), School of Science, University of Phayao. We are thankful to the staff of Doi Luang National Park for their advice and support in the fieldwork. We thank Dr. Trin Seramethakun for his main assistance in identifying tree species.

REFERENCES

Chaiyo U, Garivait S, Wanthongchai K. Carbon storage in above-ground biomass of tropical deciduous forest in Ratchaburi Province, Thailand. World Academy of Science, Engineering and Technology 2011;5(10):636-41.

Chaiyo U, Garivait S, Wanthongchai K. Structure and carbon storage in aboveground biomass of mixed deciduous forest in western region, Thailand. GMSARN International Journal 2012;6:143-50.

Department of National Parks, Wildlife and Plant Conservation (DNP). Manual for Studies of Wild Plants. Volume 1. Bangkok, Thailand: Ministry of Natural Resources and Environment; 2007a. (in Thai).

Department of National Parks, Wildlife and Plant Conservation (DNP). Manual for Studies of Wild Plants. Volume 2. Bangkok, Thailand: Ministry of Natural Resources and Environment; 2007b. (in Thai).

Food and Agriculture Organization (FAO). Global Forest Resource Assessment: Main Report. Rome, Italy: FAO; 2010.

Food and Agriculture Organization (FAO). Global Forest Resource Assessment: Main Report. Rome, Italy: FAO; 2020.

Gilmour D. Forests and Water: A Synthesis of the Contemporary Science and Its Relevance for Community Forestry in the Asia-Pacific Region. RECOFTC Issue Paper No. 3. Bangkok, Thailand: RECOFTC-The Center for People and Forests; 2014.

Intergovernmental Panel on Climate Change (IPCC). Climate Change 2001: A Scientific Basis. Cambridge, UK: University Press; 2001.

Jha N, Tripathi NK, Chanthorn W, Brockelman W, Nathalang A, P´elissier R. et al. Forest abovegroundbiomass stock and resilience in a tropical landscape of Thailand. Biogeosciences 2020;17(1):121-34.

Jia B, Guo W, He J, Sun M, Chai L, Liu J, et al. Topography, diversity, and forest structure attributes drive aboveground carbon storage in different forest types in northeast China. Forests 2022;13:Article No. 455.

Kaewkrom P, Kaekla N, Thummikkapong S, Punsang S. Evaluation of carbon storage in soil and plant biomass of primary and secondary mixed deciduous forests in the lower northern part of Thailand. African Journal of Environmental Science and Technology 2011;5(1):8-14.

Khamyong N. Plant Species Diversity, Soil Characteristics and Carbon Accumulation in Different Forests, Doi Suthep-Pui National Park, Chiang Mai Province [dissertation]. Chiang Mai, Chiang Mai University; 2009.

Khamyong N, Wangpakapattanawong P, Chairuangsri S, Inta A, Tiansawat P. Tree species composition and height-diameter allometry across three forest types in Northern Thailand. Chiang Mai University Journal of Natural Sciences 2018;17(4):289-306.

Klaydach T, Khunrattanasiri W. Using of vegetation indices from THAICHOTE satellite data for forest types classification in Doi Luang National Park, Chiang Rai Province. Proceedings of the 33rd Asian Conference on Remote Sensing 2012 (ACRS 2012); 2012 November 26-30; Pattaya, Thailand: 2012.

Krebs CJ. Ecology: The Experimental Analysis of Distribution and Abundance. New York, USA: Harper and Row Publisher; 1985. p. 800.

Lamotte S, Gajaseni J, Malaisse F. Structure diversity in three forest types of north-eastern Thailand (Sakaerat Reserve, Pak Tong Chai). Biotechnology, Agronomy and Society and Environment 1998;2(3):192-202.

Liu J, Yunhong T, Slik JWF. Topography related habitat associations of tree species traits, composition and diversity in a Chinese tropical forest. Forest Ecology and Management 2014;330:75-81.

Malhi Y, Grace J. Tropical forests and atmospheric carbon dioxide. Trends in Ecology and Evolution 2000;15:332-37.

Marod D, Hermhuk S, Sungkaew S, Thinkampheang S, Kamyo T, Nuipakdee W. Species composition and spatial distribution of dominant trees in the forest ecotone of a mountain ecosystem, northern Thailand. Environment and Natural Resources Journal 2019;17(3):40-9.

Marod D, Kutintara U, Yarwudhi C, Tanaka H, Nakashisuka T. Structural dynamics of a natural mixed deciduous forest in western Thailand. Journal of Vegetation Science 1999;10: 777-86.

Mensah S, Veldtman R, Assogbadjo AE, Glèlè Kakaï R, Seifert T. Tree species diversity promotes aboveground carbon storage through functional diversity and functional dominance. Ecology and Evolution 2016;6:7546-57.

Ogawa H, Yoda K, Kira T. A preliminary survey on the vegetation of Thailand. Nature and Life in Southeast Asia 1961;1:21-157.

Ogawa H, Yoda K, Ogino K, Kira T. Comparative ecological studies on three main type of forest vegetation in Thailand II. Plant Biomass. Nature and Life in Southeast Asia 1965;4:49-80.

Ounkerd K, Sunthornhao P, Puangchit L. Valuation of carbon stock in trees at Khao Wong Community Forest, Chaiyaphum Province. Thai Journal of Forestry 2015;34(1):29-38.

Phonchaluen S. Plant Species Diversity, Soil Characteristics and Utilization of Ban Sai Thong Community Forest, Pa Sak Sub-District, Mueang District, Lamphun Province [dissertation]. Chiang Mai, Chiang Mai University; 2009.

Phongkhamphanh T. Khamyong S, Onpraphai T. Variations in plant diversity and carbon storage among subtype community in a dry dipterocarp community forest of Mae Tha sub-district, Mae On District, Chiang Mai Province. Thai Journal of Forestry 2015;34(3):83-98.

Podong C, Poolsiri R, Katzensteiner K, Pengthamkeerati P, Thongdeenok P. Species diversity and litter dynamics in secondary mixed deciduous forest, Thung Salaeng Lung National Park, Northern, Thailand. Folia Forestalia Polonica, Serie A. Forestry 2013;55(4):196-204.

Poorter L, van der Sande MT, Thompson J, Arets EJ, Alarcón A, Álvarez-Sánchez J, et al. Diversity enhances carbon storage in tropical forests. Global Ecology and Biogeography 2015; 24:1314-28.

Royal Forest Department (RFD). Forest in Thailand. Bangkok, Thailand: Ministry of Natural Resources and Environment; 2007.

Royal Forest Department (RFD). Forestry Statistics Year 2016. Bangkok, Thailand: Ministry of Natural Resources and Environment; 2016. (in Thai).

Royal Forest Department (RFD). Forest Statistics Data. Bangkok, Thailand: Ministry of Natural Resources and Environment; 2020.

Sala OE, Chapin III FS, Armesto JJ, Berlow R, Bloomfield J, Dirzo R, et al. Biodiversity-global biodiversity scenarios for the year 2100. Science 2000;287:1770-4.

Schlesinger WH. Biogeochemistry, an Analysis of Global Change. New York, USA: Academic Press; 1991.

Seanchanthong D. Plant Species Diversity and Soil Characteristics of Forest Communities in Pang Ma Pha District, Mea Hong Son Province [dissertation]. Chiang Mai, Chiang Mai University; 2005.

Senpaseuth P. Navanugraha C, Pattanakiat S. The estimation of carbon storage in dry evergreen and dry dipterocarp forests in Sang Khom District, Nong Khai Province, Thailand. Environment and Natural Resources Journal 2009;7(2):1-11.

Sintayehu DW. Impact of climate change on biodiversity and associated key ecosystem services in Africa: A systematic review. Ecosystem Health and Sustainability 2018;4(9):225-39.

Solomon S, Qin D, Manning M, Chen Z, Marquis M, Averyt KB, et al. Climate Change 2007: The Physical Science Basis, Contribution of Working Group I to the Fourth Assessment Report of the Intergovernmental Panel on Climate Change. Cambridge, UK: University Press; 2007.

Steininger MK, Tucker CJ, Townshend JRG, Killeen TJ, Desch A, Bell V, et al. Tropical deforestation in the Bolivian Amazon. Environmental Conservation 2001;28(2):127-34.

Sungpalee W, Sri-ngernyuang K, Kanzaki M, Itoh A, Nanami S. Spatial biomass variation, biomass dynamics and species diversity in relation to topographic factors of lower tropical montane forest. Thai Journal of Forestry 2015;34(3):69-82.

Terakunpisut J, Gajaseni N, Ruankawe N. Carbon sequestration potential in aboveground biomass of Thong Pha Phum National Forest Thailand. Applied Ecology and Environmental Research 2007;5(2):93-102.

Wischmeier WH, Smith DD. Predicting Rainfall Erosion Losses. A Guide to Conservation Planning, Agriculture Handbook, No. 537. Washington DC, USA: Department of Agriculture; 1978. p. 58.

Socio-Economic Contribution of *Zanthoxylum armatum* (Timur) in the Rural Household Income of Myagdi District, Nepal

Bijaya Neupane[1,2], Navin Gautam[1], Mahamad Sayab Miya[1*], Anju Upadhyaya[1], Yajna Prasad Timilsina[1], Deepak Gautam[1,3], Shalikram Kandel[1], and Bijaya Dhami[1]

[1]*Institute of Forestry, Pokhara Campus, Tribhuvan University, Pokhara 33700, Nepal*
[2]*Department of Forest Sciences, Faculty of Agriculture and Forestry, University of Helsinki 00014, Finland*
[3]*School of Ecology and Nature Conservation, Beijing Forestry University, Beijing 100083, China*

ARTICLE INFO

Received: 28 Apr 2022
Received in revised: 22 Sep 2022
Accepted: 26 Sep 2022
Published online: 25 Nov 2022
DOI: 10.32526/ennrj/21/202200175

Keywords:
Dependency/ Households/ Income/ Livelihood/ Medicinal plant/ Regression

*** Corresponding author:**
E-mail: sayabmiya13@gmail.com

ABSTRACT

Non-timber forest products (NTFPs) contribute to livelihood of rural communities which is influenced by numerous socio-economic variables. This study assessed the financial contribution of *Zanthoxylum armatum* and the influence of respondents' various socio-economic characteristics on such contribution in Ghatan of Beni Municipality, Myagdi District, Nepal. For this study, we used semi-structured questionnaires to 80 purposively selected households, followed by 10 key informant interviews, four focus group discussions, and direct field observations. A Pearson correlation matrix was used to determine the dependence of several socio-economic variables on average annual household income from the sale of *Z. armatum*. The average annual income per household from the sale of *Z. armatum* was found to be the highest (494 USD) in Brahmin/Chhetri households and the lowest (372 USD) in Dalit households. Among five variables used in the regression model, only three of them: land holding size (khet), time taken to harvest (days), and wealth ranking (rich) were found positively significant with p-values of 0.042, 0.000, and 0.064 respectively. Whereas, the education status of the respondents (literate) and the main income source (agriculture) were found negatively significant with p-values of 0.046 and 0.064, respectively. Furthermore, we believe that this result will help to promote the conservation of *Z. armatum* and other valuable medicinal plants as well as their sustainable management in the study area and similar areas.

1. INTRODUCTION

Non-timber forest products (NTFPs) are those forest resources other than timbers that originate from plants, animals, and minerals; and also include forest services that can be marketed, or have scenic, social, cultural, and religious significance (Ahenkan and Boon, 2011). They comprise Medicinal and Aromatic Plants (MAPs), fruits, bamboo and rattan, wild vegetables, tannin, gums, dyes, resins, and others (Hammet, 2004). NTFPs are well-known in the local and international markets for their multiple uses, as an ingredient, for example in herbal medicines, cosmetics, tea, food, etc. (Banjade and Paudel, 2008). They are one of the possible alternatives for the enhancement of the local economy and sustainable forest management (Wiersum and Ros-Tonen, 2005; Mukul et al., 2010; Kar and Jacobson, 2012). Additionally, NTFPs are considered important for their potential for socio-cultural value, poverty alleviation, and biodiversity conservation (Shackleton and Pullanikkatil, 2019; Reta et al., 2020; Sahoo et al., 2020).

Among the NTFPs of Nepal, *Zanthoxylum armatum* (Nepali name: Timur) is one of the prioritized species for cultivation and economic development (DPR, 2006; Phuyal et al., 2019). *Z. armatum* is a shrub or small tree which reaches up to 6 m in height. It has glabrous branches with reddish brown stipular spines, imparipinnate leaves, minute and polygamous flowers, and a small drupe, reddish, ovoid, and glandular warted fruits (enclosing single rounded and shining black seeds) (Grierson and Long,

Citation: Neupane B, Gautam N, Miya MS, Upadhyaya A, Timilsina YP, Gautam D, Kandel S, Dhami B. Socio-economic contribution of *Zanthoxylum armatum* (Timur) in the rural household income of Myagdi District, Nepal. Environ. Nat. Resour. J. 2023;21(1):58-66. (https://doi.org/10.32526/ennrj/21/202200175)

1991; Nair and Nayar, 1997). The species grows well in moist areas with deep soils exposed to sun, degraded slopes, open pastures, wastelands, shrub lands, and forests (natural as well as secondary scrub with adequate rainfall) (Phuyal et al., 2019). According to the IUCN (2022), it is under the least concerned species category. *Z. armatum* is distributed from hot valleys of subtropical to the temperate region of several Asian countries (Nair and Nayar, 1997). In Nepal, it is distributed at an elevation range of 1,100-2,900 m from east to west (Shrestha et al., 2022).

The rural people of Nepal, as a source of their household income, have been trading *Z. armatum* since the early 80s (Manandhar, 1986; Malla et al., 1993; Kunwar et al., 2018). Due to its increasing demand and market price, rural people have started to cultivate the plant commercially (Phuyal et al., 2019). According to the DoF (2014), Nepal exports roughly 90% of *Z. armatum* in raw form to India. It is also exported to China (He et al., 2018), and a small quantity to European countries (Phuyal et al., 2019). In Nepal, many herbal and ayurvedic medicine companies use *Z. armatum* in various products. A total of 2,990.71 USD royalty was collected from the trade of 418,179 kg of *Z. armatum* from Nepal in 2015 only. It was 2,448.41 USD for 17,896 kg in 2011 and 16,709.98 USD for 240,206 kg in 2013 (DoF, 2013; DoF, 2015). The Salyan District (which includes pocket areas of *Z. armatum*) alone contributed 16,658.73 USD to 272,200 kg in 2015 (DFO, 2015). According to Lamichhane et al. (2021), it covered 28% of the total traded volume of NTFPs in the fiscal year 2019-2020 in the Jajarkot District. *Z. armatum* has played an important role in uplifting the economic status of rural communities (Phuyal et al., 2019). The species could be promoted as an alternative cash crop to increase the income of rural farmers, which may improve their livelihoods and contribute to rural poverty alleviation.

The Myagdi District of Nepal has favorable environment and climate for diverse MAPs (such as *Paris polyphylla*, *Bergenia ciliata*, *Acorus calamus*, *Asparagus racemosus*, *Swertia chirayita*, and *Nardostachys grandiflora*). Hence, Ghatan village of ward No. 9 of Beni Municipality was allocated as the *Z. armatum* pocket area of the district, and the people of this area have been regularly involved in its cultivation. But despite being selected as a pocket area, there has been limited research on the linkage of the species to the household's income. Since proper attention has not been paid to the value and conservation of *Z. armatum* and its contribution to livelihood at a local level. This study was conducted to document the economic potential and contribution of *Z. armatum* to the household income of rural people. Furthermore, this study may contribute to the conservation of *Z. armatum* and other valuable medicinal plants, as well as their long-term management in the study area and similar other areas.

2. METHODOLOGY

2.1 Study area

The study was carried out in the Ghatan Village of Beni Municipality, Myagdi District, Nepal. The district has a total area of 2,297 km^2, an elevation range of 792 m to 8,167 m, and is located between 83º20'10.28'E and 28º36'10.42'N. The temperature ranges from 3ºC to 36ºC. Beni Municipality lies in the headquarter of the district and comprises 10 wards. Ghatan lies in ward No. 9 of the municipality, about 7 km north of Beni Bazar (district headquarter). This ward combines the former Ghatan and Toripani Villages, and its altitude ranges from 1,400 m to 2,500 m (Figure 1). According to data provided by the municipality office, the ward has 800 households and a population of 4,132 people. Due to its exceptionally suitable cultivating conditions in ward No. 9, the village of Ghatan was assigned as a pocket area for *Z. armatum* production by the Division Forest Office (DFO), Myagdi. The people of the village are involved in agriculture, cultivation of *Z. armatum*, foreign employment, government jobs, and livestock rearing. No research activities about *Z. armatum* as well as other medicinal plants have been conducted in this area to date. So, this area was selected for conducting our research after a discussion with the DFO, Myagdi.

2.2 Data collection

2.2.1 Household survey

Among the total 800 households of the study area, 80 households were purposively selected that were directly involved in cultivation and collection of *Z. armatum* for the questionnaire survey. We interviewed the selected households by using the semi-structured questionnaire (Iponga et al., 2018). The questionnaire mainly consisted of the household information related to the household and commercial uses of *Z. armatum*, whether cultivated or not in the private farmland, yearly contribution to the household income, quantities harvested or collected annually, etc. The total annual income of each respondent's household was the variable used for determining the wealth rankings of households. The questionnaires were pre-tested and finalized before conducting the household survey.

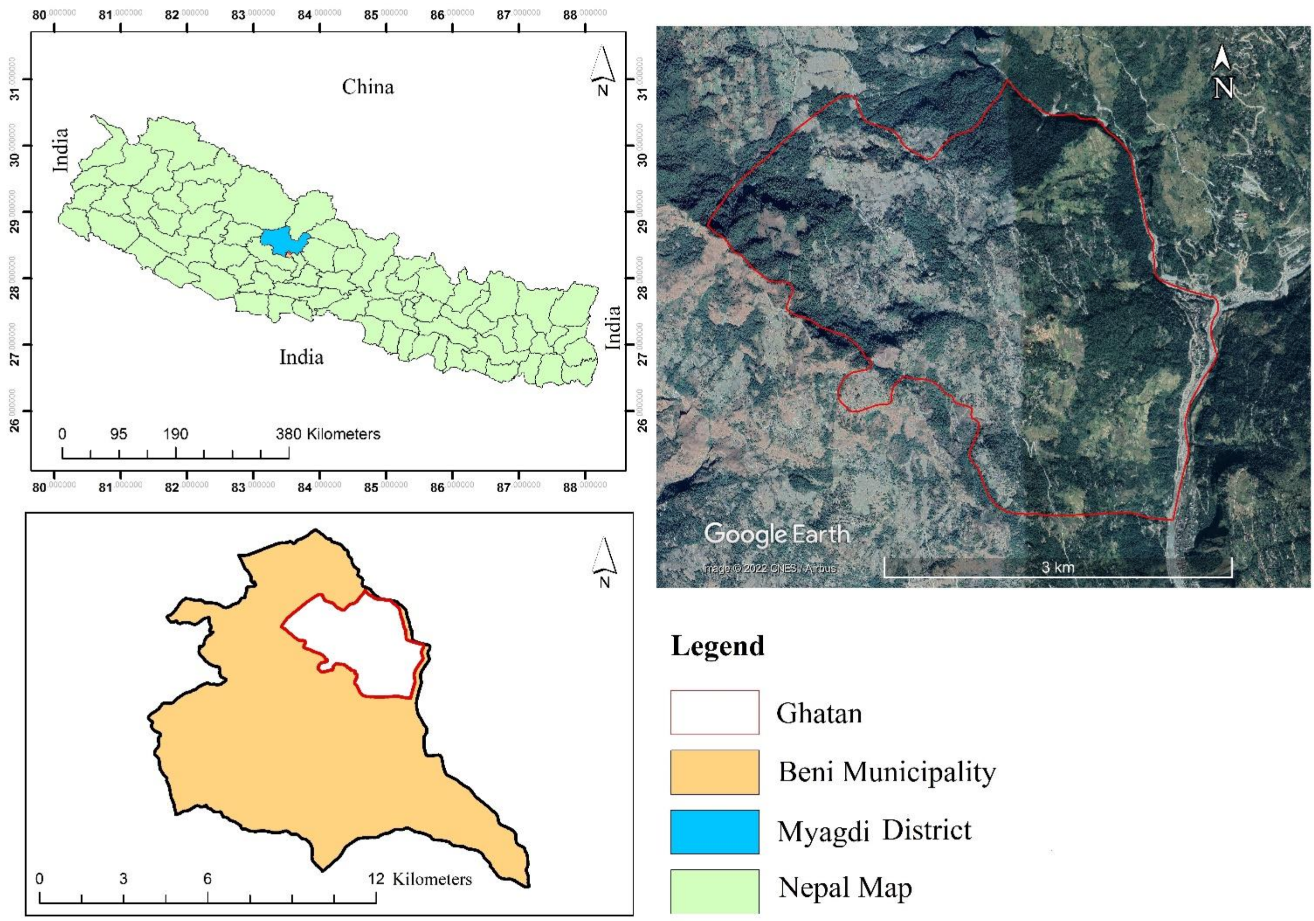

Figure 1. Map of the study area showing Ghatan Village

2.2.2 Key informant interview

A total of five key informants including local leader, teacher, local *Z. armatum* trader, elderly person, and local *Z. armatum* nursery (seedling production place) caretaker were interviewed purposively to collect information on *Z. armatum* and its status, market condition, dependency of people, mechanism involved in the sale of *Z. armatum*, threats prevalent and measures that could be taken to minimize them. Similarly, five domestic market retailers were interviewed about the collection system and market price of *Z. armatum*.

2.2.3 Focus group discussion

A total of four focus group discussion each consisting of eight to ten participants including Community Forest Users Groups (CFUGs) member, women, local NTFPs collectors, local leaders, teachers, etc. were performed to inform them about the type of study that was being carried out there. Participatory resource mapping was carried out in the group discussions to assess the trend of availability of *Z. armatum* and distribution ranges in the study area. Various information about *Z. armatum* cultivation, such as from when they started to cultivate it commercially, average quantity of annual production, market availability etc. were also collected.

2.2.4 Z. armatum nurseries and plantation sites observation

After completing the household questionnaire survey, we also visited the two nurseries within the study site that were regularly producing and supplying the *Z. armatum* seedlings to the cultivators in Myagdi and its neighboring districts of Nepal. During the visit to those nurseries, we collected detailed information on how and at what season and months of the year the seedlings were produced. In addition, we observed the plantation sites or farmlands of the local people and captured the field evidence regarding the *Z. armatum* species.

2.3 Data analysis

Qualitative data analysis was done through descriptive measures including mean, percentage, and pie chart in Microsoft Excel 10. Pearson correlation matrix was used on SPSS 22 to identify whether the various pre-determined socio-economic variables of respondents: caste, gender, literacy, wealth ranking, family size, land holding size, and distance from the forest are dependent or not with the average annual household income from the sale of *Z. armatum*. To classify respondents into various wealth ranking classes, three wealth ranking classes were selected: rich, middle-class, and poor households. The households having a total annual income less than 1,709.53 USD were considered poor households, households having a total annual income between 1,709.53 to 4,273.82 USD were considered as middle-class households, and households having a total annual income more than 4,273.82 USD were considered rich households. Gauli and Hauser (2011) had previously applied a similar technique to classify wealth ranking based on their field scenario. We also applied this ranking method based on field observation and consultation with DFO officials. All these socio-economic variables of respondents were considered independent variables and the average annual income from the sale of *Z. armatum* was a dependent variable. With the help of the Pearson correlation matrix, we were able to determine which independent variables played a significant role with our pre-defined dependent variable.

3. RESULTS

3.1 Socio-economic characteristics of the respondents

Out of the total respondents, 66% (n=53) were male and 34% (n=27) were female. Regarding the education level of the respondents, 75% were literate and 25% were illiterate. Among them, 39% have completed their primary level education, 24% have completed secondary level, and only 12% have completed higher secondary level. Concerning to caste or ethnic groups, 69% were Brahmin/Chhetri, followed by 20% Dalit and 11% indigenous. Among the total respondents, 37% (n=30) were from the rich class, 44% (n=35) were from the middle class and 19% (n=15) were from households that fell under the poor class. The result shows that the number of respondents was highest from the middle class (Table 1).

3.2 Sources of income

Among the respondents, cultivation and collection of *Z. armatum* was the chief source of household income for 37% of the respondents. While, 32% of the respondents were involved in other income sources such as private jobs, business, and government jobs for the primary source of income, though they were cultivating *Z. armatum* in small quantity. In addition, 31% of the respondents were engaged in agriculture and livestock husbandry primarily, being less involved in *Z. armatum* cultivation (Figure 2).

Table 1. Socio-economic characteristics of the respondents

Variable	Category	Frequency	Percentage (%)
Sex	Male	53	66
	Female	27	34
Education	Illiterate	20	25
	Literate	60	75
Ethnic group	Brahmin/Chhetri	55	69
	Indigenous	9	11
	Dalit	16	20
Wealth ranking	Poor	15	19
	Middle	35	44
	Rich	30	37
Occupation	Farmer	51	64
	Non farmer	29	36

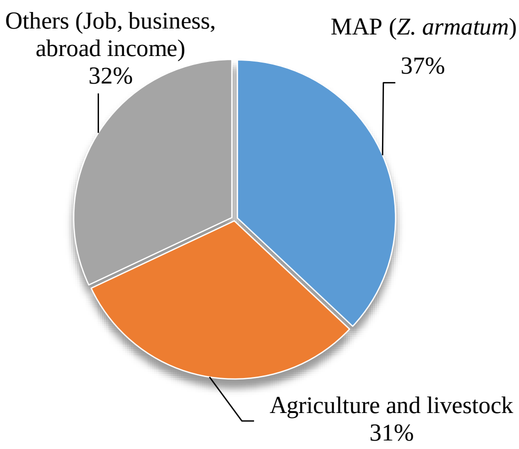

Figure 2. Sources of income of respondents

3.3 Contribution of *Z. armatum* for commercial and household use

Among the various medicinal plants found in the study area, only *Z. armatum* was cultivated and collected from the forest and private lands for commercial use as well as household use. About 90% of the collected *Z. armatum* was used for commercial purposes and 10% for household use. But some other high-value NTFPs such as *Paris polyphylla*, *Bergenia ciliata*, *Acorus calamus*, *Asparagus racemosus*, *Swertia chirayita*, and *Nardostachys grandiflora* were collected from the forest in very few amounts and for household use only.

3.4 Contribution with respect to education status

With concern to respondents' education status, the mean annual income from the sale of *Z. armatum* was slightly higher in illiterate households with an average income of 477 USD per household followed by literate households with an average income of 461 USD per household (Table 2).

3.5 Contribution with respect to caste/ethnicity

Regarding respondents' caste/ethnicity, the mean annual income from the sale of *Z. armatum* was highest in Brahmin/Chhetri households, with an average annual income of 494 USD per household. This was followed by indigenous households with an average annual income of 460 USD, showing that *Z. armatum*'s sales made income to all caste/ethnicity homes. Dalit households showed the lowest average yearly income, with 372 USD (Table 3).

3.6 Contribution with respect to wealth class

For the respondents' wealth ranking category, the mean annual income from the sale of *Z. armatum* was highest in the rich households with an average annual income of 613 USD, indicating that all the households of this class were making income from the sale of *Z. armatum*. Middle-class households with an average annual income of 460 USD followed this. The mean annual income was lowest in poor households with an average annual income of 184 USD (Table 4).

Table 2. Education-wise average annual contribution of *Z. armatum* (USD)

	Education category	Mean	Std. deviation	Std. error mean
Average annual household income from sale of *Z. armatum*	Illiterate	477	341	76
	Literate	461	504	65

Table 3. Caste-wise average annual contribution of *Z. armatum* (USD)

	Caste	Mean	Std. deviation	Std. error	Minimum	Maximum
Average annual household income from sale of *Z. armatum*	Dalit	372	3,323	81	0	1,043
	Indigenous	460	190	63	174	696
	Brahmin/Chhetri	494	530	71	0	3,478
	Total	466	467	52	0	3,478

Table 4. Wealth ranking-wise average annual contribution of *Z. armatum* (USD)

	Wealth rank	Mean	Std. deviation	Std. error	Minimum	Maximum
Average annual household income from sale of *Z. armatum*	Poor	184	146	38	0	391
	Middle	460	336	57	0	1,304
	Rich	613	622	114	70	3,478
	Total	465	467	52	0	3,478

3.7 Socio-economic variables influencing the household income from *Z. armatum*

Multiple linear regressions indicated that the three variables: land holding size (khet), time taken to harvest (days), and wealth ranking (rich) were positively significant with average annual household revenue from the sale of *Z. armatum* with p-values of 0.042, 0.000, and 0.064 respectively. While two variables: education status of respondents (literate) and main income source (agriculture) were negatively significant with average annual income from the sale of *Z. armatum* with p-values 0.046 and 0.064, respectively (Table 5). The correlation matrix is shown in Table 6.

Table 5. Factors influencing the annual income from sale of *Z. armatum*

Independent variables	Coefficients		T	Sig.
	B	Std. error		
Constant	9.935	0.449	22.121	0.000
ln khet1	0.258	0.124	2.075	0.042**
ln bari1	-0.195	0.129	-1.505	0.138
Time taken to harvest (days)	0.037	0.005	7.063	0.000***
Ln family size (no.)	0.040	0.154	0.259	0.797
Sex (Dummy, Male=1)	0.040	0.128	0.315	0.754
Education (Dummy, Literate=1)	-0.260	0.127	-2.040	0.046**
Ethnicity (Dummy, Non- Dalit=1)	-0.033	0.166	-0.198	0.844
Wealth (Dummy, Rich=1)	0.339	0.179	1.890	0.064*
Main income (Dummy, agriculture=1)	-0.235	0.125	-1.883	0.064*

*Significant at $p<0.1$, **significant at $p<0.05$, ***significant at $p<0.01$; Over all model significant, $F=10.216$ ($p<0.01$); Adjusted Coefficient of determination (R^2) =0.54; Results of social data has level of significant up to 10%

Table 6. Correlations matrix

		Age of respondent	Total annual income of respondent	Average annual household income from sale of *Z. armatum*	Family size of respondent	Land holding of respondent -Bari	Land holding of respondent-khet	Distance from the forest
Age of respondent	Pearson Correlation	1.000	0.112	0.163	0.531**	0.146	0.233*	0.088
	p-value		0.325	0.148	0.000	0.195	0.038	0.440
Total annual income of respondent	Pearson Correlation		1.000	0.477**	0.383**	0.342**	0.256**	0.146
	p-value			0.000	0.000	0.002	0.022	0.197
Average annual household income from sale of *Z. armatum*	Pearson Correlation			1.000	0.210	0.373**	0.038	0.437**
	p-value				0.062	0.001	0.738	0.000
Family size of respondent	Pearson Correlation				1.000	0.261*	0.280*	0.001
	p-value					0.019	0.012	0.994
Land holding of respondent-Bari	Pearson Correlation					1.000	0.623**	0.069
	p-value						0.000	0.541
Land holding of respondent-khet	Pearson Correlation						1.000	-0.089
	p-value							0.432
Distance from the forest	Pearson Correlation							1.000
	p-value							

**: Correlation is significant at the 0.01 level (2-tailed)
*: Correlation is significant at the 0.05 level (2-tailed)

4. DISCUSSION

Only *Z. armatum* was cultivated and collected for commercial purposes among the various medicinal plants found in this area, while the rest were only used for household purposes. Figure 2 shows how dependency on agriculture and livestock husbandry has been reduced since more household members have been involved in the production of *Z. armatum* and other jobs, including foreign employment. The culture of collection and sale of *Z. armatum* in Nepal has a long history and can be dated back to the early 80s when the trade started with India. Before trading in India, local people utilized it for their household uses only (Malla et al., 1993). The NTFPs collection predominately for household consumption (43% out of collected NTFPs) was also reported by Maharjan and Dangal (2020) in their study in Dolakha District. Similarly, the majority of the NTFPs were used for household purposes (55%) in the study in Bajhang District (Singh et al., 2021).

The households earned an average of 465 USD annually from the sale of *Z. armatum*, which comprises about 8% of the total annual income of households. This demonstrates that it has played an important role in the rural economy and contributed to the household income of the locals in the study area. Shrestha et al. (2020) revealed that the local people of Nepal draw between 15-50% of their household income from the NTFP sub-sector. Likewise, in the Baitadi District of Nepal, MAPs, including *Z. armatum*, have contributed to up to 9.5% of the total annual household income (Pyakurel et al., 2017). In Darchula, Baitadi, and Dadeldhura Districts, the contribution from the NTFPs sub-sector was 20% of the annual household income (Kunwar et al., 2013) and Olsen and Larsen (2003) estimated 12% in the higher region of Nepal. All of these studies include the contribution made by various NTFPs, but we only include the contribution made by *Z. armatum*. That's why the average annual household contribution in our study is slightly less than in those studies. In the past, rural people started to trade different medicinal plants, including *Z. armatum*, as a source of income (Manandhar, 1986; Kunwar et al., 2018). Similarly, according to the focus group discussion, commercial cultivation of *Z. armatum* in Ghatan village started in 2011 after the implementation of one village, one product program for *Z. armatum* cultivation supported by the Federation of Nepal Chambers of Commerce and Industry and DFO of Myagdi.

The participation of the poor in the collection of *Z. armatum* was lower than that of the middle and upper classes. It can be further clarified that the average annual income from the sale of *Z. armatum* for poor households is USD 184, whereas rich households receive 613 USD annually. Gauli and Hauser (2011) also found that the economic contribution of NTFPs is higher in rich households than in poor households. Though rich people were not directly involved in the collection of *Z. armatum*, they did work as middlemen and/or intermediate contractors and thus earned more money than the poor and middle-class people. Another important reason for rich people contributing more than poor people is that most of the *Z. armatum* collection was done on their private land rather than in community forests (CF), and rich people have larger land holding sizes (11.62 Ropani land per household) than poor people (4.2 Ropani land per household). Likewise, while analyzing the financial contribution of *Z. armatum* among literate and illiterate households, the contribution among illiterate people was found greater than that of literate households. This is because most literate people were found to be involved in various other professions such as government jobs, and business rather than the cultivation and collection of *Z. armatum*. Our finding was quite similar to the result shown by Piya et al. (2011).

While analyzing socio-economic factors affecting the income earned from the sale of *Z. armatum* by a household using a multiple linear regression model, we found that land holding size (khet), time taken to harvest (days), and wealth ranking (rich) were positively significant in the average annual household income respectively. Whereas, the education status of respondents (literate) and main income source (agriculture) were negatively significant. This result shows that people having greater land holding size are getting more income from the sale of *Z. armatum* than people having less land holding size. Other research studies have also demonstrated that dependence on NTFPs is influenced by various socioeconomic characteristics, including distance from the market (Lacuna-Richman, 2004), income (Heubes et al., 2012), and possession of livestock and age of household head (Melaku et al., 2014). The other factors that also influence household dependence include labor availability, involvement in non-agriculture activities (which are similar to our findings), and incorporation into markets (Hasan et al., 2013).

5. CONCLUSION

The study showed that the financial contribution of *Z. armatum* was greatest in higher castes and in wealthy households. The wealth ranking of respondents, land holding size, and time taken to harvest *Z. armatum* were positively significant in the total annual income from its sale, whereas education status and main income source were negatively significant. The study concludes that *Z. armatum* contributes significantly to household income and that it varies significantly across households depending on the influence of various socioeconomic factors. This finding of the study will be useful for the long-term conservation and management of Z. *armatum* in the study area and similar other areas, focusing on its socio-economic contribution. *Z. armatum* should be prioritized for commercial cultivation and collection on community land, as opposed to cultivation on rich households' private land. The responsible authorities should provide technical and financial assistance to cultivators. Additionally, lower caste people should also be given more priority in *Z. armatum* cultivation in the study area.

ACKNOWLEDGEMENTS

We would like to acknowledge the University Grant Commission (UGC), Nepal for funding this research under the UGC's Small Research Development and Innovation Grant. We are grateful to Mr. Saroj Rijal and his team for assisting us during our field work, as well as Mr. Yiba Giri, a *Z. armatum* cultivator and farmer, for his continuous support and the field assistants for their help during the field survey. Likewise, we are thankful to the Division Forest Office, Myagdi team for their continuous motivation and support during our research. Similarly, we would like to express our heartfelt gratitude to the respondents for their time and hospitality in providing the information.

REFERENCES

Ahenkan A, Boon E. Commercialization of non-timber forest products in Ghana: Processing, packaging and marketing. Food Agriculture and Environment 2011;8:962-9.

Banjade MR, Paudel NS. Economic potential of non-timber forest products in Nepal: Myth or reality. Journal of forest and Livelihood 2008;7(1):36-48.

Department of Forest (DoF). Hamro Ban, Annual Report of the Department of Forests for FY 2012/13. Kathmandu: Department of Forest; 2013.

Department of Forest (DoF). Hamro Ban, Annual Report of the Department of Forests for FY 2013/14. Kathmandu: Department of Forest; 2014.

Department of Forest (DoF). Hamro Ban, Annual Report of the Department of Forests for FY 2014/15. Kathmandu: Department of Forest; 2015.

Department of Plant Resources (DPR). NTFPs Prioritized for Economic Development of Nepal (Nepal Ko Aarthik Bikaska Lagi Prathamikta Prapta Jadibutiharu). Kathmandu, Nepal: Department of Plant Resources; 2006.

District Forest Office (DFO). Annual Progress Report. Salyan, Khalanga: District Forest Office; 2015.

Gauli K, Hauser M. Commercial management of non-timber forest products in Nepal's community forest user's groups: Who benefits? International Forestry Review 2011;13(1):35-45.

Grierson AJC, Long DG. Flora of Bhutan, Volume 2, Part 1. Edinburgh: Royal Botanic Garden; 1991.

Hammet AL. Non-timber forest products: Profits and panacea. In: A Synthesis Report on the Current Status of NTFPs in the Terai Region of Nepal. Kathmandu, Nepal: Ministry of Forests and Soil Conservation; 2004.

Hasan MK, Gatto P, Jha PK. Traditional uses of wild medicinal plants and their management practices in Nepal: A study in Makawanpur District. International Journal of Medicinal and Aromatic Plants 2013;3(1):102-12.

He J, Yang B, Dong M, Wang Y. Crossing the roof of the world: Trade in medicinal plants from Nepal to China. Journal of Ethnopharmacology 2018;224:100-10.

Heubes J, Heubach K, Schmidt M, Wittig R, Zizka G, Nuppenau EA, et al. Impact of future climate and land use change on non-timber forest product provision in Benin, West Africa: Linking niche-based modeling with ecosystem service values. Economic Botany 2012;66(4):383-97.

Iponga DM, Mikolo-Yobo C, Lescuyer G, Assoumou FM, Levang P, Tieguhong JC, et al. The contribution of NTFP-gathering to rural people's livelihoods around two timber concessions in Gabon. Agroforestry Systems 2018;92(1):157-68.

International Union for Conservation of Nature (IUCN). The IUCN red list of threatened species. Version 2022-1 [Internet]. 2022 [cited 2022 Oct 22]. Available from: https://www.iucnredlist.org.

Kar SP, Jacobson MG. NTFP income contribution to household economy and related socioeconomic factors: Lessons from Bangladesh. Forest Policy and Economics 2012;14(1):136-42.

Kunwar RM, Mahat L, Acharya RP, Bussmann RW. Medicinal plants, traditional medicine, markets and management in far-west Nepal. Journal of Ethnobiology and Ethnomedicine 2013;9:Article No. 24.

Kunwar RM, Fadiman M, Cameron M, Bussmann RW, Thapa-Magar KB, Rimal B, et al. Cross-cultural comparison of plant use knowledge in Baitadi and Darchula Districts, Nepal Himalaya. Journal of Ethnobiology and Ethnomedicine 2018;14:Article No. 40.

Lacuna-Richman C. Subsistence strategies of an indigenous minority in the Philippines: Nonwood forest product use by the Tagbanua of Narra, Palawan. Economic Botany 2004: 58:266-85.

Lamichhane R, Gautam D, Miya MS, Chhetri HB, Timilsina S. Role of non-timber forest products in national economy: A case of Jajarkot District, Nepal. Grassroots Journal of Natural Resources 2021;4(1):94-105.

Malla SB, Shakya PR, Rajbhandari KR, Bhattarai NK, Subedi MN. Minor Forest Products of Nepal: General Status and Trade. Kathmandu: Forest Resource Information System Project; 1993.

Maharjan S, Dangal MR. Economic contribution of non-timber forest products in rural livelihood of Dolakha, Nepal. Open Journal for Research in Economics 2020;3(2):55-66.

Manandhar NP. Ethnobotany of Jumla District, Nepal. International Journal of Crude Drug Research 1986;24(2):81-9.

Melaku E, Ewnetu Z, Teketay D. Non-timber forest products and household incomes in Bonga forest area, southwestern Ethiopia. Journal of Forestry Research 2014;25:215-23.

Mukul SA, Uddin MB, Manzoor RAZM, Fox J. Integrating livelihoods and conservation in protected areas: Understanding the role and stakeholder views on prospects for nontimber forest products: A Bangladesh case study. International Journal of Sustainable Development and World Ecology 2010;17(2):180-8.

Nair KN, Nayar MP. Rutaceae. In: Hajra PK, Nair VJ, Daniel P, editors. Flora of India (Malpighiceae - Dichapetalaceae) Vol. 4. Calcutta, India: Botanical Survey of India; 1997. p. 259-408.

Olsen CS, Larsen HO. Alpine medicinal plant trade and Himalayan mountain livelihood strategies. Geographical Journal 2003;169:243-54.

Phuyal N, Jha PK, Raturi PP, Rajbhandary S. *Zanthoxylum armatum* DC.: Current knowledge, gaps and opportunities in Nepal. Journal of Ethnopharmacology 2019;229:326-41.

Piya L, Maharjan KL, Joshi NP, Dangol DR. Collection and marketing of non-timber forest products by Chepang Community in Nepal. Journal of Agriculture and Environment 2011;12:10-21.

Pyakurel D, Sharma IB, Ghimire SK. Trade and conservation of medicinal and aromatic plants in western Nepal. Botanica Orientalis: Journal of Plant Science 2017;11:27-37.

Reta Z, Adgo Y, Girum T, Mekonnen N. Assessment of contribution of non-timber forest products in the socioeconomic status of peoples in Eastern Ethiopia. Open Access Journal of Biogeneric Science and Research 2020;4(4):1-8.

Sahoo SR, Panda NK, Subudhi SN, Das HK. Contribution of non-timber forest produces (NTFPs) in the socio-economic development of forest dwellers in Odisha. Journal of Pharmacognosy and Phytochemistry 2020;9(4):81-5.

Shackleton CM, Pullanikkatil D. Considering the links between non-timber forest products and poverty alleviation. In: Pullanikkatil D, Shackleton C, editors. Poverty Reduction Through Non-Timber Forest Products, Sustainable Development Goals Series. Springer Cham; 2019. p. 15-28.

Shrestha KK, Bhandari P, Bhattarai S. Plants of Nepal (Gymnosperms and Angiosperms). Kathmandu, Nepal: Heritage Publishers and Distributors Pvt. Ltd; 2022.

Shrestha S, Shrestha J, Shah KK. Non-timber forest products and their role in the livelihoods of people of Nepal: A critical review. Grassroots Journal of Natural Resources 2020; 3(2):42-56.

Singh J, Miya MS, Adhikari A, Das LK. Potentiality of income generation through non-timber forest products: A case study from the Sallipatan Trishakti Community Forest, Bajhang district, Nepal. International Research Journal of MMC 2021:2(2):1-15.

Wiersum KF, Ros-Tonen MAF. The Role of Forests in Poverty Alleviation: Dealing with Multiple Millennium Development Goals. Wageningen UR: North-South Policy Brief; 2005.

Preparation of C-based Magnetic Materials from Fruit Peel and Hydrochar using Snake Fruit (*Salacca zalacca*) Peel as Adsorbents for the Removal of Malachite Green Dye

Mauizatul Hasanah[1,3], Alfan Wijaya[2], Fitri Suryani Arsyad[3], Risfidian Mohadi[3], and Aldes Lesbani[2,3*]

[1]Department of Pharmacy, School of Pharmacy Bhakti Pertiwi, Jl. Ariodillah III No. 22A, Palembang 30128, South Sumatera, Indonesia
[2]Research Center of Inorganic Materials and Coordination Complexes, Faculty of Mathematics and Natural Sciences, Sriwijaya University, Jl. Padang Salasa No. 524 Ilir Barat 1, Palembang 30139, South Sumatera, Indonesia
[3]Doctoral Program, Faculty of Mathematics and Natural Sciences, Sriwijaya University, Jl. Padang Selasa No. 524 Ilir Barat 1, Palembang 30139, Indonesia

ARTICLE INFO

Received: 6 Sep 2022
Received in revised: 7 Nov 2022
Accepted: 10 Nov 2022
Published online: 23 Nov 2022
DOI: 10.32526/ennrj/21/202200192

Keywords:
Hydrothermal treatment/ Snake fruit peel/ Hydrochar/ Magnetic material/ Adsorption/ Malachite green dye

*** Corresponding author:**
E-mail:
aldeslesbani@pps.unsri.ac.id

ABSTRACT

In this study, fruit peel-based magnetic (M-Sp) and hydrochar-based magnetic (M-HSp) materials were successfully synthesized by hydrothermal and magnetization treatments. Characterization using X-ray diffraction, Fourier-transform infrared spectroscopy, vibrating sample magnetometry, and scanning electron microscopy-energy dispersive spectroscopy confirmed their successful synthesis. The materials were applied as adsorbents for the removal of malachite green (MG) dye. Equilibrium adsorption occurred at 90 min according to the PSO kinetic model, and the adsorption followed the Langmuir isotherm. The adsorption capacity of the materials was improved by the hydrothermal and magnetic treatments compared to that of the untreated initial material. The adsorption capacities of M-Sp and M-HSp were 69.444 and 88.889 mg/g, respectively. The M-Sp and M-HSp adsorbents could be reused for up to four regeneration cycles compared to the three cycles for the initial material. The adsorption mechanism of MG dye by the M-Sp and M-HSp adsorbents was suggested to occur via hydrogen bond, electrostatic, π-π, and physical interactions. The magnetic materials prepared in this study had a high adsorption capacity and adsorbent reusability, rendering them promising for use in dye removal and to facilitate separation between adsorbents and adsorbates.

1. INTRODUCTION

Snake fruit (*Salacca zalacca*) is a tropical fruit found in Southeast Asia; it is known by the name “Salak” in Indonesia (Zubaidah et al., 2018). Snake fruit peel (Sp) is an easily obtainable biomass produced from agricultural waste. As it has no market value, it has rarely been investigated and has not been widely utilized warranting further study (Yvonne et al., 2018). Previous research (Azizah and Fatimah, 2020) (Rahmayanti et al., 2022) utilizing Sp as an adsorbent to remove dyes and heavy metals reported fairly high adsorption capacity. Thus, Sp has many advantages in that it can be easily obtained and has good adsorption capabilities, rendering it promising for application as an adsorbent to eliminate waste water or organic pollutants.

The adsorption ability of Sp can be enhanced by hydrothermal treatment to obtain hydrochar. Hydrochar has been widely used as an effective adsorbent to remove dye pollutants with a high adsorption capacity (Haris et al., 2022; Hasanah et al., 2022). One of the most studied dye pollutants is malachite green (MG), which is a cationic dye and widely used in the textile, leather, and other industries; it is considered an organic pollutant in wastewater. It has been reported that the MG dye has many adverse effects on humans upon exposure owing to its high toxicity, teratogenicity, carcinogenicity and mutagenicity (Mohadi et al., 2022;

Citation: Hasanah M, Wijaya A, Arsyad FS, Mohadi R, Lesbani A. Preparation of c-based magnetic materials from fruit peel and hydrochar using snake fruit (*Salacca zalacca*) peel as adsorbents for the removal of malachite green dye. Environ. Nat. Resour. J. 2023;21(1):67-77. (https://doi.org/10.32526/ennrj/21/202200192)

Wu et al., 2022; Qiao et al., 2022). In addition, MG dye can irritate the respiratory tract, affect digestion, and cause skin problems such as rashes or swelling, as well as permanent damage to the eyes from contact (Das et al., 2021). MG dye also blocks the transmission of light, which can adversely affect the growth of aquatic organisms (Wang et al., 2022). Therefore, it is necessary to investigate methods for the removal of this dye. The adsorption method has been extensively advocated by researchers for the removal of dye pollutants owing to its simple process, low cost, and high removal efficiency (Karthi et al., 2022; Gajera et al., 2022; Alqadami et al., 2018; Dil et al., 2018).

Research conducted in recent years has particularly focused on the development of magnetic materials based on carbon to separate adsorbents from adsorbates at the end of the adsorption process (Cojocaru et al., 2019). Magnetic materials are also widely used in the removal of dye pollutants, both as adsorbents and as photocatalysts. Magnetic materials used in the removal of dye pollutants include carbon-based materials such as chitosan-magnetic Fe_3O_4/activated carbon nanocomposites that adsorb cationic and anionic dyes (Kaveh and Bagherzadeh, 2022), a chitosan-based magnetic material that could adsorb acid orange 7 dye with an adsorption capacity of 97 mg/g (Cojocaru et al., 2019), a magnetic cellulose-based ionic liquid that could adsorb MG and Congo Red dyes with adsorption capacities of 1,299.3 mg/g and 1,068.1 mg/g, respectively (Ling et al., 2022), a superb natural magnetic material that could adsorb crystal violet dye with an adsorption capacity of 117 mg/g (Sanad et al., 2021), and a biochar-based magnetic material that could adsorb rhodamine B and MG dyes with adsorption capacities of 334.89 mg/g and 576.73 mg/g, respectively (Cheng et al., 2022). Thus, carbon-based magnetic materials are promising novel adsorbents to remove dye pollutants.

In this study, Sp (from *Salacca zalacca*) which has rarely been employed in related studies was subjected to hydrothermal and magnetization treatments to improve its properties. The obtained materials were analyzed using X-ray diffraction (XRD), Fourier-transform infrared spectroscopy (FT-IR), vibrating sample magnetometer (VSM), and scanning electron microscopy with energy dispersive spectroscopy (SEM-EDS). The materials were then applied as adsorbents to remove MG dye and study the effect of the pH pzc, contact time, as well as study the adsorption isotherm, adsorption thermodynamics, and regeneration ability.

2. METHODOLOGY

2.1 Chemicals and instrumentation

The Sp used in this study was sourced from Palembang, South Sumatera, Indonesia. The chemicals used included ortho-phosphoric acid (H_3PO_4; Merck, Germany), iron(III) chloride ($FeCl_3$; Sigma Aldrich, Germany), iron(II) sulfate heptahydrate ($FeSO_4 \cdot 7H_2O$; Smart Lab, Indonesia), ammonia solution (NH_3 25%; Merck, Germany), hydrochloric acid (HCl; Mallinckrodt LabGuard, France), sodium hydroxide (NaOH; Merck, Germany), and sodium chloride (NaCl; Merck, Germany). The MG powder (cationic dye) was obtained from a textile factory in Palembang, South Sumatera, Indonesia (its chemical structure is shown in Figure 1). Distilled water was purchased from Brataco Inc., Indonesia. The material was characterized using a Rigaku Miniflex-600 X-ray diffractometer (Japan), Shimadzu Prestige-21 FTIR spectrophotometer (Japan), OXFORD VSM1.2H vibrating sample magnetometer (England), and Quanta 650 SEM-EDS apparatus (England). Absorbance measurements of the dye solution were conducted using (UV) visible Biobase spectrophotometer UV BK-1800PC (China).

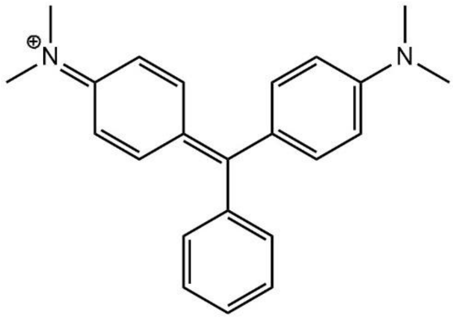

Figure 1. Chemical structure of malachite green dyes

2.2 Preparation of hydrochar from Sp

The thoroughly washed Sp was dried in the sun, ground until smooth, and filtered using a 40 mesh-sized sieve. Hydrochar from the snake fruit peel (HSp) was produced through hydrothermal carbonization treatment, which was carried out by adding as much as 2 g Sp powder to 50 mL of H_3PO_4. The solution was placed in a hydrothermal stainless steel-autoclave (volume: 100 mL), then placed in the oven for 6 h at 150°C (Çatlıoğlu et al., 2020). The mixture was subsequently filtered and washed using distilled water, and then dried in the oven for 6 h at 110°C. The initial and obtained materials were characterized using XRD, FTIR, and SEM-EDS analyses.

2.3 Preparation of fruit peel-based magnetic material (M-Sp)

$FeCl_3$ (0.004 mol) and $FeSO_4 \cdot 7H_2O$ (0.003 mol) were each dissolved in 3 mL of distilled water and the solution was mixed using a stirrer for 3 h. Ammonia (3.5 mL of 25% solution) was then slowly dripped into the mixture. Subsequently, 1 g of Sp was added and stirred for 30 min. The mixture was then placed in a hydrothermal stainless-steel autoclave for 3 h at 150°C. Next, it was filtered and washed using distilled water, and dried in the oven at 100°C. The material was characterized using XRD, FTIR, VSM, and SEM-EDS analyses.

2.4 Preparation of hydrochar-based magnetic material (M-HSp)

$FeCl_3$ (0.004 mol) and $FeSO_4 \cdot 7H_2O$ (0.003 mol) were each dissolved in 25 mL of distilled water, and the solution was mixed and stirred using a stirrer for 3 h. Ammonia (3.5 mL of 25% solution) was then slowly dripped into the mixture, after which 1 g of the HSp was added and stirred for 30 min. Subsequently the mixture was placed in hydrothermal stainless-steel autoclave for 3 h at 150°C. It was then filtered and washed using distilled water, and then dried in the oven at 100°C. The obtained material was characterized using XRD, FTIR, VSM, and SEM-EDS analyses.

2.5 Adsorption process and regeneration ability

Adsorption was performed by considering several parameters, including the pH pzc, contact time, concentration, and temperature. The pH pzc was determined by varying the pH of the NaCl solution, and then adding 0.02 g of the material to the solution and stirring for 24 h, after which the final pH of the solution was measured. The effect of the contact time for the adsorption of MG dye was measured by varying the contact time during adsorption. As much as 0.02 g of the adsorbent was added to an Erlenmeyer flask containing 20 mL of the dye solution at a concentration of 50 mg/L. The mixture was stirred, following which the absorbance of the filtrate was measured using a UV-visible spectrophotometer for the specified time variation. The effects of the concentration and temperature were determined by varying these parameters during adsorption. As much as 0.02 g of the adsorbent was added to an Erlenmeyer flask containing 20 mL of the dye solution for a specified concentration variation and stirred for 60 min at the specified temperature; subsequently, the absorbance of the filtrate was measured. The regeneration ability of the adsorbent was determined by performing adsorption-desorption cycles, where the latter process was performed to remove the adsorbate from the adsorbent. For this, 0.1 of the adsorbent was added to the dye solution at a concentration of 50 mg/L. The mixture stirred for 2 h, and the absorbance of the filtrate was measured. Desorption was carried out using an ultrasonic system with a water bath. The adsorbent that subjected to desorption was dried and reused in the subsequent adsorption process.

3. RESULTS AND DISCUSSION

The initial material (Sp), and the prepared hydrochar and magnetic materials are shown in Figure 2. The initial material changes in color to black in HSp due to the hydrothermal carbonization treatment, while it changes to brown in the magnetic material, indicating the presence of iron. Figures 2(c) and 2(d), show the testing procedure for the magnetic material using an external magnet, confirming its successful preparation. The data in Table 1 show that the yield weight of the resulting material reaches 70-90%.

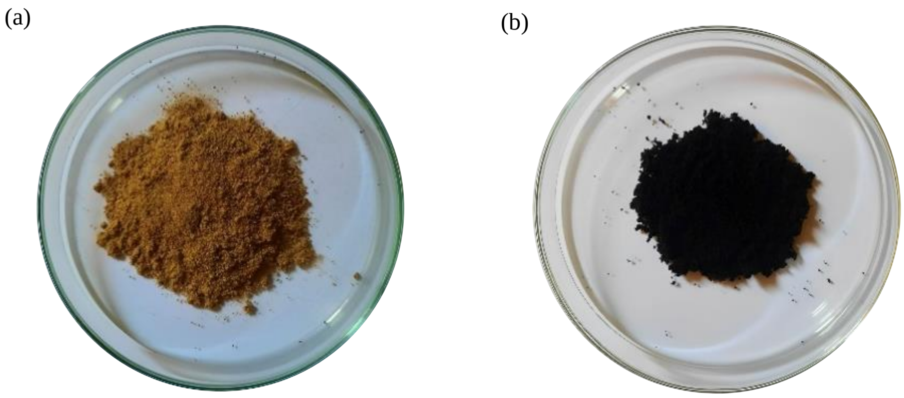

Figure 2. Materials of Sp (a), HSp (b), M-Sp (c), and M-HSp (d)

(c) (d)

Figure 2. Materials of Sp (a), HSp (b), M-Sp (c), and M-HSp (d) (cont.)

Table 1. Percent yield weight of materials

Materials	Yield weight (%)
HSp	90.455
M-Sp	99.703
M-HSp	72.068

The XRD patterns of Sp, HSp, M-Sp, and M-HSp are shown in Figure 3. The patterns for Sp and HSp show diffraction peaks at 2θ≈=20º (002) indicating that these materials are amorphous with a low crystallinity (Venkatesan et al., 2022). The diffraction peaks of M-Sp and M-HSp are located at 2θ≈=20º (002), indicating the presence of the initial material; and peaks are also found at 2θ≈=30º (311), 35º (400), and 65º (440), originating from Magnetite (Chekalil et al., 2019).

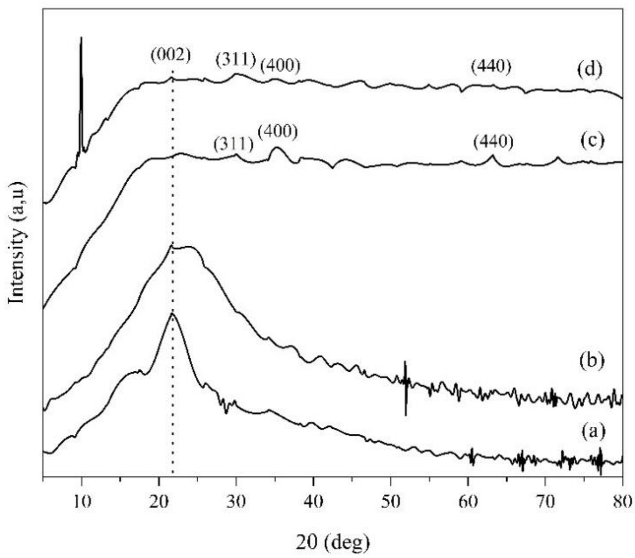

Figure 3. Diffraction patterns of Sp (a), HSp (b), M-Sp (c), and M-HSp (d)

The FT-IR spectra of Sp, HSp, M-Sp, and M-HSp are shown in Figure 4. The peak at 3,425 cm^{-1} is assigned to the O-H bond from the phenolic hydroxyl group, while the peaks at 2,924, 1,630, and 1,003 cm^{-1} correspond to the C-H, C=C, and C-O functional groups, respectively. The spectra of the M-Sp and M-HSp materials show a peak at 560 cm^{-1}, indicating the presence of the Fe-O bond. The magnetic curves of M-Sp and M-HSp were measured using VSM and are shown in Figure 5; both materials are paramagnetic with magnetizations of 17.69 emu/g and 5.65 emu/g, respectively. The hysteresis curve is at the null position, implying that M-Sp and M-HSp are superparamagnetic.

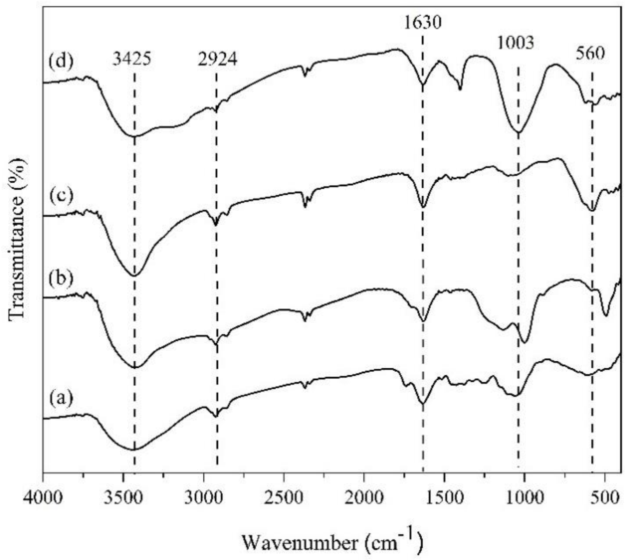

Figure 4. FT-IR Spectrum of Sp (a), HSp (b), M-Sp (c), and M-HSp (d)

The SEM–EDS results are shown in Figure 6 and Table 2. Figure 2 shows that the materials forms aggregates and is heterogeneous. Hsp and M-Hsp exhibit a smoother morphology than Sp and M-Sp. Table 2 show the EDS data with percentages of the C, O, and Fe atoms. HSp has a higher C content than Sp due to hydrothermal carbonization. This proves the success of the hydrothermal carbonization treatment carried out in this study. M-Sp and M-HSp exhibit Fe content due to the magnetization process in the materials; M-Sp has a higher Fe content than M-Hsp. This is reflected in the magnetization of M-Sp, which is higher than that of M-HSp.

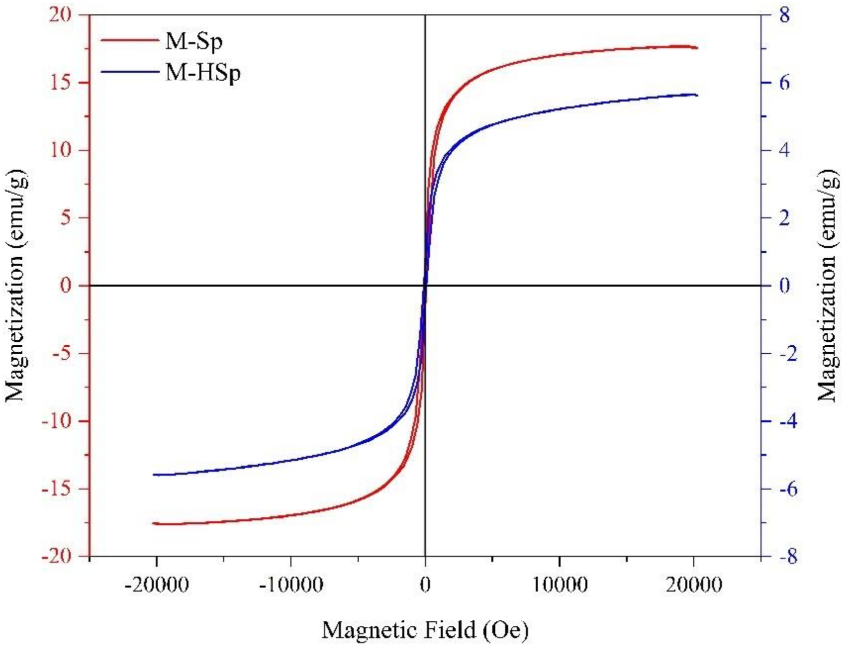

Figure 5. Magnetization curve

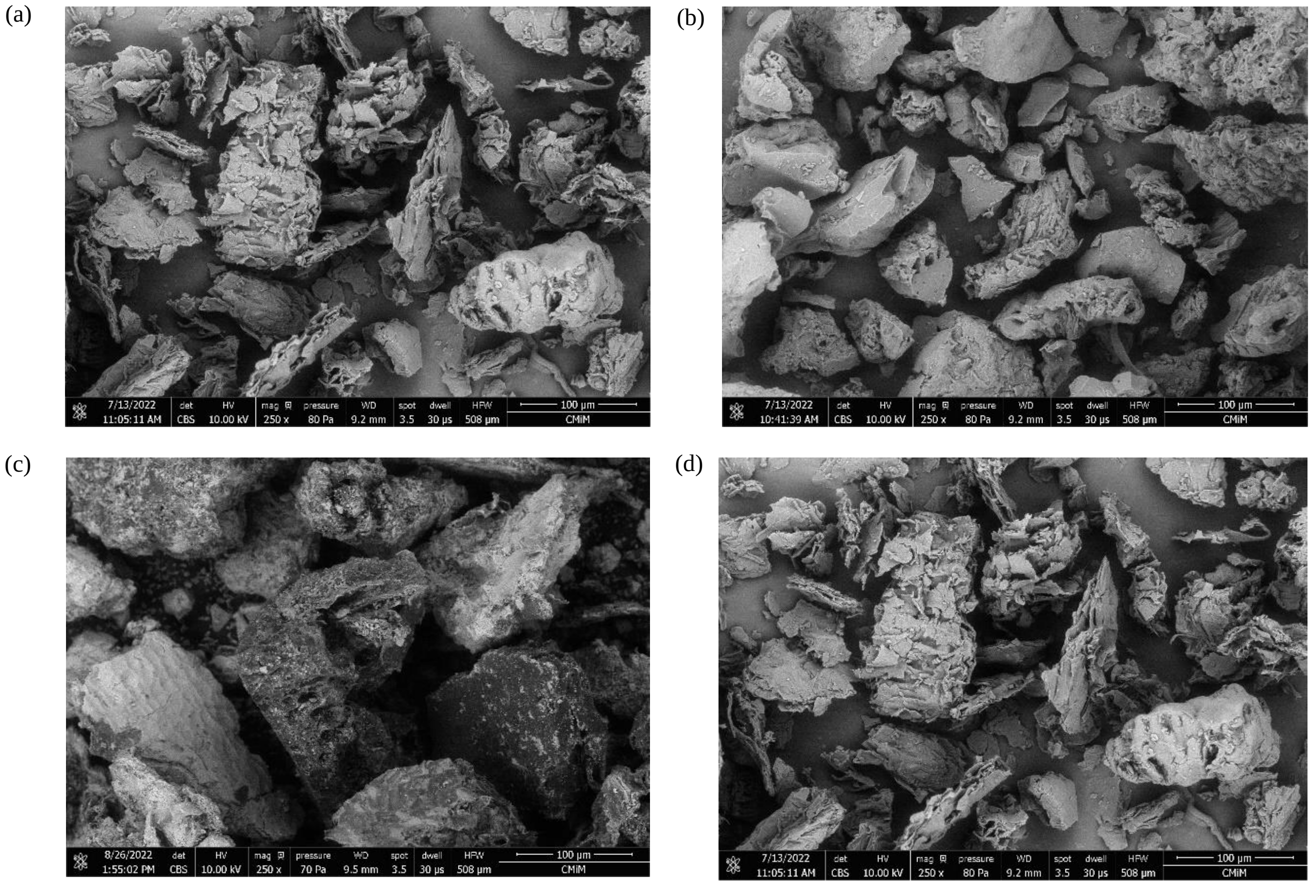

Figure 6. SEM images of Sp (a), Hsp (b), M-Sp (c), and M-Hsp (d)

Table 2. EDS data of materials

Materials	Weight (%)		
	C	O	Fe
Sp	55.9	32.8	-
HSp	68	26.3	-
M-Sp	17.7	31.6	46.9
M-HSp	18.2	34.6	36.4

The results of the pH pzc measurements are shown in Figure 7. The pH pzc of the materials is approximately in the range of 4.5-5.9. This implies that for this pH range, the material surfaces are neutral and carry zero charge, enabling optimal adsorption without the influence of positive or negative charges. The pH pzc of each material was evaluated for the adsorption of MG dye. The adsorption kinetic parameters are shown in Figure 8 and Table 3. The equilibrium adsorption of MG dye occurs at 90 min. Table 3 shows that the adsorption kinetics follow the PSO model, with a linear regression coefficient (R^2) close to 1. The kinetic rate of the PSO model is lower than of the PFO model, indicating that the reaction proceeds faster with the former model.

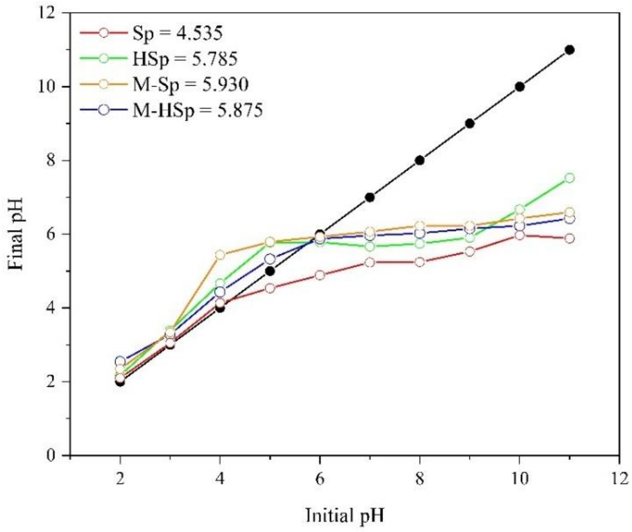

Figure 7. pH pzc of materials

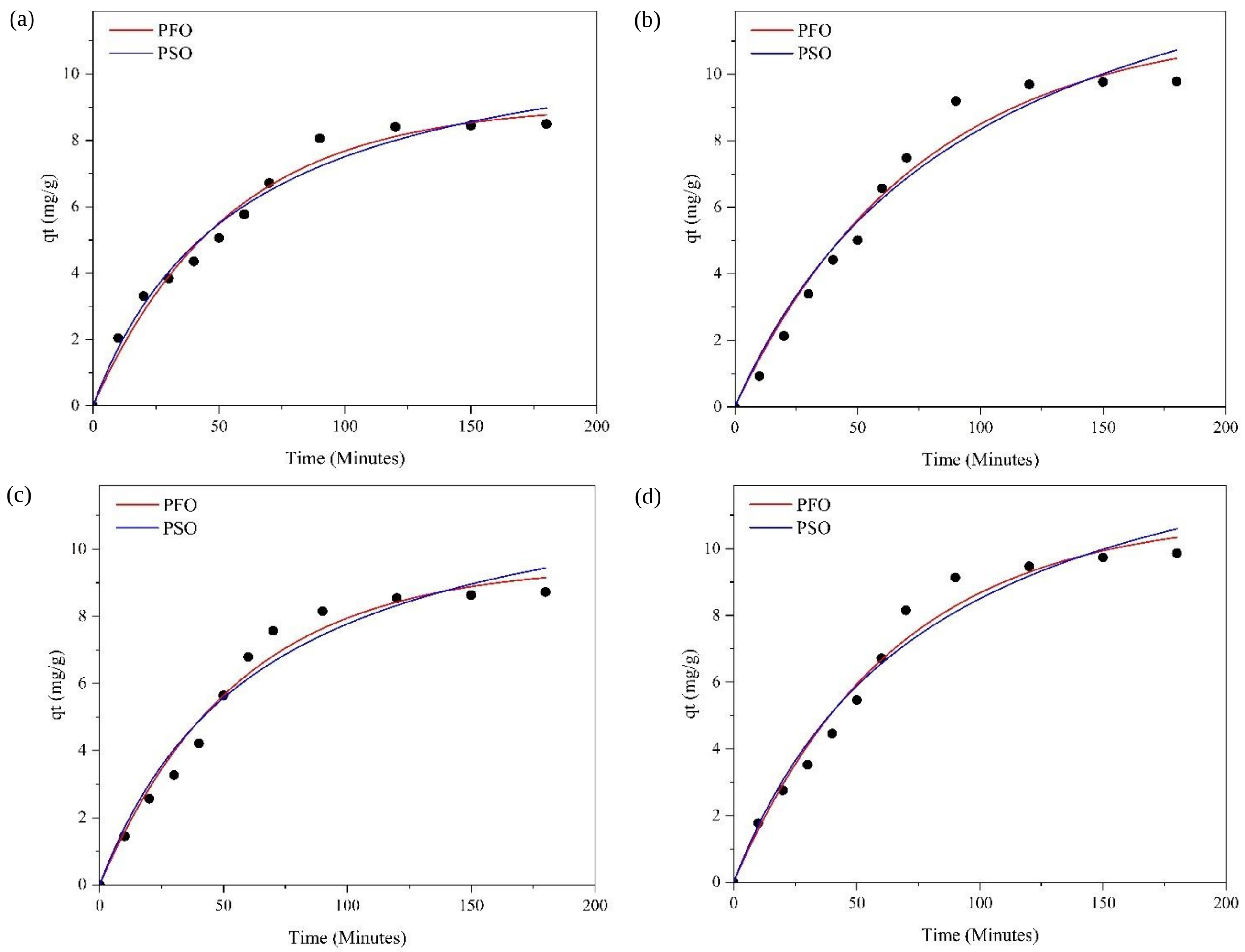

Figure 8. Adsorption kinetic models and equilibrium condition of Sp (a), HSp (b), M-Sp (c), and M-HSp (d)

Table 3. Adsorption kinetic parameters

Adsorbents	Initial concentration (mg/L)	$Qe_{experiment}$ (mg/g)	PFO			PSO		
			Qe_{Calc} (mg/g)	R^2	k1	Qe_{Calc} (mg/g)	R^2	k2
Sp	10.586	8.496	13.813	0.944	0.037	11.364	0.963	0.0017
HSp	10.586	9.785	22.930	0.926	0.044	16.155	0.900	0.0006
M-Sp	10.586	8.726	12.272	0.969	0.033	13.158	0.934	0.0010
M-HSp	10.586	9.867	13.868	0.971	0.030	15.337	0.937	0.0008

The adsorption isotherm models are shown in Figure 9 and Table 4, and indicate that the increasing temperature causes an increase in the adsorption concentration. The adsorption capacity of the materials is enhanced by the hydrothermal and magnetic treatments compared to that of the initial material. The adsorption capacities of Sp, HSp, M-Sp, and M-HSp are 66.667, 86.957, 69.444, and 88.889 mg/g, respectively. Based on isotherm data, the Langmuir model is better than the Freundlich model for the adsorption process in this study, with R^2 close to 1. The adsorption thermodynamic parameters are shown in Table 5. The adsorption process that occurs in this study is an endothermic process, as indicated by the positive ΔH; the ΔS value indicates the degree of irregularity of the adsorption process.

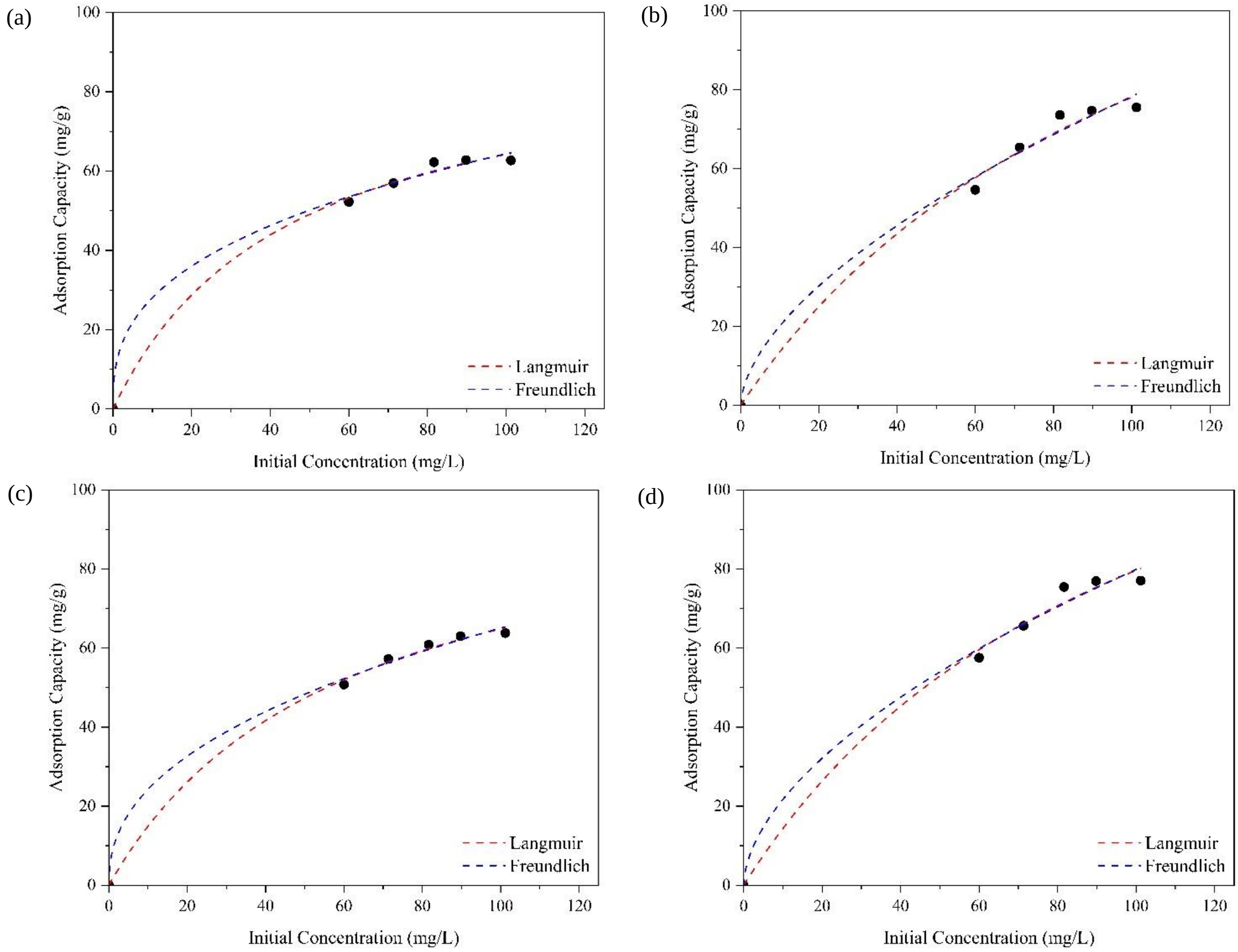

Figure 9. Adsorption isotherm models of Sp (a), HSp (b), M-Sp (c), and M-HSp (d)

Table 4. Adsorption isotherm parameters

Adsorbents	Adsorption isotherm	Adsorption constant	T (K)				
			30ºC	40ºC	50ºC	60ºC	70ºC
Sp	Langmuir	Q_{max}	59.524	60.976	62.112	65.359	66.667
		kL	0.239	0.281	0.338	0.371	0.514
		R^2	0.996	0.998	0.998	0.997	0.998
	Freundlich	n	8.078	7.862	8.439	7.905	8.110
		kF	33.963	35.099	37.575	38.833	41.295
		R^2	0.870	0.939	0.935	0.859	0.863
HSp	Langmuir	Q_{max}	86.957	67.568	71.429	76.336	80.645
		kL	0.477	0.712	0.654	0.630	0.639
		R^2	0.999	0.999	0.998	0.996	0.994
	Freundlich	n	3.709	3.719	3.610	3.674	3.897
		kF	23.281	24.820	25.598	28.379	32.240
		R^2	0.858	0.882	0.936	0.992	0.995
M-Sp	Langmuir	Q_{max}	63.291	64.103	64.516	68.966	69.444
		kL	0.138	0.198	0.278	0.240	0.319
		R^2	0.992	0.990	0.997	0.999	0.999
	Freundlich	n	4.785	5.848	6.549	5.705	6.094
		kF	24.826	30.444	34.096	33.281	36.249
		R^2	0.894	0.816	0,909	0.967	0.924
M-HSp	Langmuir	Q_{max}	70.922	74.627	76.336	77.519	88.889
		kL	0.716	0.558	0.697	0.921	1.103
		R^2	0.999	0.998	0.996	0.997	0.998
	Freundlich	n	4.026	3.561	3.970	4.444	5.048
		kF	27.983	26.309	30.740	34.898	39.967
		R^2	0.991	0.958	0.999	0.999	0.996

Table 5. Adsorption thermodynamic parameters

Adsorbents	Concentration (mg/L)	T (K)	Q_e (mg/g)	ΔH (kJ/mol)	ΔS (J/mol. K)	ΔG (kJ/mol)
Sp	101.185 mg/L	303	54.926	6.990	0.024	-0.389
		313	56.481			-0.633
		323	58.111			-0.876
		333	60.889			-1.120
		343	62.704			-1.363
HSp	101.185 mg/L	303	62.296	13.070	0.047	-1.091
		313	64.926			-1.559
		323	67.778			-2.026
		333	71.592			-2.494
		343	75.555			-2.961
M-Sp	101.185 mg/L	303	54.704	8.186	0.045	-5.436
		313	57.285			-5.886
		323	58.926			-6.335
		333	62.259			-6.785
		343	63.815			-7.234
M-HSp	101.185 mg/L	303	67.370	9.714	0.038	-1.716
		313	70.111			-2.093
		323	72.000			-2.470
		333	73.889			-2.847
		343	77.074			-3.224

The regeneration ability of the material in Figure 10 shows that the initial material (Sp) can only be used for three regeneration cycles, while the materials subjected to the hydrothermal and magnetic treatments can be used for four regeneration cycles. Table 6 lists the adsorption capacities for reported magnetic materials. The table shows that the magnetic material prepared in this study has a higher adsorption capacity, rendering it promising for dye removal. Figure 11 illustrates the possible adsorption mechanism of MG dye by M-Sp and M-HSp, involving hydrogen bond, electrostatic, π-π, and physical interactions. It shows that the adsorption process of MG dye involves not only physical interactions, but also chemical interactions.

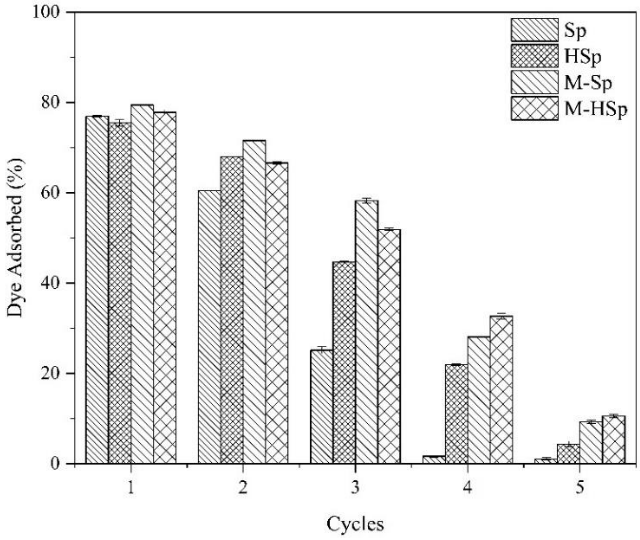

Figure 10. Regeneration ability of materials

Table 6. Comparison of several adsorbents on the adsorption of MG

Adsorbents	Adsorption capacity (mg/g)	Equilibrium time (minutes)	References
Fe_3O_4@chitosan@ZIF-8	3.282	40	Zadvarzi et al. (2021)
Polyaniline–nickel ferrite magnetic nanocomposite	4.09	210	Patil and Shrivastava (2015)
Magnetic $CuFe_2O_4$ nano-adsorbent	22	30	Vergis et al. (2018)
Sodium alginate-coated Fe_3O_4 nanoparticles	47.84	20	Mohammadi et al. (2014)
Magnetic GO/Fe_3O_4	59	90	Li et al. (2021)
Magnetic litchi pericarps	70.42	60	Zheng et al. (2015)
Cobalt ferrite silica magnetic nanocomposite	75.5	40	Amiri et al. (2017)
Magnetic reduced graphene oxide nanocomposite	77.15	20	Sadegh et al. (2021)
Magnetic chitosan-DES nanoparticles	87.72	120	Sadiq et al. (2021)
M-Sp	69.444	90	This work
M-HSp	88.889	90	This work

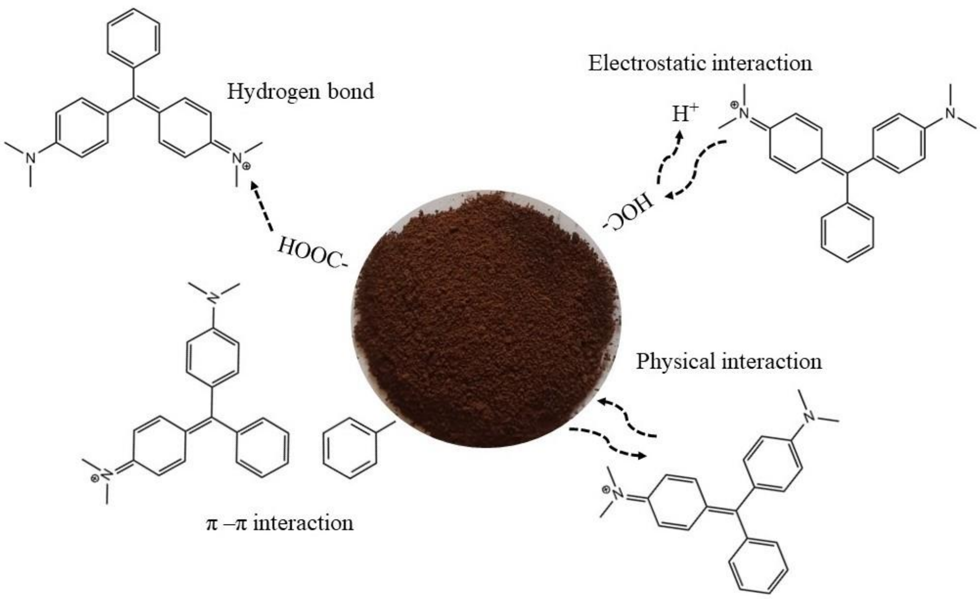

Figure 11. Plausible adsorption mechanism of MG by M-Sp and M-HSp

4. CONCLUSION

In this study, fruit-peel-based magnetic materials (M-Sp and M-HSp) were successfully synthesized by hydrothermal and magnetization treatments. The materials were used as adsorbents for the removal of MG dye. Equilibrium adsorption occurred at 90 min; the adsorption kinetics followed the PSO model and the adsorption isotherm fitted well to the Langmuir isotherm. The adsorption capacities of M-Sp and M-HSp were 69.444 and 88.889 mg/g, respectively. The adsorbent reusabilities of M-Sp and M-HSp were high, and both materials could be reused for up to four regeneration cycles compared to the three cycles for the untreated initial material. The adsorption mechanism of MG by M-Sp and M-HSp was suggested to involve hydrogen bonds, electrostatic, π-π, and physical interactions.

ACKNOWLEDGEMENTS

The authors acknowledge support by the Ministry of Education, Culture, Research and Technology Republic Indonesia through the Hibah Disertasi Doctor main contract number (142/E5/PG.02.00.PT/2022) by derivative contract number (0145.009/UN9.3.1/PL/2022). The authors also thank the Research Center of Inorganic Materials and Complexes, Universitas Sriwijaya for the analysis, apparatus, support, and discussion of this research.

REFERENCES

Alqadami AA, Khan MA, Siddiqui MR, Alothman ZA. Development of citric anhydride anchored mesoporous MOF through post synthesis modification to sequester potentially toxic lead (II) from water. Microporous and Mesoporous Materials 2018;261:198-206.

Amiri M, Salavati NM, Akbari A, Gholami T. Removal of malachite green (a toxic dye) from water by cobalt ferrite silica magnetic nanocomposite: Herbal and green sol-gel autocombustion synthesis. International Journal of Hydrogen Energy 2017;42(39):24846-60.

Azizah U, Fatimah I. Salacca zalacca skin and its modified form as biosorbents for Hg^{2+} removal from aqueous solution. Green Chemistry Letters and Reviews 2020;13(3):42-50.

Çatlıoğlu FN, Akay S, Gözmen B, Turunc E, Anastopoulos I, Kayan B, et al. Fe-modified hydrochar from orange peel as adsorbent of food colorant Brilliant Black: Process optimization and kinetic studies. International Journal of Environmental Science and Technology 2020;17(4):1975-90.

Chekalil N, Tarhini M, Elaissari A, Saïdi-Besbes S. Multi-step synthesis of core-shell magnetic nanoparticles bearing acid-chelating functional moieties. Research on Chemical Intermediates 2019;45(10):4847-61.

Cheng S, Zhao S, Xing B, Liu Y, Zhang C, Xia H. Preparation of magnetic adsorbent-photocatalyst composites for dye removal by synergistic effect of adsorption and photocatalysis. Journal of Cleaner Production 2022;348(3):Article No. 131301.

Cojocaru C, Samoila P, Pascariu P. Chitosan-based magnetic adsorbent for removal of water-soluble anionic dye: Artificial neural network modeling and molecular docking insights. International Journal of Biological Macromolecules 2019; 123:587-99.

Das P, Debnath P, Debnath A. Enhanced sono-assisted adsorptive uptake of malachite green dye onto magnesium ferrite nanoparticles: Kinetic, isotherm and cost analysis. Environmental Nanotechnology, Monitoring and Management 2021;16:Article No. 100506.

Dil AA, Vafaei A, Ghaedi AM, Ghaedi M, Dil EA. Multi-responses optimization of simultaneous adsorption of methylene blue and malachite green dyes in binary aqueous system onto Ni:FeO(OH)-NWs-AC using experimental design: Derivative spectrophotometry method. Applied Organometallic Chemistry 2018;32(3):1-13.

Gajera R, Vardhan R, Yadav A, Kumar P. Adsorption of cationic and anionic dyes on photocatalytic flyash/TiO_2 modified chitosan biopolymer composite. Journal of Water Process Engineering 2022;49(7):Article No. 102993.

Haris M, Khan MW, Paz-Ferreiro J, Mahmood N, Eshtiaghi N. Synthesis of functional hydrochar from olive waste for simultaneous removal of azo and non-azo dyes from water. Chemical Engineering Journal Advances 2022;9:Article No. 100233.

Hasanah M, Wijaya A, Arsyad FS, Mohadi R, Lesbani A. Preparation of hydrochar from *Salacca zalacca* peels by hydrothermal carbonization: Study of adsorption on congo red dyes and regeneration ability. Science and Technology Indonesia 2022;7(3):372-8.

Karthi S, Sangeetha RK, Arumugam K, Karthika T, Vimala S. Removal of methylene blue dye using shrimp shell chitin from industrial effluents. Materials Today: Proceedings 2022; 5:Article No. 428.

Kaveh R, Bagherzadeh M. Simultaneous removal of mercury ions and cationic and anionic dyes from aqueous solution using epichlorohydrin cross-linked chitosan@magnetic Fe_3O_4/ activated carbon nanocomposite as an adsorbent. Diamond and Related Materials 2022;124(2):Article No. 108923.

Li W, Xu M, Cao Q, Luo J, Yang S, Zhao G. Magnetic GO/Fe_3O_4 for rapid malachite green (MG) removal from aqueous solutions: A reversible adsorption. RSC Advances 2021; 11(32):19387-94.

Ling C, Yimin D, Qi L, Chengqian F, Zhiheng W, Yaqi L, et al. Novel High-efficiency adsorbent consisting of magnetic cellulose-based ionic liquid for removal of anionic dyes. Journal of Molecular Liquids 2022;353:Article No. 118723.

Mohadi R, Normah N, Fitri ES, Palapa NR. Unique adsorption properties of cationic dyes malachite green and rhodamine-B on longan (*Dimocarpus longan*) peel. Science and Technology Indonesia 2022;7(1):115-25.

Mohammadi A, Daemi H, Barikani M. Fast removal of malachite green dye using novel superparamagnetic sodium alginate-coated Fe_3O_4 nanoparticles. International Journal of Biological Macromolecules 2014;69:447-55.

Patil MR, Shrivastava VS. Adsorption of malachite green by polyaniline-nickel ferrite magnetic nanocomposite: An isotherm and kinetic study. Applied Nanoscience (Switzerland) 2015;5(7):809-16.

Qiao Q, Zhou H, Guo F, Shu R, Liu S, Xu L, et al. Facile and scalable synthesis of mesoporous composite materials from coal gasification fine slag for enhanced adsorption of malachite green. Journal of Cleaner Production 2022; 22(110):Article No. 131932.

Rahmayanti A, Firdaus A, Tamyiz M, Hamidah LN, Oktavia L, Rosyidah E, et al. Synthesis and effectiveness of snake fruit (*Salacca zalacca*) seed charcoal bio-adsorbent in reducing remazol brilliant blue. IOP Conference Series: Earth and Environmental Science 2022;1030(1):Article No. 012016.

Sadegh N, Haddadi H, Arabkhani P, Asfaram A, Sadegh F. Simultaneous elimination of rhodamine B and malachite green dyes from the aqueous sample with magnetic reduced graphene oxide nanocomposite: Optimization using experimental design. Journal of Molecular Liquids 2021; 343:Article No. 117710.

Sadiq AC, Olasupo A, Rahim NY, Ngah WSW, Suah FBM. Comparative removal of malachite green dye from aqueous solution using deep eutectic solvents modified magnetic chitosan nanoparticles and modified protonated chitosan beads. Journal of Environmental Chemical Engineering 2021;9(5):Article No. 106281.

Sanad MMS, Farahat MM, Abdel KMA. One-step processing of low-cost and superb natural magnetic adsorbent: Kinetics and thermodynamics investigation for dye removal from textile wastewater. Advanced Powder Technology 2021;32(5): 1573-83.

Venkatesan S, Ahmed H, Ali I, Rafique N. Evaluation of the production of hydrochar from spent coffee grounds under different operating conditions. Journal of Water Process Engineering 2022;49(7):Article No. 103037.

Vergis BR, Hari KR, Kottam N, Nagabhushana BM, Sharath R, Darukaprasad B. Removal of malachite green from aqueous solution by magnetic $CuFe_2O_4$ nano-adsorbent synthesized by one pot solution combustion method. Journal of Nanostructure in Chemistry 2018;8(1):1-12.

Wang Z, Ren D, Zhang X, Zhang S, Chen W. Adsorption-degradation of malachite green using alkali-modified biochar immobilized laccase under multi-methods. Advanced Powder Technology 2022;33(11):Article No. 103821.

Wu J, Yang J, Feng P, Wen L, Huang G, Xu C, et al. Highly efficient and ultra-rapid adsorption of malachite green by recyclable crab shell biochar. Journal of Industrial and Engineering Chemistry 2022;113:206-14.

Yvonne KS, Mahani Y, Razak W, Sofiyah MR, Razali MH. Properties of epoxy-hybrid composite using bamboo fiber and *Salacca zalacca* fruit skin powder. Materials Today: Proceedings 2018;5(10):21759-64.

Zadvarzi SB, Khavarpour M, Vahdat SM, Baghbanian SM, Rad AS. Synthesis of Fe_3O_4@chitosan@ZIF-8 towards removal of malachite green from aqueous solution: Theoretical and experimental studies. International Journal of Biological Macromolecules 2021;168:428-41.

Zheng H, Qi J, Jiang R, Gao Y, Li X. Adsorption of malachite green by magnetic litchi pericarps: A response surface methodology investigation. Journal of Environmental Management 2015;162:232-9.

Zubaidah E, Dewantari FJ, Novitasari FR, Srianta I, Blanc PJ. Potential of snake fruit (*Salacca zalacca* (Gaerth.) Voss) for the development of a beverage through fermentation with the *Kombucha consortium*. Biocatalysis and Agricultural Biotechnology 2018;13(9):198-203.

Treating Tapioca Starch Industrial Wastewater Using Two-Phase Multi-Staged Up-Flow Anaerobic Sludge Blanket (MS-UASB)

Thanapat Thepubon[1,2], Pairaya Choeisai[1,2*], Krit Choeisai[1], and Kazuaki Syutsubo[3,4]

[1]Faculty of Engineering, Khon Kaen University, Khon Kaen 40002, Thailand
[2]Research Center for Environmental and Hazardous Substance Management, Khon Kaen University, Khon Kaen 40002, Thailand
[3]Regional Environment Conservation Division, National Institute for Environmental Studies, Tsukuba, Ibaraki, Japan
[4]Research Center for Water Environment Technology, School of Engineering, The University of Tokyo, Bunkyo, Tokyo, Japan

ARTICLE INFO

Received: 26 Sep 2022
Received in revised: 22 Nov 2022
Accepted: 1 Dec 2022
Published online: 22 Dec 2022
DOI: 10.32526/ennrj/21/202200210

Keywords:
Two-phase UASB/ Acidification unit/ MS-UASB reactor/ Tapioca starch wastewater/ Sludge flotation

*** Corresponding author:**
E-mail: pairaya@yahoo.com

ABSTRACT

A laboratory-scale, two-phase multi-staged up-flow anaerobic sludge blanket (MS-UASB) treatment system was monitored over time in order to evaluate its treatment efficiency and performance when treating non-diluted industrial tapioca starch wastewater under ambient temperature in Thailand. The system consisted of an acidification (AC) reactor and MS-UASB reactor and was operated for 280 days. The two-phase MS-UASB achieved a maximum organic loading rate (OLR) of 8 kg-COD/m^3/day for the overall system and reached 80.5% of chemical oxygen demand (COD) removal efficiency. Based on the inlet wastewater of each reactor, the AC reactor removed 61.85% of suspended solids and achieved acidification of the wastewater to produce volatile fatty acids at over 50%. Meanwhile, the MS-UASB reactor achieved 74.5% COD removal efficiency. Further analysis found that the increase in soluble extracellular polymeric substances per bound extracellular polymeric substances (S-EPS/B-EPS) was related to the floating sludge phenomenon, which occurred under excess OLR condition.

1. INTRODUCTION

Tapioca (*Manihot esculenta* Crantz), also known as cassava, is a crop cultivated in tropical and sub-tropical regions that can grow in extreme agro-ecologies. The crop can survive infertile land and withstand drought, and its harvests are less affected by diseases. These attributes have made tapioca an important crop, serving as a dietary energy source throughout the world, especially in African and South American regions. While Thailand is one of the major producers of tapioca, the country does not count the crop as a main staple for consumption (Sowcharoensuk, 2020). Accordingly, the majority of tapioca harvested in Thailand is processed into tapioca products, especially tapioca starch, and is bound for export. Tapioca starch is flexible in terms of functional properties and can be used in a wide range of food and non-food industries (Breuninger et al., 2009; Li et al., 2017). Thailand is known as the world's largest exporter of tapioca starch, accounting for as much as 80 percent of world tapioca starch exports (FAO, 2018) and with an annual production volume of 2 million tons (TTSA, 2021; TTDI, 2000).

The tapioca starch production process involves seven major steps: washing the roots, chopping and grinding the plant, extracting and separating the starch, dewatering and separating the protein, drying, and packaging. The process requires a large volume of water, which becomes a massive amount of wastewater. In Thailand, the industry creates an average of 19 m^3 of wastewater per one ton of produced tapioca starch. This wastewater is high in organic content and acidity (Chavalparit and Ongwandee, 2009; Intanoo et al., 2014; Jiraprasertwong et al., 2019; Thepubon et al., 2020), and the discharge of untreated tapioca starch wastewater into the environment can lead to terrible environmental problems. Generally, anaerobic ponds and anaerobic covered lagoon systems are well-known wastewater treatment systems and are considered solutions for various wastewater producing industries, including the tapioca starch industry (Akunna, 2018; Khanal, 2011; Rajbhandari and Annachhatre, 2004).

Citation: Thepubon T, Choeisai P, Choeisai K, Syutsubo K. Treating tapioca starch industrial wastewater using two-phase multi-staged up-flow anaerobic sludge blanket (MS-UASB). Environ. Nat. Resour. J. 2023;21(1):78-89. (https://doi.org/10.32526/ennrj/21/202200210)

However, such systems have low loading rates, require high hydraulic retention times (HRT), and are associated with large land area requirements and high implementation costs. These limitations have led to the development and promotion of various alternatives. An up-flow anaerobic sludge blanket (UASB) reactor is one such treatment system with potential to achieve a high organic loading rate (OLR) with high removal efficiency of chemical oxygen demand (COD) (Annachhatre and Amatya, 2000; Lu et al., 2015; Van Lier et al., 2015). However, failures in long-term operation of UASB reactors while treating tapioca starch wastewater have been observed, including sludge flotation and washout, which have been ascribed to inappropriate operating conditions (Lu et al., 2015; Wang et al., 2018; Wu et al., 2020).

Previous research by Syutsubo et al. (1998) has found that vigorous biogas production during excessive OLR can increase washout of granular sludge in a UASB reactor. In order to solve this problem, biogas production is reduced by installing multiple gas-liquid-solid separators (GLSs) along the height of the UASB reactor, transforming the system into what is known as a multi-staged UASB (MS-UASB). This solution has been applied toward treating various industrial wastewater types, such as lipid and protein, molasses, and high strength vinasses wastewater (Choeisai et al., 2014; Onodera et al., 2011; Tagawa et al., 2002). In addition, a recent study showed that the two-phase UASB, which adds an acidification unit, can enhance stability in treatment performance and greatly improve stability in the morphology of granular sludge in UASB reactors (Wu et al., 2020). This can be attributed to the separation of ideal operating conditions for major microorganisms in the anaerobic treatment process into acidogenesis and methanogenesis. Therefore, research suggests that the combination of an acidification unit and MS-UASB, otherwise known as a two-phase MS-UASB system, may be able to enhance treatment efficiency and stability of granular sludge when treating tapioca starch wastewater.

This study, therefore, initiated testing using a laboratory-scale, two-phase MS-UASB installation, which was operated under ambient temperatures in Northeast Thailand, the nation's major agricultural region for tapioca production and 54.5% of its total agricultural land (KURDI, 2015), to comprehensively evaluate the installation's performance and efficiency in treating high-strength industrial tapioca starch wastewater. The effect of the OLR on system stability was examined by varying HRT to optimize operational conditions. Furthermore, retained sludge properties, including methane producing activity (MPA), sludge concentration, sludge volume index (SVI), and extracellular polymeric substances (EPS), were periodically evaluated in order to assess operating conditions as well as operational stability.

2. METHODOLOGY

2.1 Experimental set-up

A schematic diagram of the laboratory-scale proposed anaerobic treatment system used in this study is shown in Figure 1. The system consisted of an acidification (AC) reactor and an MS-UASB reactor, with working volumes of 8.5 L (10-cm diameter and 100-cm height internally) and 12.7 L (10-cm width, 20-cm length, and 100-cm height), respectively. The MS-UASB reactor was equipped with three GLSs along its height, as illustrated in Figure 1. The AC reactor was initiated without inoculation. The MS-UASB was initiated with 77.7 g-VSS seed sludge. The seed sludge, at a concentration of 6,100 mg-VSS/L, was obtained from an anaerobic cover lagoon treating tapioca starch wastewater located in a Khon Kaen, Thailand tapioca starch factory.

2.2 Characteristics of tapioca starch wastewater

The influent was tapioca starch wastewater (TSW) obtained from the tapioca starch extraction process within Khon Kaen Province, Thailand's tapioca starch industry. The wastewater had a pH of 4.11-4.24; a COD of 13,800-21,400 mg/L, with a biochemical oxygen demand (BOD)/COD ratio of 0.58-0.65; a total suspended solids (SS) value of 2,800-7,340 mg/L, with a volatile suspended solid (VSS) per SS ratio of 0.58-0.69; a total carbohydrates value of 1,080-1,770; and a protein value of 930-1,625 mg/L. Settleable solids were removed from the influent by gravity settling for 1 h, increasing methane production capability by an average of 15.5% with SS concentration removal (Thepubon et al., 2020). Influent pH was adjusted to 7.0 by the addition of sodium bicarbonate ($NaHCO_3$). Neither nutrients nor trace elements were added to adjust influent nutrient composition.

2.3 System operating conditions

The intention of the present study was to enhance the COD removal and biogas production rates in the anaerobic digestion process using the MS-UASB. The system was operated using a semi-continuous feeding pattern controlled by a mechanical electric timer switch. The influent was fed into the system for 15-minute periods along the experimental period. The system's operating conditions are summarized in Table 1. The experimental period was divided into a start-up period (phases 1 and 2) and an acclimation period (phases 3 to 6), operating with diluted wastewater and non-diluted wastewater, respectively.

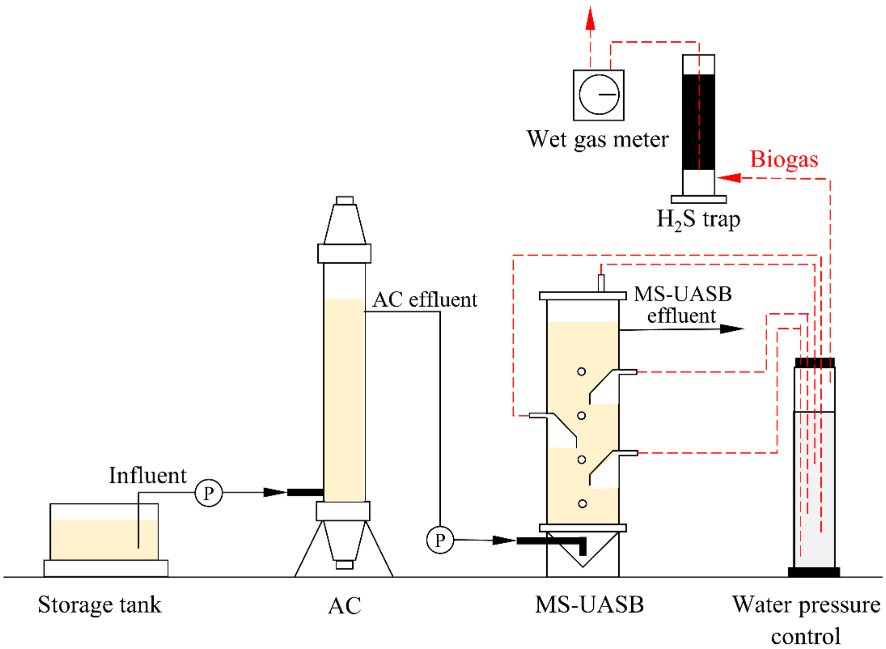

Figure 1. Schematic diagram of laboratory-scale, two-phase MS-UASB system

Table 1. Operating conditions of the two-phase MS-UASB system

Phase	Operation period (day)	Influent COD (mg/L)	AC		MS-UASB	
			HRT (h)	OLR*	HRT (h)	OLR*
1	1-35	2,910.5±388.0	68	1.0±0.1	108	0.5±0.1
2	36-110	5,861.2±498.4	68	2.1±0.2	108	0.8±0.1
3	111-152	15,711.5±2488.6	38	9.8±1.6	58	4.5±0.8
4	153-210	15,116.6±1,692.6	21	17.7±2.7	30	9.1±1.3
5	211-223	10,972.8±1,556.6	10	33.6±1.2	16	17.1±2.4
6	224-280	11,872.1±1,627.8	21	19.8±3.0	30	10.5±1.8

*OLR is given in units of kg-COD/m^3/day

2.4 Analytical methods

The room temperature and internal liquid temperature at mid-height of both the AC and MS-UASB reactors were measured daily. Wastewater samples, including influent, AC effluent, and MS-UASB effluent, were collected to measure COD, SS, and VSS following standard methods (Baird et al., 2017), and volatile fatty acids (VFAs) were measured by direct titration method (Dilallo and Albertson, 1961), in order to monitor the efficiency and performance of the treatment system. In addition, the samples were measured twice for carbohydrate and protein content at each operational phase when COD removal of both reactors was in a steady state. Protein and carbohydrate content were evaluated by Lowry's method (Lowry, 1951) using albumin as a reference solution and phenol-sulfuric acid method (Nielsen, 2017) using glucose as a reference solution, respectively. Biogas production was measured daily by a wet gas meter (Tokyo Shinagawa, model WS-1A), and biogas composition was analyzed using gas chromatography (Shimadzu, GC-8A) with a thermal conductivity detector (TCD).

2.5 Analysis of retained sludge behavior

Retained sludge samples were periodically collected from the 0.15-m high MS-UASB reactor to investigate physicochemical sludge properties, including mixed liquor suspended solids (MLSS), mixed liquor volatile suspended solids (MLVSS), and SVI. Moreover, each sludge sample was measured for EPS, including bound EPS (B-EPS) and soluble EPS (S-EPS) forms. EPS were extracted using formaldehyde-sodium hydroxide (Liu and Fang, 2002; Chabalina et al., 2008), after which variations in carbohydrate and protein content in both forms of extracted EPS were determined.

In order to investigate methane producing capability, retained sludge samples were collected on Day 0 (seed sludge), Day 132, and Day 223 and were evaluate for MPA. Serum vials were used following the method described by Harada et al. (1994) and Syutsubo et al. (2001), under mesophilic conditions (35±1ºC) at a food/microorganism (F/M) ratio of 0.4 mg-COD/mg-VSS. The substrates used in MPA testing included acetate, H_2/CO_2 (80/20, v/v), and tapioca starch wastewater.

3. RESULTS AND DISCUSSION

3.1 Performance of two-phase MS-UASB system

The two-phase MS-UASB system was operated for 280 days, divided into the six phases described in Table 1, under ambient temperatures. Figure 2 shows the system's operating conditions and performance over time along the experimental period. Ambient and liquid temperatures inside both reactors remained between 20-33ºC and averaged 28±2.4ºC (as shown in Figure 2(a)). During the start-up period, in phases 1 and 2, the COD removal efficiency of the overall system was maintained above 80%. After successful start-up, non-diluted TSW was fed to the system in phases 3-6. Phases 3-5 could be considered an acclimation period and phase 6 a recovery period. During the acclimation period, OLR was increased by decreasing HRT. Phase 4 was the most stable period, with the overall system reaching its highest OLR of up to approximately 7 kg-COD/m^3/day (18 kg-COD/m^3/day at the AC reactor and 9 kg-COD/m^3/day at the MS-UASB reactor), and an average total COD (T-COD) removal efficiency of 80.5% (22.3% at the AC reactor and 74.5% at the MS-UASB reactor). However, sludge flotation and washout occurred in the MS-UASB in phase 5 on Day 223, which was 12 days after operation had been characterized by an HRT of 26 h and OLR of 14 kg-COD/m^3/day (33 kg-COD/m^3/day at the AC reactor and 17 kg-COD/m^3/day at the MS-UASB reactor).

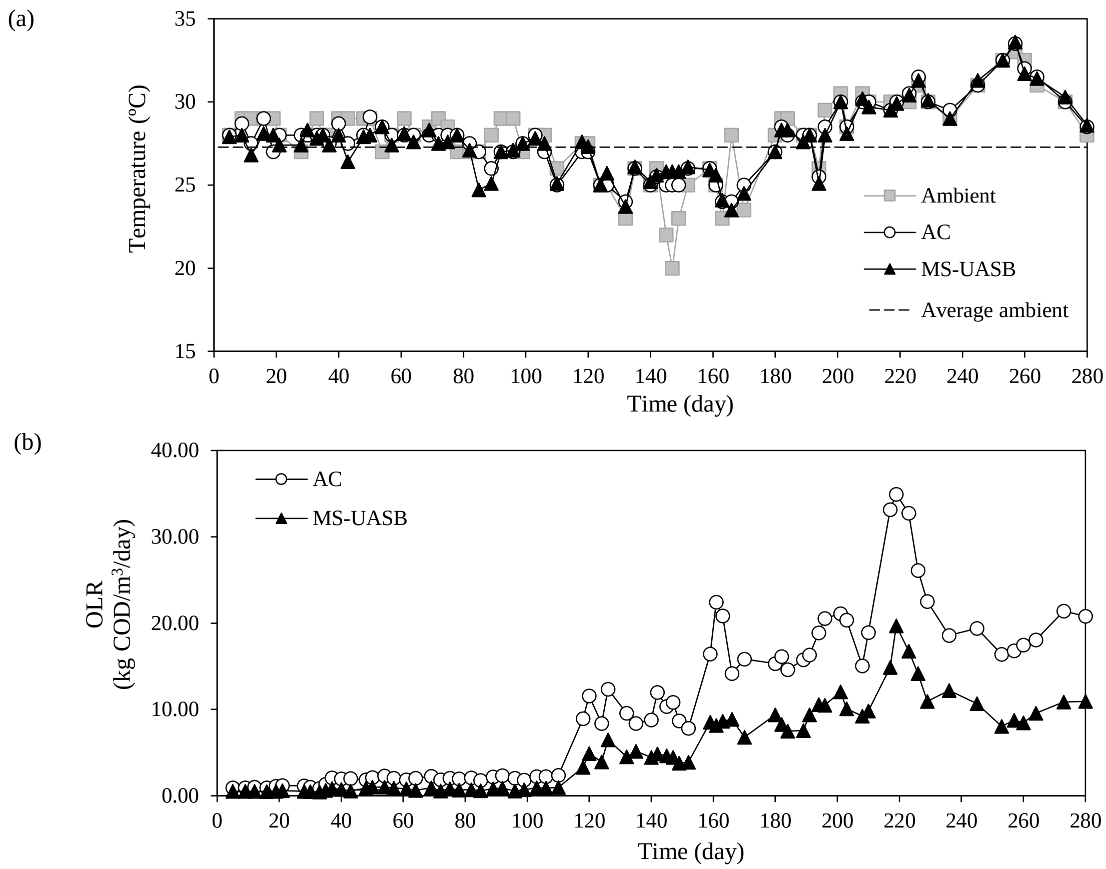

Figure 2. Operational performance of two-phase MS-UASB system during experimental period

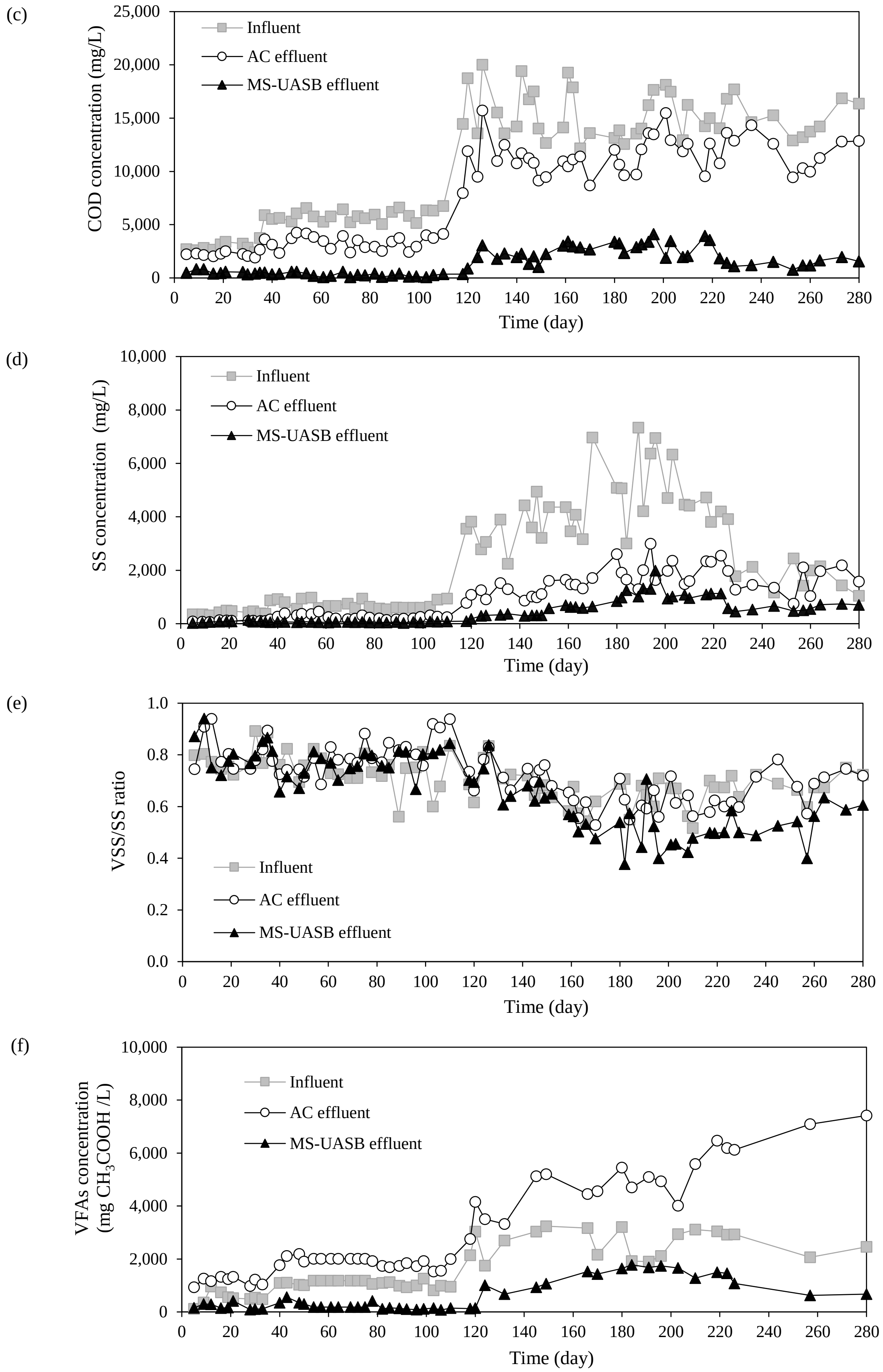

Figure 2. Operational performance of two-phase MS-UASB system during experimental period (cont.)

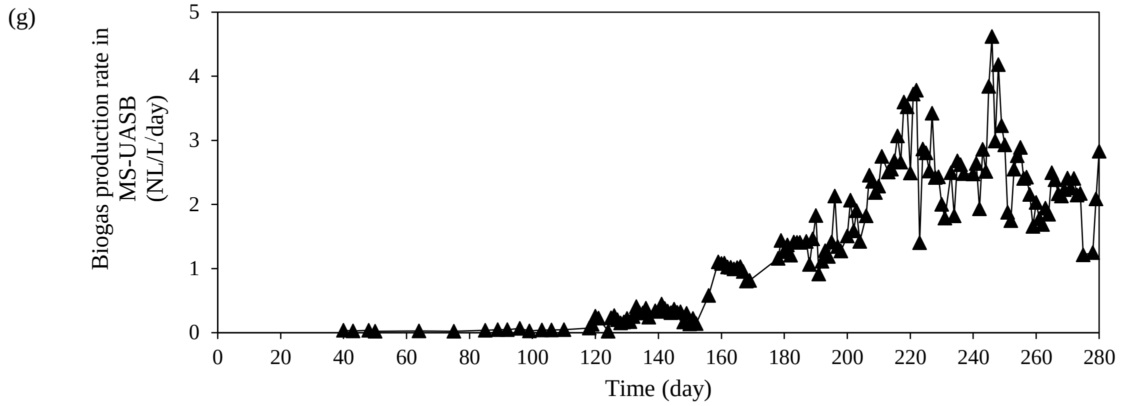

Figure 2. Operational performance of two-phase MS-UASB system during experimental period (cont.)

In order to solve this problem, the HRT was immediately extended to 51 h as in phase 4. The HRT remained at 51 h throughout phase 6, or the recovery period, from Days 224-280. In the recovery period, the average T-COD removal efficiency of the AC reactor was 20.9%, while that of the MS-UASB increased to 88.8% based on inlet COD, indicating a higher efficiency than that measured under similar HRT conditions in phase 4, during the acclimation period. The increase of COD removal efficiency was attributed to an increase in the average ambient temperature by approximately 3ºC as a result of seasonal weather changes in Thailand, as shown in Figure 2 (a). It could be concluded that the two-phase MS-UASB for treating high-strength industrial TSW was able to achieve a maximum available OLR of 8 kg-COD/m^3/day with an HRT of 51 h for the overall system. Based on inlet wastewater for each reactor, the AC reactor and the MS-UASB reactor achieved an OLR of 19 kg-COD/m^3/day and 9 kg-COD/m^3/day, respectively.

During phase 4, the AC reactor achieved SS removal at an average of 61.8±10.1% and the VSS/SS ratio of the AC reactor influent and effluent showed similar characteristics, averaging 0.62±0.06 and 0.61±0.06, respectively. Differences in average T-COD and soluble COD of the AC reactor's influent and effluent (data not shown) revealed that the COD caused by suspended solids (SS-COD) in the influent and effluent was at 23.9% and 12.3%, based on each T-COD, respectively. SS-COD removal at the AC reactor was 56.2% based on SS-COD influent, or 16.6% based on T-COD influent (T-COD removal at the AC reactor was 22.3% based on T-COD influent). Consequently, the AC reactor trapped more than 50% of the influent SS without changing VSS/SS ratio characteristics, and 74.4% of T-COD removal was COD removal from the trapped SS fraction. The MS-UASB reactor, on the other hand, achieved SS removal at an average of 43.5%. The VSS/SS ratio of the MS-UASB effluent changed to 0.50±0.08, a 10% decrease from the AC reactor effluent. This indicated that the MS-UASB reactor achieved removal of the organic fraction of SS particulate matter to a modest degree.

In terms of VFAs concentration (Figure 2(f)), that of the AC reactor effluent increased by more than 50% throughout the experimental period, indicating that an acidogenesis reaction occurred in the AC reactor. Subsequently, the MS-UASB reactor, fed with AC reactor effluent, decreased the VFAs concentration by up to 60%. VFAs concentration of the MS-UASB effluent in phase 4 averaged 1,600 mg/L as acetic acid, and VFAs effluent concentration was stabilized.

The methane content in the biogas depended on a variety of factors, including the particulate matter in the wastewater, the pH in the reactor, and nutrient limitations. The methane potential of each wastewater sample needed to be evaluated using small scale batch reactor performance test results (Angelidaki and Sanders, 2004). In phase 4, the MS-UASB influent, or the AC-reactor effluent, had a high SS concentration, averaging 1,820±475 mg SS/L, the pH of the effluent averaged 7.94±0.07, and the methane content (as shown in Figure 2(g)) was measured and averaged at 76.5±10.2%. However, it should be noted that fluctuations in biogas production (data not shown) occurred within the MS-UASB reactor, and the methane potential was calculated to be 0.69±0.28 NL-CH_4/L-TSW, equivalent to a methane yield of 0.27±0.16 NL-CH_4/g-$COD_{removed}$.

The aforementioned two-phase MS-UASB performance results indicate that the installation of an AC reactor as a pre-treatment unit enhanced treatment performance and reduced the risk of inhibition within the MS-UASB reactor. Clearly, the use of a two-phase

MS-UASB could help to reduce retention time from approximately four days of degradation duration time as measured by the biochemical methane potential test to two days for achieving maximum biodegradation potential (Thepubon et al., 2020).

3.2 Biodegradation of macro-pollutants in TSW

As shown in Figure 3(a) and 3(b), carbohydrate and protein, the major macro-pollutants in starch wastewater (Devereux et al., 2011), were measured under all operating conditions throughout the experimental period. The AC reactor achieved a carbohydrate removal efficiency of over 80% under all operating conditions while protein removal levels fluctuated. Protein removal efficiency, varying between 30-67%, mainly occurred at the MS-UASB reactor. These results clearly indicate that carbohydrates were effectively converted to acetic acids and other VFAs during the acidification that occurred at the AC reactor, similar to findings from previous research (Wu et al., 2020). In contrast, the protein was largely hydrolyzed and acidified under methanogenesis conditions, consistent with research by Miron et al. (2000). In addition, protein was a macro-pollutant requiring a longer HRT, with a lower biodegradation rate than carbohydrates (Akunna, 2018; Cremonez et al., 2021). This suggests that optimal conditions for the acidification unit should be further investigated in order to enhance the performance of the two-phase MS-UASB when treating tapioca starch wastewater.

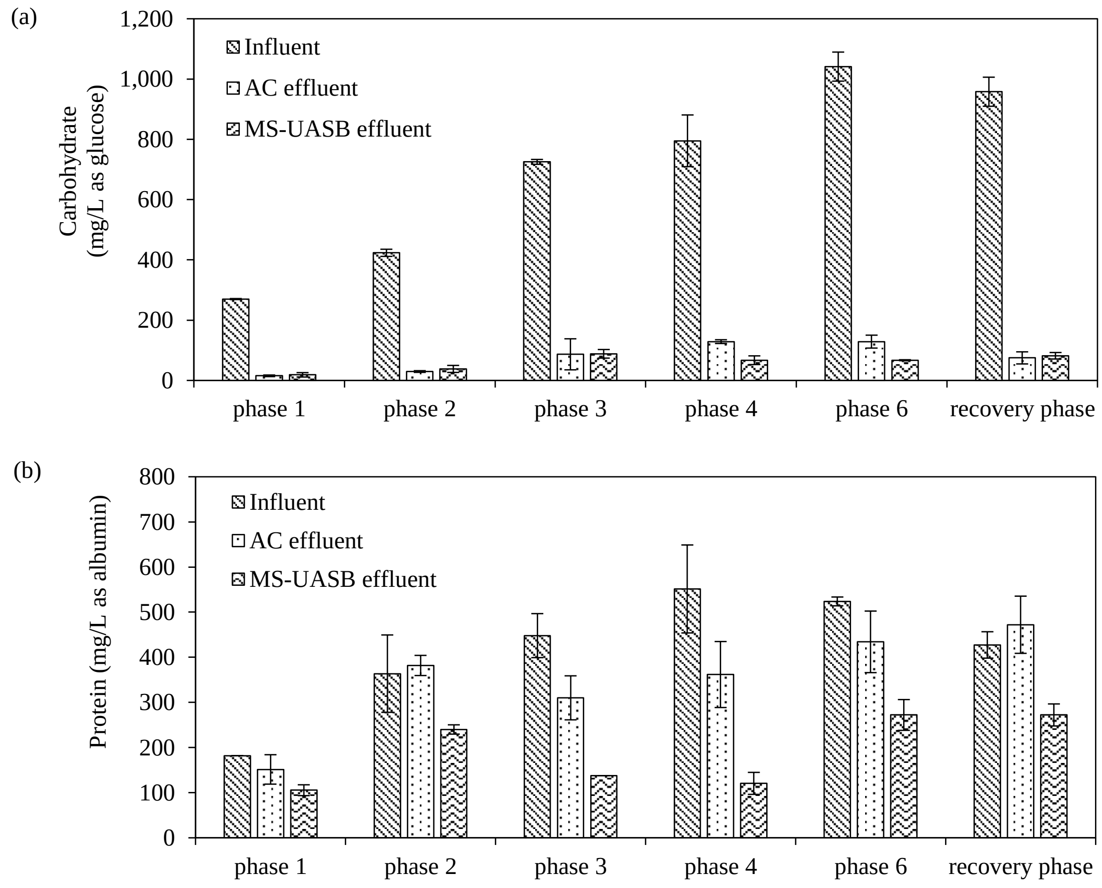

Figure 3. Treatment performance of the system in terms of (a) carbohydrate and (b) protein components

3.3 Methanogenic producing activities (MPA) of the retained sludge

Methanogenesis in anaerobic digestion stages is generally separated into *Acetoclastic methanogen* and *Hydrogenophilic methanogen* (Akunna, 2018). *Acetoclastic methanogen* uses acetic acid to produce methane, with 72% of methane produced from *Acetoclastic methanogen*, and the remaining 28% of methane produced from *Hydrogenophilic methanogen* by utilizing H_2 and CO_2 (Khanal, 2011). In the MPA test conducted for the present study, acetate and H_2/CO_2 (80/20) were used as test substrates to uncover the activity of these two types of methanogens, and TSW was used as a test substrate to evaluate the MPA of the retained sludge from the TSW. The changes in MPA of the retained sludge are shown in Figure 4. The sludge samples included seed sludge (day 0), retained sludge from the acclimation period in phase 3 (Day 132), and retained sludge from the first day that sludge flotation occurred in phase 5 (Day 223). The results showed that when using acetate as the test substrate, the MPA of the retained sludge had increased 2.1 times by Day 132 and 4.6 times by Day 223 compared to that of the seed sludge; when using H_2/CO_2 as the test substrate, changes in MPA in the retained sludge were insignificant when compared to that of the seed sludge; when TSW was used as the test substrate, the MPA of the retained sludge was shown to have increase 1.6 times by Day 132 and 5.9 times by Day 223 compared to that of the seed sludge. These results indicate that the TSW was acclimated in the MS-UASB, and the two-phase MS-UASB did separate between the acidogenesis and methanogenesis reactions under ex-situ conditions. Consequently, MPA was shown to significantly increase when acetate was used as the source for methane production. This is typical degradation that occurs due to *Acetoclastic methanogen*.

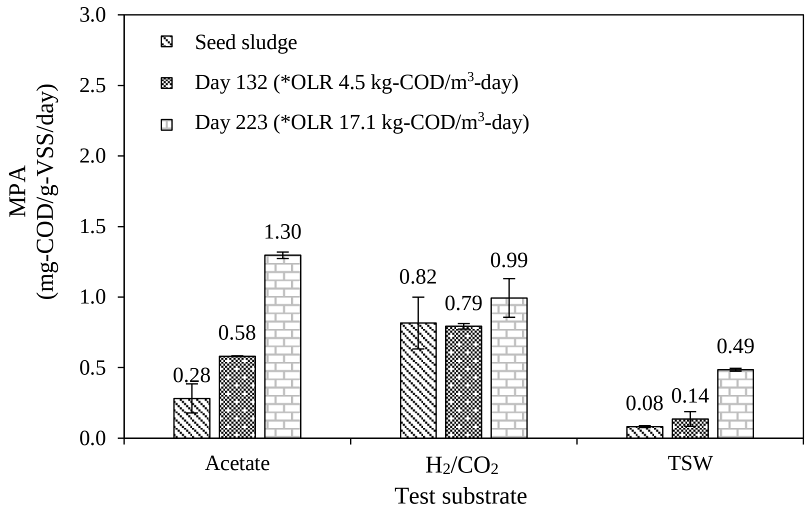

Figure 4. MPA of seed sludge and retained sludge sampled on Days 132 and 223 (OLR*: the average OLR of all phases of the MS-UASB reactor)

3.4 Physicochemical properties of retained sludge

Aside from the operational conditions, physical and chemical properties of the retained sludge in terms of MLVSS concentration, SVI, B-EPS, and S-EPS were analyzed and are shown in Figure 5. Sludge properties can influence performance and stability of anaerobic wastewater treatment systems (Wang et al., 2018). Higher MLVSS concentrations (ranging from 30,000-50,000 mg/L) and lower SVI values (<20 mL/g MLVSS) are preferable for obtaining good granulation of UASB retained sludge (Cervantes et al., 2006). As shown in Figure 5(a), during the acclimation period, the MLVSS concentration of the MS-UASB retained sludge increased and stabilized at 9,300 mg/L, with a low SVI of 17.7 mL/g-MLVSS. This was better than the MLVSS concentration of the seed sludge, which was 6,120 mg/L, with an SVI of 40.4 mL/g-VSS. These results confirm these advantageous properties of MS-UASB retained sludge.

Moreover, TSW's SS concentration of over 500 mg/L is considered high for a UASB system, as SS adsorption has been evidenced to affect granular sludge properties (Stronach et al., 2012; Van Lier et al., 2015). EPS biosynthesis, achieved either by microorganism secretion or adsorption of certain organic compounds, significantly influences sludge properties (Sheng et al., 2010). Consequently, retained sludge and floating sludge were evaluated for EPS along the experimental period. EPS is separated into two forms: B-EPS and S-EPS. B-EPS is described as an inner layer tightly and closely bound with cells, while S-EPS is weakly bound with cells dispersed in the solution. Normally, microbial aggregates contain higher B-EPS content than S-EPS content. Both forms of EPS are comprised largely of polysaccharides (carbohydrates), with proteins as the major substance. Previous studies have focused on the ratio of protein/carbohydrate as a parameter relating to sludge characteristics (Lu et al., 2015; Wu et al., 2020; Liu et al., 2010; Lu et al., 2018; Wang et al., 2018). However, the present study found protein to be a major chemical substance that significantly changed the concentration of both forms of EPS throughout the experimental period. This resulted in the retained sludge having a protein/carbohydrate ratio in line with EPS content, which may be attributed to the adsorption of protein compounds. These protein compounds were a major macro-pollutant fed into the MS-UASB reactor, as mentioned in section 3.2. Consequently, the protein/carbohydrate ratio of EPS content was not a focus in the present study; rather, S-EPS/B-EPS was considered a useful parameter relating to the retained sludge properties in this study.

As shown in Figure 5(b), total B-EPS content did not change significantly in the start-up period. Total S-EPS content, however, decreased dramatically within 32 days after the start-up period (-8.8 times from seed sludge). The S-EPS/B-EPS ratio of retained sludge on Day 32 was 0.08, an 87.5% decrease from the seed sludge, which contained an S-EPS/B-EPS ratio of 0.62. The B-EPS content of retained sludge on Days 132, 223, and 246 then increased 1.8, 3.2, and 4.4 times, respectively, relative to the retained sludge on Day 32, while the S-EPS content increased 1.5 times, 3.6 times, and 4.5 times, respectively. During this period, the S-EPS/B-EPS ratio of retained sludge remained in the range of 0.06-0.08.

In addition, a floating sludge phenomenon occurred on Day 223. The floating sludge was collected and analyzed for both forms of EPS content, then compared to the retained sludge on the same experimental day, the results of which are shown in Figure 5(c). The comparison showed that the total B-EPS content of the floating sludge was 48.1% lower than that of the retained sludge, while S-EPS content was 98.9% higher than that of the retained sludge. The S-EPS/B-EPS ratio of the floating sludge was 0.31, 3.9 times higher than that of the retained sludge.

Based on the findings described above, the decrease in S-EPS and the lower S-EPS/B-EPS ratio in the retained sludge on Day 32, relative to the seed sludge, indicated an elimination of the poor settleable sludge containing a high S-EPS/B-EPS ratio. In other words, a selection and aggregation of retained sludge occurred in this period, increasing biomass concentration and improving settleability. Then, the S-EPS/B-EPS ratio of the retained sludge during the acclimation and recovery period was maintained in the range of 0.06-0.08, and biomass concentrations and SVI remained stable. The floating sludge on Day 223, on the other hand, was shown to have an S-EPS/B-EPS ratio of 0.31, suggesting that a higher S-EPS/B-EPS ratio may indicate an increase in the production of weakly bound EPS on the sludge surface, resulting in poor settleability and sludge flotation. Meanwhile, the retained sludge with the lower S-EPS/B-EPS ratio would have a more stable structure, resulting in high settleability with low SVI.

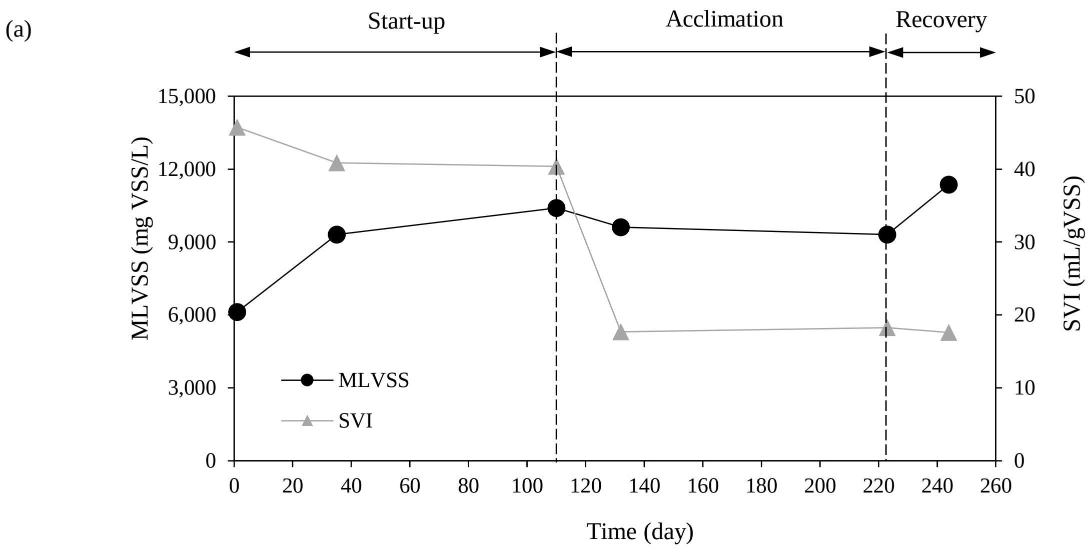

Figure 5. Physicochemical properties of sampled MS-UASB sludge over time, including (a) MLVSS and SVI, (b) EPS, and (c) comparison between EPS of retained sludge and floating sludge on Day 223

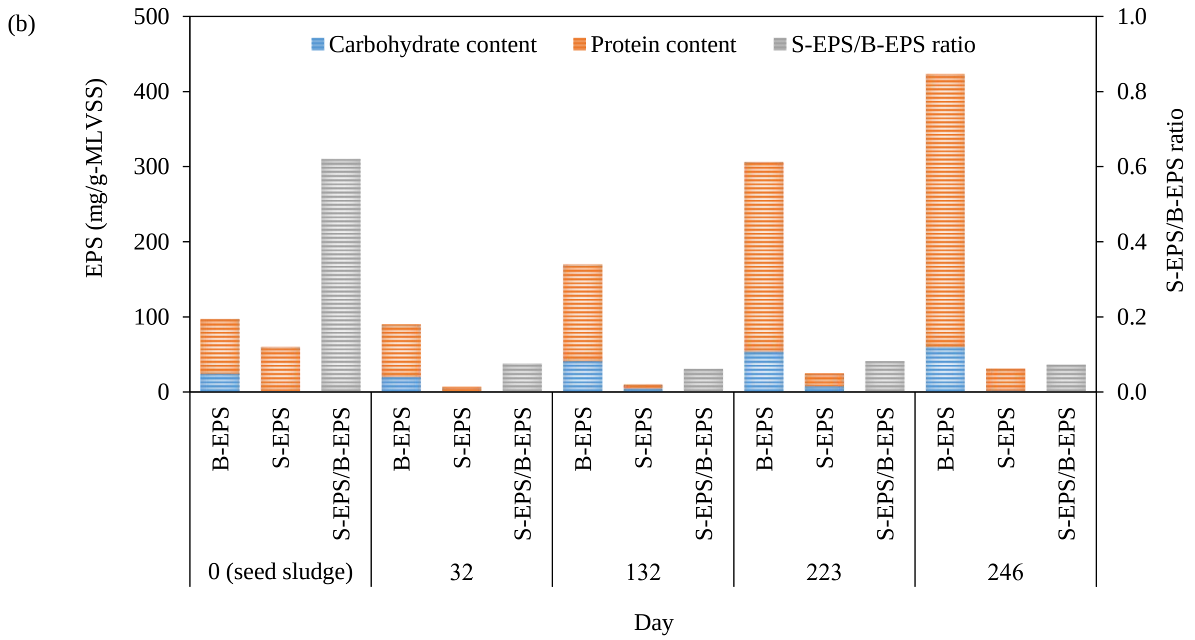

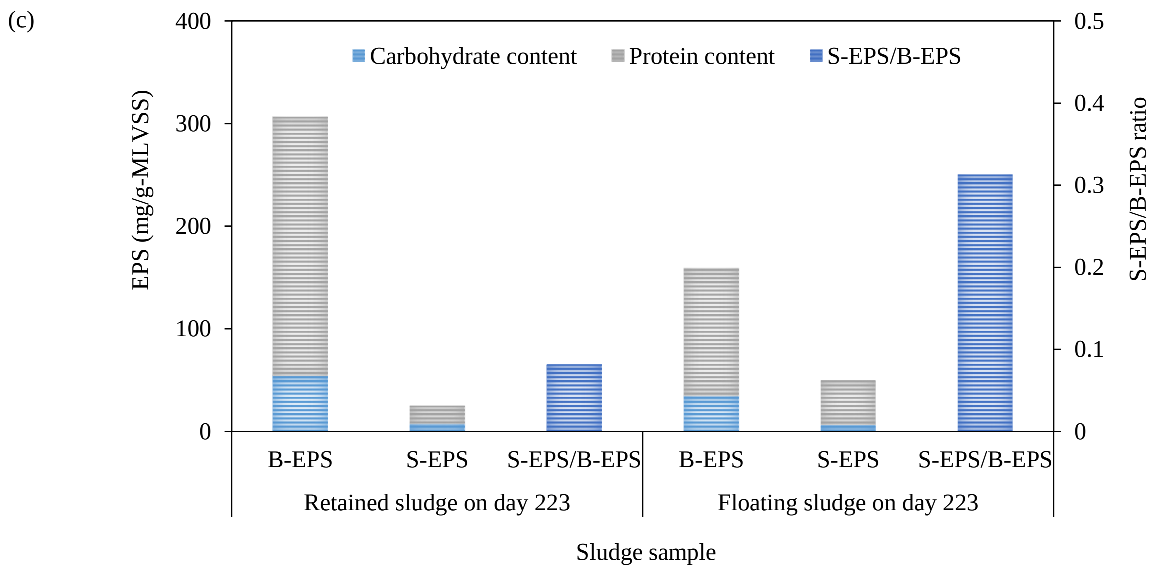

Figure 5. Physicochemical properties of sampled MS-UASB sludge over time, including (a) MLVSS and SVI, (b) EPS, and (c) comparison between EPS of retained sludge and floating sludge on Day 223 (cont.)

4. CONCLUSION

Treatment of non-diluted TSW by the two-phase MS-UASB system provided a stable performance, with the overall system averaging 80.5% COD removal under a maximum available OLR of 8 kg-COD/m^3/day and at ambient temperatures of 28.0±2.4°C. The AC reactor removed 61.8% of SS and degraded over 80% of carbohydrates into VFAs. The MPA of the MS-UASB retained sludge on Day 224 was at 1.3 g-COD/g-VSS/day using the acetate test substrate, with a high MLVSS concentration of 9,300 mg/L, a high settleability with low SVI at 17 mL/g-MLVSS, and a low S-EPS/B-EPS ratio of 0.08. The MS-UASB system achieved a methane yield of 0.27 NL-CH_4/g-$COD_{removed}$.

REFERENCES

Akunna JC. Anaerobic Waste-Wastewater Treatment and Biogas Plants: A Practical Handbook. Boca Raton, Florida: CRC Press; 2018.

Angelidaki I, Sanders W. Assessment of the anaerobic biodegradability of macropollutants. Reviews in Environmental Science and Bio/Technology 2004;3(2):117-29.

Annachhatre AP, Amatya PL. UASB treatment of tapioca starch wastewater. Journal of Environmental Engineering 2000; 126(12):1149-52.

Baird RB, Eaton AD, Rice EW. Standard Methods for the Examination of Water and Wastewater. Washington, DC: American Public Health Association (APHA), American

Water Works Association (AWWA), and Water Environment Federation (WEF); 2017.

Breuninger WF, Piyachomkwan K, Sriroth K. Tapioca/cassava starch: Production and use: In: Starch. USA: Academmic Press; 2009. p. 541-68.

Cervantes FJ, Pavlostathis SG, van Haandel A. Advanced Biological Treatment Processes for Industrial Wastewaters. London, UK: IWA Publishing; 2006.

Chabalina LD, Rodriguez M, Prats D. Study of the extracellular polymeric substances (EPS) in different types of membrane bioreactor (MBR) effluents. WIT Transactions on Ecology and the Environment 2008;111:491-500.

Chavalparit O, Ongwandee M. Clean technology for the tapioca starch industry in Thailand. Journal of Cleaner Production 2009;17(2):105-10.

Choeisai P, Jitkam N, Silapanoraset K, Yubolsai C, Yoochatchaval W, Yamaguchi T, et al. Sugarcane molasses-based bio-ethanol wastewater treatment by two-phase multi-staged up-flow anaerobic sludge blanket (UASB) combination with up-flow UASB and down-flow hanging sponge. Water Science and Technology 2014;69(6):1174-80.

Cremonez PA, Teleken JG, Meier TR, Alves HJ. Two-Stage anaerobic digestion in agroindustrial waste treatment: A review. Journal of Environmental Management 2021;281: Article No. 111854.

Devereux S, Shuttleworth PS, Macquarrie DJ, Paradisi F. Isolation and characterization of recovered starch from industrial wastewater. Journal of Polymers and the Environment 2011;19(4):971-9.

Dilallo R, Albertson OE. Volatile acids by direct titration. Journal Water Pollution Control Federation 1961:33(4);356-65.

Food and Agriculture Organization of the United Nations (FAO). Food Outlook - Biannual Report on Global Food Markets, November 2018. Rome, Italy: Trade and Markets Division of FAO; 2018.

Harada H, Uemura S, Momonoi K. Interaction between sulfate-reducing bacteria and methane-producing bacteria in UASB reactors fed with low strength wastes containing different levels of sulfate. Water Research 1994;28(2):355-67.

Intanoo P, Rangsanvigit P, Malakul P, Chavadej S. Optimization of separate hydrogen and methane production from cassava wastewater using two-stage upflow anaerobic sludge blanket reactor (UASB) system under thermophilic operation. Bioresource Technology 2014;173:256-65.

Jiraprasertwong A, Maitriwong K, Chavadej S. Production of biogas from cassava wastewater using a three-stage upflow anaerobic sludge blanket (UASB) reactor. Renewable Energy 2019;130:191-205.

Kasetsart University Research and Development Institute (KURDI). Tapioca: Planting area in Thailand [Internet]. 2015 [cited 2021 Aug 31]. Available from: https://www3.rdi.ku.ac.th/?p=18045.

Khanal SK. Anaerobic Biotechnology for Bioenergy Production: Principles and Applications. New Jersey, USA: John Wiley and Sons; 2011.

Li S, Cui Y, Zhou Y, Luo Z, Liu J, Zhao M. The industrial applications of cassava: Current status, opportunities and prospects. Journal of the Science of Food and Agriculture 2017;97(8):2280-90.

Liu H, Fang HH. Extraction of extracellular polymeric substances (EPS) of sludges. Journal of Biotechnology 2002;95(3): 249-56.

Liu XM, Sheng GP, Luo HW, Zhang F, Yuan SJ, Xu J, et al. Contribution of extracellular polymeric substances (EPS) to the sludge aggregation. Environmental Science and Technology 2010;44(11):4355-60.

Lowry OH. Protein measurement with the Folin phenol reagent. Journal of Biological Chemistry 1951;193:265-75.

Lu X, Zhen G, Estrada AL, Chen M, Ni J, Hojo T, et al. Operation performance and granule characterization of upflow anaerobic sludge blanket (UASB) reactor treating wastewater with starch as the sole carbon source. Bioresource Technology 2015; 180:264-73.

Lu X, Ni J, Zhen G, Kubota K, Li YY. Response of morphology and microbial community structure of granules to influent COD/SO_4^{2-} ratios in an upflow anaerobic sludge blanket (UASB) reactor treating starch wastewater. Bioresource Technology 2018;256:456-65.

Miron Y, Zeeman G, Van Lier JB, Lettinga G. The role of sludge retention time in the hydrolysis and acidification of lipids, carbohydrates and proteins during digestion of primary sludge in CSTR systems. Water Research 2000;34(5):1705-13.

Nielsen SS. Food Analysis Laboratory Manual. Switzerland: Springer Cham; 2017. p. 137-41.

Onodera T, Sase S, Choeisai P, Yoochatchaval W, Sumino H, Yamaguchi T, et al. High-rate treatment of molasses wastewater by combination of an acidification reactor and a USSB reactor. Journal of Environmental Science and Health, Part A 2011;46(14):1721-31.

Rajbhandari BK, Annachhatre AP. Anaerobic ponds treatment of starch wastewater: Case study in Thailand. Bioresource Technology 2004;95(2):135-43.

Sheng GP, Yu HQ, Li XY. Extracellular polymeric substances (EPS) of microbial aggregates in biological wastewater treatment systems: A review. Biotechnology Advances 2010;28(6):882-94.

Sowcharoensuk C. Industry Outlook 2020-2022: Cassava Industry [Internet]. 2020 [cited 2022 Nov 30]. Available from: https://www.krungsri.com/en/research/industry/industry-outlook/agriculture/cassava/IO/io-cassava-20.

Stronach SM, Rudd T, Lester JN. Anaerobic Digestion Processes in Industrial Wastewater Treatment. Berlin, Heidelberg: Springer; 2012.

Syutsubo K, Harada H, Ohashi A. Granulation and sludge retainment during start-up of a thermophilic UASB reactor. Water Science and Technology 1998;38(8-9):349-57.

Syutsubo K, Sinthurat N, Ohashi A, Harada H. Population dynamics of anaerobic microbial consortia in thermophilic granular sludge in response to feed composition change. Water Science and Technology 2001;43(1):59-66.

Tagawa T, Takahashi H, Sekiguchi Y, Ohashi A, Harada H. Pilot-plant study on anaerobic treatment of a lipid-and protein-rich food industrial wastewater by a thermophilic multi-staged UASB reactor. Water Science and Technology 2002;45(10): 225-30.

Thai Tapioca Development Institute (TTDI). Tapioca starch [Internet]. 2000 [cited 2021 Aug 31]. Available from: https://tapiocathai.org/English/E4_e.html.

Thai Tapioca Starch Association (TTSA). Export tapioca products [Internet]. 2021 [cited 2021 Aug 31]. Available from: https://www.thaitapiocastarch.org/en/information/statistics/export_tapioca_products.

Thepubon T, Choeisai P, Mungkarndee P, Choeisai K, Syutsubo K. Effect of suspended solids removal methods on methane production from tapioca starch wastewater. Engineering and Applied Science Research 2020;47(1):87-92.

Van Lier JB, Van der Zee FP, Frijters CT, Ersahin ME. Celebrating 40 years anaerobic sludge bed reactors for industrial wastewater treatment. Reviews in Environmental Science and Bio/Technology 2015;14(4):681-702.

Wang B, Wu D, Zhang X, Mackey HR, Chen GH. Sludge flotation, its causes and control in granular sludge upflow reactors. Applied Microbiology and Biotechnology 2018; 102(15):6383-92.

Wu J, Jiang B, Feng B, Li L, Moideen SN, Chen H, et al. Pre-acidification greatly improved granules physicochemical properties and operational stability of upflow anaerobic sludge Blanket (UASB) reactor treating low-strength starch wastewater. Bioresource Technology 2020;302:Article No. 122810.

INSTRUCTION FOR AUTHORS

Publication and Peer-reviewing processes of Environment and Natural Resources Journal

Environment and Natural Resources Journal is a peer reviewed and open access journal that is published in six issues per year. Manuscripts should be submitted online at https://ph02.tci-thaijo.org/index.php/ennrj/about/submissions by registering and logging into this website. Submitted manuscripts should not have been published previously, nor be under consideration for publication elsewhere (except conference proceedings papers). A guide for authors and relevant information for the submission of manuscripts are provided in this section and also online at: https://ph02.tci-thaijo.org/index.php/ennrj/author. All manuscripts are refereed through a **double-blind peer-review** process.

Submitted manuscripts are reviewed by outside experts or editorial board members of **Environment and Natural Resources Journal**. This journal uses double-blind review, which means that both the reviewer and author identities are concealed from the reviewers, and vice versa, throughout the review process. Steps in the process are as follows:

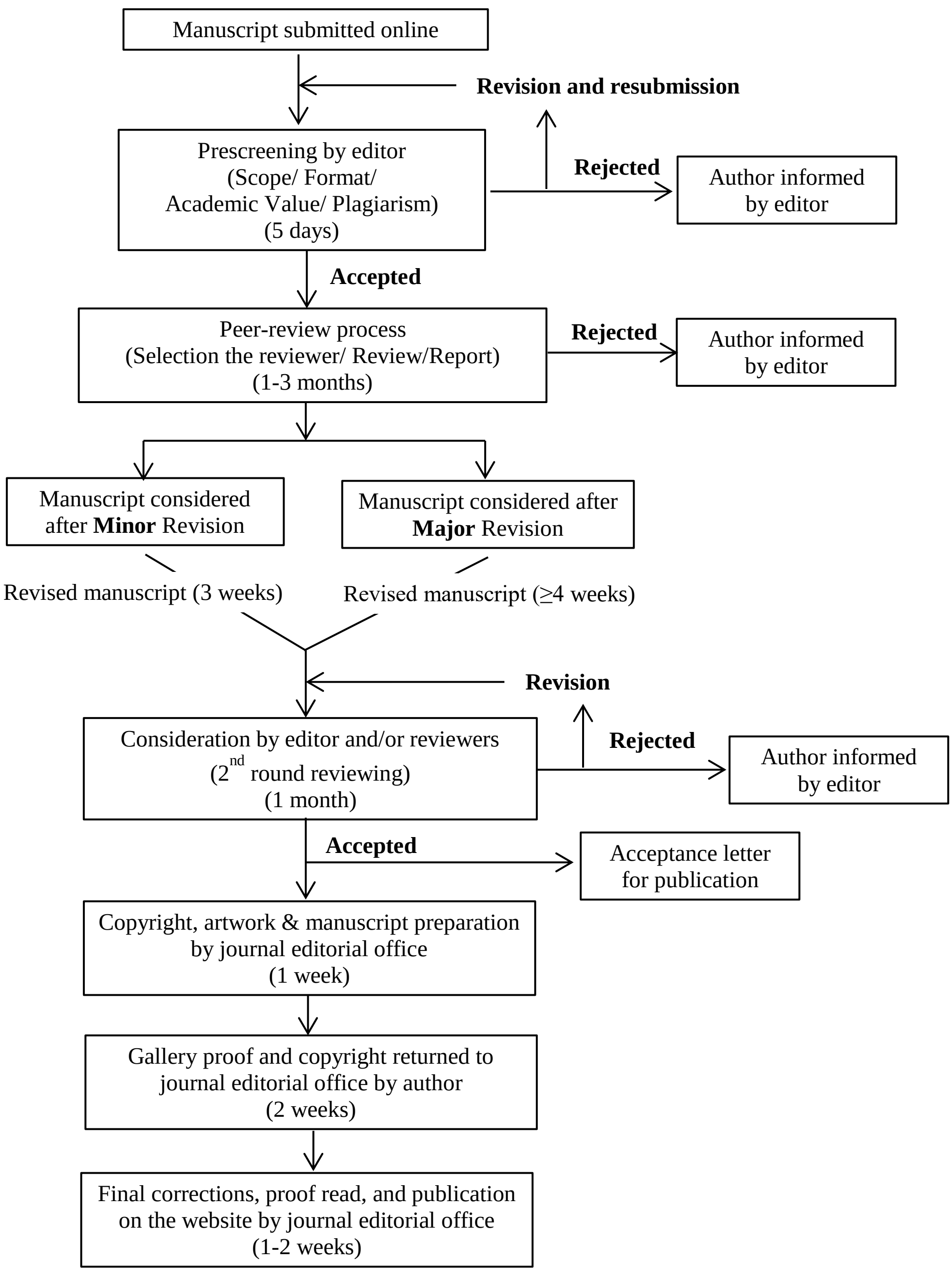

The Environment and Natural Resources Journal (EnNRJ) accepts 2 types of articles for consideration of publication as follows:

- *Original Research Article:* Manuscripts should not exceed 3,500 words (excluding references).
- *Review Article (by invitation):* This type of article focuses on the in-depth critical review of a special aspect in the environment and also provides a synthesis and critical evaluation of the state of the knowledge of the subject. Manuscripts should not exceed 6,000 words (excluding references).

Submission of Manuscript

Cover letter: Key points to include:

- Statement that your paper has not been previously published and is not currently under consideration by another journal
- Brief description of the research you are reporting in your paper, why it is important, and why you think the readers of the journal would be interested in it
- Contact information for you and any co-authors
- Confirmation that you have no competing interests to disclose

Manuscript-full: Manuscript (A4) must be submitted in Microsoft Word Files (.doc or .docx). Please make any identifying information of name(s) of the author(s), affiliation(s) of the author(s). Each affiliation should be indicated with superscripted Arabic numerals immediately after an author's name and before the appropriate address. Specify the Department/School/Faculty, University, Province/State, and Country of each affiliation.

Manuscript-anonymized: Manuscript (A4) must be submitted in Microsoft Word Files (.doc or .docx). Please remove any identifying information, such as authors' names or affiliations, from your manuscript before submission and give all information about authors at title page section.

Reviewers suggestion *(mandatory)*: Please provide the names of 3 potential reviewers with the information about their affiliations and email addresses. *The recommended reviewers should not have any conflict of interest with the authors. Each of the reviewers must come from a different affiliation and must not have the same nationality as the authors.* Please note that the editorial board retains the sole right to decide whether or not the recommended potential reviewers will be selected.

Preparation of Manuscript

Manuscript should be prepared strictly as per guidelines given below. The manuscript (A4 size page) must be submitted in Microsoft Word (.doc or .docx) with Times New Roman 12 point font and a line spacing of 1.5. *The manuscript that is not in the correct format will be returned and the corresponding author may have to resubmit*. The submitted manuscript must have the following parts:

Title should be concise and no longer than necessary. Capitalize first letters of all important words, in Times New Roman 12 point bold.

Author(s) name and affiliation must be given, especially the first and last names of all authors, in Times New Roman 11 point bold.

Affiliation of all author(s) must be given in Times New Roman 11 point italic.

Abstract should indicate the significant findings with data. A good abstract should have only one paragraph and be limited to 250 words. Do not include a table, figure or reference.

Keywords should adequately index the subject matter and up to six keywords are allowed.

Text body normally includes the following sections: 1. Introduction 2. Methodology 3. Results and Discussion 4. Conclusions 5. Acknowledgements 6. References

Reference style must be given in Vancouver style. Please follow the format of the sample references and citations as shown in this Guide below.

Unit: The use of abbreviation must be in accordance with the SI Unit.

Format and Style

Paper Margins must be 2.54 cm on the left and the right. The bottom and the top margin of each page must be 1.9 cm.

Introduction is critically important. It should include precisely the aims of the study. It should be as concise as possible with no sub headings. The significance of problem and the essential background should be given.

Methodology should be sufficiently detailed to enable the experiments to be reproduced. The techniques and methodology adopted should be supported with standard references.

Headings in Methodology section and Results and Discussion section, no more than three levels of headings should be used. Main headings should be typed (in bold letters) and secondary headings (in bold and italic letters). Third level headings should be typed in normal and no bold, for example;

2. Methodology
2.1 Sub-heading
2.1.1 Sub-sub-heading

Results and Discussion can be either combined or separated. This section is simply to present the key points of your findings in figures and tables, and explain additional findings in the text; no interpretation of findings is required. The results section is purely descriptive.
<u>Tables</u> Tables look best if all the cells are not bordered; place horizontal borders only under the legend, the column headings and the bottom.
<u>Figures</u> should be submitted in color; make sure that they are clear and understandable. Please adjust the font size to 9-10, no bold letters needed, and the border width of the graphs must be 0.75 pt. *(Do not directly cut and paste them from MS Excel.)* Regardless of the application used, when your electronic artwork is finalized, please 'save as' or convert the images to TIFF (or JPG) and separately send them to EnNRJ. The images require a resolution of at least 300 dpi (dots per inch). If a label needed in a figure, its font must be "Times New Roman" and its size needs to be adjusted to fit the figure without borderlines.

All Figure(s) and Table(s) should be embedded in the text file.

Conclusions should include the summary of the key findings, and key take-home message. This should not be too long or repetitive, but is worth having so that your argument is not left unfinished. Importantly, don't start any new thoughts in your conclusion.

Acknowledgements should include the names of those who contributed substantially to the work described in the manuscript but do not fulfill the requirements for authorship. It should also include any sponsor or funding agency that supported the work.

References should be cited in the text by the surname of the author(s), and the year. This journal uses the author-date method of citation: the last name of the author and date of publication are inserted in the text in the appropriate place. If there are more than two authors, "et al." after the first author' name must be added. Examples: (Frits, 1976; Pandey and Shukla, 2003; Kungsuwas et al., 1996). If the author's name is part of the sentence, only the date is placed in parentheses: "Frits (1976) argued that . . ."

Please be ensured that every reference cited in the text is also present in the reference list (and vice versa).

In the list of references at the end of the manuscript, full and complete references must be given in the following style and punctuation, arranged alphabetically by first author's surname. Examples of references as listed in the References section are given below.

Book

Tyree MT, Zimmermann MH. Xylem Structure and the Ascent of Sap. Heidelberg, Germany: Springer; 2002.

Chapter in a book

Kungsuwan A, Ittipong B, Chandrkrachang S. Preservative effect of chitosan on fish products. In: Steven WF, Rao MS, Chandrkachang S, editors. Chitin and Chitosan: Environmental and Friendly and Versatile Biomaterials. Bangkok: Asian Institute of Technology; 1996. p. 193-9.

Journal article

Muenmee S, Chiemchaisri W, Chiemchaisri C. Microbial consortium involving biological methane oxidation in relation to the biodegradation of waste plastics in a solid waste disposal open dump site. International Biodeterioration and Biodegradation 2015;102:172-81.

Published in conference proceedings

Wiwattanakantang P, To-im J. Tourist satisfaction on sustainable tourism development, amphawa floating marketSamut songkhram, Thailand. Proceedings of the 1st Environment and Natural Resources International Conference; 2014 Nov 6-7; The Sukosol hotel, Bangkok: Thailand; 2014.

Ph.D./Master thesis

Shrestha MK. Relative Ungulate Abundance in a Fragmented Landscape: Implications for Tiger Conservation [dissertation]. Saint Paul, University of Minnesota; 2004.

Website

Orzel C. Wind and temperature: why doesn't windy equal hot? [Internet]. 2010 [cited 2016 Jun 20]. Available from: http://scienceblogs.com/principles/2010/08/17/wind-and-temperature-why-doesn/.

Report organization:

Intergovernmental Panel on Climate Change (IPCC). IPCC Guidelines for National Greenhouse Gas Inventories: Volume 1-5. Hayama, Japan: Institute for Global Environmental Strategies; 2006.

Remark

** Please be note that manuscripts should usually contain at least 15 references and some of them must be up-to-date research articles.*

** Please strictly check all references cited in text, they should be added in the list of references. Our Journal does not publish papers with incomplete citations.*

Changes to Authorship

This policy of journal concerns the addition, removal, or rearrangement of author names in the authorship of accepted manuscripts:

Before the accepted manuscript

For all submissions, that request of authorship change during review process should be made to the form below and sent to the Editorial Office of EnNRJ. Approval of the change during revision is at the discretion of the Editor-in-Chief. The form that the corresponding author must fill out includes: (a) the reason for the change in author list and (b) written confirmation from all authors who have been added, removed, or reordered need to confirm that they agree to the change by signing the form. Requests form submitted must be consented by corresponding author only.

After the accepted manuscript

The journal does not accept the change request in all of the addition, removal, or rearrangement of author names in the authorship. Only in exceptional circumstances will the Editor consider the addition, deletion or rearrangement of authors after the manuscript has been accepted.

Copyright transfer

The copyright to the published article is transferred to Environment and Natural Resources Journal (EnNRJ) which is organized by Faculty of Environment and Resource Studies, Mahidol University. The accepted article cannot be published until the Journal Editorial Officer has received the appropriate signed copyright transfer.

Online First Articles

The article will be published online after receipt of the corrected proofs. This is the official first publication citable with the Digital Object Identifier (DOI). After release of the printed version, the paper can also be cited by issue and page numbers. DOI may be used to cite and link to electronic documents. The DOI consists of a unique alpha-numeric character string which is assigned to a document by the publisher upon the initial electronic publication. The assigned DOI never changes.

Mahidol University

Wisdom of the Land

Research and Academic Service Section, Faculty of Environment and Resource Studies, Mahidol University
999 Phutthamonthon 4 Rd, Salaya, Nakhon Pathom 73170, Phone +662 441-5000 ext. 2108 Fax. +662 441 9509-10
E-mail: ennrjournal@gmail.com Website: https://www.tci-thaijo.org/index.php/ennrj

Crossref

Google Scholar